

Distribution Agreement

In presenting this thesis or dissertation as a partial fulfillment of the requirements for an advanced degree from Emory University, I hereby grant to Emory University and its agents the non-exclusive license to archive, make accessible, and display my thesis or dissertation in whole or in part in all forms of media, now or hereafter known, including display on the world wide web. I understand that I may select some access restrictions as part of the online submission of this thesis or dissertation. I retain all ownership rights to the copyright of the thesis or dissertation. I also retain the right to use in future works (such as articles or books) all or part of this thesis or dissertation.

Signature:

Kathryn Paschal MacPherson

Date

Peripheral immune traffic to the AD brain: role of soluble TNF signaling and
peripheral inflammation

By

Kathryn Paschal MacPherson
Doctor of Philosophy

Graduate Division of Biological and Biomedical Science
Neuroscience

Malú G. Tansey, Ph.D.
Advisor

W. Michael Caudle, Ph.D.
Committee Member

Mandy L. Ford, Ph.D.
Committee Member

Allan I. Levey, M.D., Ph.D.
Committee Member

Lary C. Walker, Ph.D.
Committee Member

Accepted:

Lisa A. Tedesco, Ph.D.
Dean of the James T. Laney School of Graduate Studies

Date

Peripheral immune traffic to the AD brain: role of soluble TNF signaling and
peripheral inflammation

By

Kathryn P MacPherson
B.S., Biology and Neuroscience, Indiana University Bloomington

Advisor: Malú G. Tansey, Ph.D.

An abstract of a dissertation submitted to the Faculty of the James T. Laney School of
Graduate Studies of Emory University in partial fulfillment of the requirements for the
degree of Doctor of Philosophy in Neuroscience
2017

Abstract

Peripheral immune traffic to the AD brain: role of soluble TNF signaling and peripheral inflammation

By Kathryn Paschal MacPherson

Recent evidence has shifted our understanding of the origin and longevity of microglia and perivascular macrophages as well as the role the immune system plays in brain health and disease. However, it remains unclear when during the course of disease peripheral immune cells traffic to the brain. Subsets of immune cells from both the innate and adaptive immune system have proposed protective and harmful roles in mediation of neuroinflammatory disease, while chronic peripheral inflammation has been linked to increased risk of developing neuroinflammatory disease. We hypothesize that the inflammatory phenotype of peripheral immune cells changes as a function of age and in response to progressive neurodegeneration. However, it is not yet understood how chronically inflamed central and peripheral immune cell populations impact brain health and disease course outcome. At terminal stages of neuroinflammatory diseases such as Alzheimer's disease (AD), evidence suggests that populations of peripheral immune cells exist within the parenchyma; however, the kinetics of trafficking have yet to be established. Understanding when subsets of immune cells traffic to the brain will reveal novel opportunities for disease-modulating therapies. Here we used mouse models to investigate the extent to which markers of inflammation and immune cell population profiles centrally and peripherally change as a function of AD-like pathology progression, and whether these changes represent adaptive or maladaptive responses. Trafficking of peripheral immune cells to inflamed tissues is regulated by several mechanisms, including cytokine and chemokine signaling. The cytokine soluble Tumor Necrosis Factor (sTNF) has been shown in multiple studies to be elevated in patients with AD, and sTNF regulates the permeability of the blood-brain barrier (BBB). sTNF is produced by both brain-resident and peripheral immune cells. Therefore, we hypothesize that sTNF is a key mediator of peripheral immune cell contributions to AD-like pathology. Here we have investigated the extent to which inhibition of sTNF signaling in the periphery and within the brain modulates not only neuroinflammation and peripheral immune cell trafficking to the CNS, but also the extent of progression of AD-like pathology. In addition, we investigated the extent to which chronic peripheral inflammation induced by high-caloric diet or lipopolysaccharide, alters brain neuroinflammatory kinetics and AD-like pathology to support a role for therapeutic intervention of sTNF signaling in the clinic to delay onset or slow progression of AD.

Peripheral immune traffic to the AD brain: role of soluble TNF signaling and
peripheral inflammation

By

Kathryn P MacPherson

B.S., Biology and Neuroscience, Indiana University Bloomington

Advisor: Malú G. Tansey, Ph.D.

A dissertation submitted to the Faculty of the
James T. Laney School of Graduate Studies of Emory University
in partial fulfillment of the requirements for the degree of
Doctor of Philosophy
in Neuroscience

2017

Table of Contents

<u>Chapter 1: Peripheral and brain immune mediators in brain health and AD:</u>	1
1.1 Introduction.....	2
1.2 Contributors to the CNS inflammatory environment	3
1.2.1 Microglia.....	3
1.2.2 Macrophages.....	6
1.2.3 T cells.....	9
1.2.4 Astrocytes.....	13
1.3 Regulation of Neuroinflammation.....	16
1.3.1 Lymphatics and Deep Cervical Lymph Nodes.....	17
1.3.2 Blood-brain Barrier.....	19
1.3.3 Cytokine signaling - focus on tumor necrosis factor.....	21
1.4 Role of peripheral inflammation in AD.....	23
1.4.1 Inflammatory risk factors for AD.....	24
1.4.2 Alteration in trafficking of peripheral immune cells to the brain.....	25
1.5 Dissertation overview.....	27
<u>Chapter 2: Peripheral administration of the soluble TNF inhibitor XPro1595 modifies brain immune cell profiles, decreases beta-amyloid plaque load, and rescues impaired long-term potentiation in 5xFAD mice.</u>	30
2.1 Context, Author’s Contribution, and Acknowledgement of Reproduction.....	31
2.2 Abstract.....	31
2.3 Significance statement.....	32
2.4 Introduction.....	33
2.5 Methods.....	35
2.5.1 Animals.....	35
2.5.2 Multiplexed Immunoassays.....	36
2.5.3 Brain Dissociation for Immune Cell Isolation	37
2.5.4 Spleen Dissociation for Immune Cell Isolation	38
2.5.5 Deep Cervical Lymph Node Dissociation (DCLN) for Immune Cell Isolation.....	38

2.5.6 Multi-color Flow Cytometry.....	38
2.5.7 XPro1595 Administration.....	40
2.5.8 Electrophysiology.....	41
2.5.9 Brain Dissection for RNA Extraction.....	43
2.5.10 Real-time PCR (QPCR).....	44
2.5.11 Brain Dissection for Immunohistochemistry and Histological Analysis.....	45
2.5.12 Statistical Analysis.....	46
2.6 Results.....	46
2.6.1 Age-dependent pro-inflammatory cytokine expression in 5xFAD mice.....	46
2.6.2 Altered peripheral immune cell populations in the pro-inflammatory Tg CNS environment.....	47
2.6.3 Altered naïve and effector T cell populations in deep cervical lymph node of Tg mice.....	49
2.6.4 Inhibition of soluble TNF decreases brain populations of activated CD11b ⁺ immune cells and CD4 ⁺ T cells.....	50
2.6.5 Inhibition of soluble TNF increases the naïve T cell populations in the DCLNs of Tg mice.....	53
2.6.6 Inhibition of soluble TNF decreases amyloid β and cytokine expression in the hippocampus of Tg mice.....	54
2.6.7. XPro1595 blocked LTP deficits in 5xFAD mice.....	55
2.7 Discussion.....	56
2.8 Summary.....	64

Chapter 3: The role of high caloric diet on central and peripheral inflammation and immune cell profiles..... 87

3.1 Context, Author’s Contribution, and Acknowledgement of Reproduction....	88
3.2 Abstract.....	88
3.3 Introduction.....	89
3.4 Methods.....	92
3.4.1 Animals.....	92
3.4.2 High-fat high-fructose (HFHF) diet.....	93
3.4.3 Low-dose (LD) LPS administration.....	94
3.4.4 Brain Dissociation for Immune Cell Isolation.....	94

3.4.5 Plasma and Peripheral blood mononuclear cell (PBMC) isolation...	95
3.4.6 Multi-color Flow Cytometry.....	95
3.4.7 Bioluminescence imaging (BLI) Measurements.....	97
3.4.8 Statistical Analysis.....	98
3.5 Results.....	99
3.5.1 PBMC populations in male mice are altered by low-dose LPS-induced peripheral inflammation.....	99
3.5.2 HFHF diet induced dynamic changes within CD11b ⁺ myeloid PBMC populations in both male and female C57Bl/6Jmice.....	101
3.5.3 T cell populations show resistance to changes induced by HFHF-dependent peripheral inflammation.....	103
3.5.4 PBMC populations in female 5xSBE mice are resilient to changes induced by diet-dependent chronic peripheral inflammation.....	105
3.5.6 HFHF diet reduces frequency of CD3 ⁺ T cell populations trafficking to the brain in CCR2 RFP/+ mice.....	106
3.5.7 HFHF diet alters CD11b ⁺ microglia/macrophage population within and trafficking to the brain.....	107
3.5.8 Peripheral inflammation from both LD LPS and HFHF diet alters the neuroinflammatory response in 5xTg_SBE mice.....	109
3.6 Discussion.....	110
3.7 Summary.....	116

Chapter 4: Conclusions.....141

4.1 Summary of Results.....	142
4.1.1 Peripheral immune cell trafficking patterns in a mouse model of AD-like pathology.....	142
4.1.2 Regulation of peripheral immune cell trafficking patterns via soluble TNF (sTNF)-dependent signaling.....	143
4.1.3 Effects of chronic inflammation on peripheral immune cell trafficking and brain neuroinflammatory response.....	145
4.2 Implications and Future Directions.....	146
4.2.1 Modulation of peripheral immune cell activation and/or their trafficking may be a potential therapeutic target.....	146
4.2.2 Second-hit model of progression of AD-like pathology.....	148
4.2.3 Assessing changes in peripheral immune cell populations in at-risk human populations.....	149

4.2.4 Revitalization of an aging immune system.....	150
4.3 Conclusions.....	152

<u>Appendix: Complete list of publications to which the author has contributed during her graduate training</u>	153
--	-----

<u>References</u>	154
--------------------------------	-----

Figure Index

Figure 1.1: Modeling the effects of peripheral inflammation and soluble TNF signaling on peripheral immune cell traffic to the brain and AD-like pathology.....	28
---	----

Supplementary figure S2.1. XPro1595 penetrates into the brain parenchyma when dosed peripherally.....	66
---	----

Table 2.1: Increased expression of inflammatory cytokines in the brain of Tg mice without evidence of inflammation in the CSF	68
---	----

Table 2.2: Inhibition of sTNF partially mitigates inflammatory profile in Tg mice.....	70
--	----

Figure 2.1. Altered peripheral immune cell populations in the pro-inflammatory AD-like brain environment.....	72
---	----

Figure 2.2. Altered naïve and effector T cell populations in deep cervical lymph nodes of 5xFAD mice.....	75
---	----

Figure 2.3. Inhibition of soluble TNF with XPro1595 decreases populations of activated CD11b ⁺ immune cells and CD4 ⁺ T cells in the brain of 5xFAD mice.....	77
---	----

Figure 2.4. Inhibition of soluble TNF with XPro1595 increases the naïve T cell population in the deep cervical lymph nodes (DCLNs) of 5xFAD mice.....	79
---	----

Figure 2.5. Inhibition of soluble TNF with XPro1595 decreases amyloid beta in the subiculum and decreases pro-inflammatory mRNA in the hippocampus of 5xFAD mice.....	81
---	----

Figure 2.6. Inhibition of soluble TNF with peripheral XPro1595 administration <i>in vivo</i> rescued LTP impairment in 5xFAD mice.....	83
--	----

Figure 2.7. Specific targeting of sTNF/TNFR1 signaling rescues AD-like synaptic deficits and modulates AD-like associated immune cell population alterations.....	85
---	----

Table 3.1 – Special diet ingredient composition.....	118
Table 3.2 – Calculated nutrient composition and fatty acid profile.....	120
Supplementary figure S3.1 – PBMC gating.....	122
Supplementary figure S3.2 – CCR2 gating.....	124
Figure 3.1 PBMC populations in male mice are altered by low-dose LPS-induced peripheral inflammation.....	126
Figure 3.2 HFHF diet induced dynamic changes within CD11b ⁺ myeloid PBMC populations in both male C57Bl/6Jmice.....	128
Figure 3.3 T cell populations show resistance to changes induced by HFHF-dependent peripheral inflammation.....	130
Figure 3.4 PBMC populations in female 5xSBE mice are resilient to changes induced by diet-dependent chronic peripheral inflammation.....	132
Figure 3.5 HFHF diet reduces frequency of CD3 ⁺ T cell populations trafficking to the brain in CCR2 RFP/+ mice.....	134
Figure 3.6 HFHF diet alters CD11b ⁺ microglia/macrophage population within and trafficking to the brain.....	136
Figure 3.7 Peripheral inflammation from both LD LPS and HFHF diet alters the neuroinflammatory response in 5xTg_SBE mice.....	139

Chapter 1:

Peripheral and brain immune mediators in brain health and AD

1.1 INTRODUCTION

Once thought to be immunologically inert, the central nervous system (CNS) is now recognized as a highly regulated and immune-competent system. It is now accepted that the CNS parenchyma is immune-specialized and has a unique relationship with the peripheral immune system, such that initiation of antigen-driven proinflammatory, adaptive immune responses are tightly regulated and the kinetics of innate immune responses are modulated in health and disease. The blood-brain barrier (BBB) acts as a physical barrier that separates the brain from cells and solutes that mediate peripheral immune responses, however this does not prevent interaction with the peripheral immune system or immune cell extravasation into the CNS (Ransohoff and Engelhardt, 2012). Under homeostatic conditions inflammatory responses in the brain are influenced by BBB permeability, cytokine and chemokine signaling, neuron-microglia crosstalk, microglial activation, regulation of T cell responses, and entry of peripheral immune cells into the CNS (Carson et al., 2006). Together, this close regulation allows for immune surveillance, i.e., innate and adaptive immune responses to invasion of foreign pathogens that can be quickly resolved while minimizing negative outcomes on neuronal function and survival.

Evidence supports a role for peripheral inflammatory mechanisms in the regulation of brain function and brain health as well as a tight relationship with neuroinflammatory processes. Increasing evidence supports a role of neuroinflammation in the regulation of synaptic organization and development of mature circuits (Schafer et al., 2012). Cellular and signaling contributions of the peripheral immune system, including macrophages and neutrophils of the innate arm and T cells and B cells of the adaptive arm, in conjunction with brain-resident microglia, have increasingly been shown to play a role, not only in

autoimmune disease of the nervous system, but also in other neuroinflammatory diseases such as Alzheimer's disease (AD) (Ransohoff et al., 2015). How these populations of peripheral immune cells work with or against the brain-resident immune cells to influence health and risk or progression of disease is a topic of intense investigation. Knowledge of how these cells contribute to brain and BBB health and dysfunction is an essential part of understanding their role in neuroinflammatory pathology and neurodegenerative diseases, and will reveal opportunities for development of novel immunomodulatory interventions to prevent, delay, or arrest these diseases.

1.2 CONTRIBUTORS TO THE CNS INFLAMMATORY ENVIRONMENT

1.2.1 Microglia

Once thought to merely provide the 'glue' to support the neuronal networks, glial cells are now known to be an integral part of maintaining a healthy brain. New studies have identified the majority of microglia, originally thought to derive from monocyte-derived macrophages, originate from the embryonic yolk sac (Ginhoux et al., 2013; Tay et al., 2016). However, newly developed techniques and models have led investigators to conclude that non-yolk-sac contributions to the adult microglial pool cannot be ruled out (reviewed here (Tay et al., 2016)). Yolk sac-derived microglia populate the brain early in embryogenesis, dependent upon development of the circulatory system, where they persist in the brain into adulthood (Ginhoux et al., 2010). In contrast, yolk-sac derived macrophages, present early in development, are no longer found in blood in adulthood, having been replaced by bone-marrow derived macrophages (Ginhoux et al., 2010).

Development of yolk-sac microglia is dependent on colony stimulating factor-1 receptor (CSF-1R) expression and its ligand interleukin-34 (IL-34), which plays an important role in microglial homeostasis and are highly expressed by cortical and hippocampal neurons, and less so in the brain stem and cerebellum (Greter et al., 2012). Thus, environmental cues from the developing brain contribute to microglial longevity as well as region-specific microglial maintenance.

Microglia serve as the primary mediators of immunological defense in the brain, capable of cytokine and chemokine production, phagocytosis, and antigen presentation. Microglia are known to play diverse roles in maintaining brain health and function. Microglia have been shown to rapidly respond to localized brain injury in response to ATP (Davalos et al., 2005), a response that is impaired following systemic inflammation (Gyoneva et al., 2014). Recently, a role for microglia in the formation of mature neuronal circuit organization through complement-directed synaptic pruning has been reported (Schafer et al., 2012). These same mechanisms of complement-directed phagocytosis have also been implicated in Alzheimer's disease pathogenesis. Increased levels of complement proteins have recently been shown to precede early synapse loss, correlate with levels of soluble amyloid-beta ($A\beta$) oligomers, and are necessary for $A\beta$ oligomer-induced synaptic loss and $A\beta$ oligomer-induced LTP impairment (Hong et al., 2016). The complement protein C3 and its receptor CR3 have also been shown to play a role in microglial phagocytosis of $A\beta$ fibrils (Fu et al., 2012). Increased levels of C1qa and CD68 implicate microglia as the main source of complement and the mediators of synaptic loss in a manner similar to developmental synaptic pruning, which could be mediated via cytokine signaling or microglial activation (Hong et al., 2016). Complement component C1q has also been

shown to activate microglia to produce soluble TNF, a proinflammatory cytokine that can activate pro-apoptotic signaling pathways (Farber et al., 2009). Dysregulation of these developmentally crucial neuroinflammatory mechanisms may be contributing factor to the development and progression of neurodegenerative diseases such as AD.

Within the CNS, microglia are a major source of cytokines such as TNF, IL-1, IL-6, and IFN γ , as well as a source of neurotropic factors including neuronal growth factor (NGF) and brain-derived neurotrophic factor (BDNF). The nature of the activating stimulus, the specific microglial response, as well as the duration of activation, such as chronic activation, have been implicated as potential mechanisms of neurodegenerative disease (Smith et al., 2012). Regulation of microglial activation through neuronal ‘off’ signals like, TGF- β , CD22, CD200, and CX3CL1, and ‘on’ signals, like TREM2 and ATP, protects the brain from potentially harmful immune responses, and evidence suggests that these signals are deficient in neurodegenerative disease (Biber et al., 2007). CD200, expressed on the neuronal membrane, and its receptor, expressed on microglia, have been shown to play an inhibitory function in brain inflammation: blocking antibodies worsened neuroinflammatory disease models and macrophage infiltration (Biber et al., 2007). CD200R is also expressed on T cells (Rijkers et al., 2008), suggesting that T cells infiltrating into the brain may also be regulated via neuronal input. Fractalkine (CX3CL1), expressed in neurons, binds to microglial CX3CR1 and has been shown to play a role in regulation of microglial-neuronal interaction throughout life, including neurotoxicity and cytokine production (Reviewed here (Limatola and Ransohoff, 2014)). Microglial activation and IL-6 and TNF levels were increased with the loss of CX3CR1 and further increased with the addition of AD-like pathology. While CX3CR1 loss did not alter A β

accumulation, cognitive deficits were enhanced in an AD model with loss of CX3CR1 (Cho et al., 2011). Dysfunction of these regulatory mechanisms of microglial activation have been linked with increased risk for development of AD and impaired phagocytosis of A β reviewed here (Meyer-Luehmann and Prinz, 2015), and may serve as potential therapeutic targets as our understanding of the microglial contribution to neurodegenerative disease increases.

1.2.2 Macrophages

Macrophages are bone marrow-derived monocytes that traffic to the brain and differentiate into antigen-presenting macrophages (Hickey and Kimura, 1988). Recently, subtypes of macrophages have been identified in distinct locations of the brain; perivascular macrophages, meningeal macrophages, and choroid plexus macrophages (Prinz et al., 2011a). These macrophage populations can sample the contents of the cerebrospinal fluid (CSF) and present antigen via major histocompatibility complex II (MHCII) to contribute to immune surveillance of the brain and play an important role in response to neuroinflammatory disease, such as AD (Meyer-Luehmann and Prinz, 2015). Perivascular CX3CR1⁺ macrophages extend dendritic arms into CNS vessel lumen to present CNS antigens to circulating T cells under homeostatic conditions, and with increasing frequency in neuroinflammatory disease (Barkauskas et al., 2013). Understanding the role of these distinct populations in mediating immune regulation via their cross-talk with microglia may be a key to understanding neuroinflammatory disease. However, to study these populations of macrophages in the brain, as well as macrophages that have trafficked into the parenchyma, is challenging. In the periphery, macrophages can

be identified by the markers CD11b, CD45, and lack of Ly6G; however, these same markers also identify microglia in the brain. To distinguish between microglia and peripheral monocytes that have infiltrated the brain and differentiated into macrophages, the markers of CCR2 and Ly6C have been used to identify macrophages, while CX3CR1 has been used to identify microglia (Saederup et al., 2010). Importantly, the traditional markers for microglia (CD45, Iba1, and CD68) will also label macrophage populations. The markers of CCR2 and Ly6C, however, are down-regulated by macrophages a short while after differentiating in inflamed tissue; thus, these markers (CCR2 and Ly6C) are able to identify recently infiltrated macrophage populations (Greter et al., 2015). A majority of the peripheral macrophages that infiltrate the CNS will be CD45^{high} as compared to homeostatic/resting populations of CD45^{low} microglia. The relative levels of CD45 expression thus might potentially distinguish between macrophages and microglia among CD11b⁺ populations; however, upon activation, microglia are able to express CD45 at higher levels (Sedgwick et al., 1991), thus, CD45 is not a specific marker that can distinguish between microglia and macrophage populations.

Studies that assess RNA at the cellular level in conjunction with lineage tracking are viewed as key towards advancing the field because they will reveal novel markers to distinguish between microglia and macrophages in the CNS. A recent study by Goldmann and colleagues assessed microglia, subdural meningeal macrophages (Iba1⁺, CX3CR1⁺ and close to fibroblasts expressing ER-TR7), perivascular macrophages (Iba1⁺, CX3CR1⁺ and close to the abluminal side of CD31⁺ endothelial cells), and choroid plexus macrophages (in the stroma and epithelial layer of the choroid plexus) and found evidence suggesting that not all brain macrophage populations are derived from bone-marrow

populations. Fate mapping and chimeric studies revealed that microglia, perivascular macrophages, and meningeal macrophages are all embryonic-derived cells that, under homeostatic conditions, are stable populations not replaced by bone-marrow derived macrophages after birth, while choroid plexus macrophages are short-lived and repopulated by bone-marrow-derived macrophages (Goldmann et al., 2016). In addition, unbiased quantitative single-cell RNA sequencing revealed that, while perivascular macrophages are transcriptionally similar to microglia, they are distinguishable by *Mrc1* (encoding CD206), CD36 expression, and higher *Ptprc* (encoding CD45) expression, while microglia are distinguishable by higher *P2ry12* and *Hexb* gene expression (Goldmann et al., 2016). These distinct populations were also shown to display unique motility; meningeal macrophages were more amoeboid in shape, and as a population less mobile than microglia, while perivascular macrophages rarely displaced their cell bodies and constantly extended and retracted their protrusions along the blood vessel wall (Goldmann et al., 2016). Together, the evidence from this study refines our understanding of the origin of these macrophage populations and their potential role in neuroinflammatory disease.

As discussed above, only perivascular macrophages are replaced by peripheral blood monocytes under homeostatic conditions. This is also supported by studies of chimeric animals obtained by parabiosis, a model in which the BBB is not compromised by lethal irradiation; these experiments have shown microglia are maintained independent of bone-marrow-derived progenitors even in neuroinflammatory conditions (Ajami et al., 2007). However parabiosis generally yields lower levels of chimerism than does irradiation; in addition, a model independent of irradiation and parabiosis that uses busulfan to ablate bone marrow cells while preserving BBB integrity found minimal myeloid cell

recruitment in homeostatic conditions that was somewhat enhanced during neurodegeneration (Kierdorf et al., 2013). Recent studies suggest that, under conditions of inflammation, there is evidence that macrophages do traffic into the parenchyma and play a necessary role in plaque clearance. In an AD pre-clinical mouse model, microglial depletion induced monocyte infiltration into the brain, and over time these cells adopted features similar to microglia; however, unexpectedly the cells did not alter amyloid plaque deposition (Varvel et al., 2015), suggesting that macrophages alone are not sufficient to clear plaques. In fact, macrophages may contribute to the progression of pathology. Specifically, TREM2-positive CD45^{high}Ly6C⁺ myeloid cells, but not P2RY12 positive microglia, have been shown to contribute to AD pathogenesis (Jay et al., 2015). Together, these studies highlight the importance of elucidating the role of peripheral macrophages in AD.

1.2.3 T cells

T cells of the adaptive immune system are increasingly shown to play a role in regulation of brain immunity and mediating neuroinflammatory disease (Kipnis, 2016). CNS-specific CD4⁺ T cells have been shown to support cognition and brain health, while the choroid plexus plays an important role in the accumulation and recruitment of T cells as the neuro-immunological interface between the brain and peripheral immune system (Baruch and Schwartz, 2013). In the healthy brain, T cells patrol the CSF and become activated once they encounter their specific antigen presented to them by brain antigen-presenting cells (APCs), such as microglia, macrophages, and even astrocytes under certain conditions (Engelhardt and Ransohoff, 2005). Once active, T cells are able to enter the

brain parenchyma, and other inflamed tissues, and carry out their effector functions (Engelhardt and Ransohoff, 2012a) that may contribute to disease pathology. Blockade of LFA-1 (lymphocyte function-associated antigen 1), mediator of T cell, B cell, macrophage, neutrophil, and NK cell trafficking, reduced pathology and cognitive deficits in the 5xFAD mouse model (Zenaro et al., 2015). Following termination of the inflammatory event the effector T cell population contracts and memory T cells remain that are able to rapidly mount recall responses to antigens. Effector memory T cells migrate to tissue and display immediate effector functions, while central memory T cell home to lymphoid organs and proliferate, increasing the effector population (Sallusto et al., 2004).

Naïve CD4⁺ T cells become activated when encountering an antigen specific to their T cell receptor presented on MHC II expressed by APCs, and receiving co-stimulatory input. Once activated, naïve T cells will differentiate into effector T cells influenced by the inflammatory and cytokine milieu. There are many subsets of CD4⁺ T cells that each have distinct effector functions: Th1 cells are IFN γ -producing T cells known to play an essential role in phagocytic macrophage activation; Th2 cells produce IL-10, among other cytokines, and play a role in terminating immune responses; Th17 cells lead to the induction of proinflammatory cytokines and chemokines at sites of inflammation; regulatory CD4⁺ T cells (Treg) are also producers of IL-10 and play a role in suppression of the immune response (Luckheeram et al., 2012). Tregs, which suppress effector immune responses, have been shown to be elevated in elderly populations, and while not further elevated with AD pathology were also shown to have increased suppressive activity (Rosenkranz et al., 2007). Removal of the Treg suppressive effect on the immune system via transient depletion or inhibition of Tregs in an AD mouse model has been shown to increase

leukocyte trafficking at the choroid plexus, increase brain CD45^{high}CD11b⁺ and Treg populations, decrease plaque burden, decrease pro-inflammatory cytokine mRNA expression, and improve cognitive function (Baruch et al., 2015).

Naïve CD8⁺ T cells are activated when encountering their T cell receptor-specific antigen presented on MHCI, which is expressed on essentially all nucleated cells; CD8⁺ T cells expand into populations of effector CD8⁺ T cells producing pro-inflammatory cytokines such as IFN γ and TNF. Effector CD8⁺ T cells are cytotoxic and capable of inducing apoptosis through release of the pore-forming molecule perforin, granule enzymes, and upregulating programmed cell death triggers (CD95L) in target cells (Harty et al., 2000). MHCI and CD8⁺ T cells have been shown to play a role in brain function and neurodegenerative diseases (reviewed here (Cebrian et al., 2014a)). MHCI, expressed by neurons and present at synapses, has been shown to limit synapse density by forming a macromolecular complex with the insulin receptor, inhibiting synapse-promoting insulin receptor signaling (Dixon-Salazar et al., 2014). Expression of neuronal MHCI is increased in postmortem human samples in regions with neurodegenerative disease pathology and on murine primary neuronal cultures in response to IFN γ and activated microglia (Cebrian et al., 2014b). In EAE models, CD8⁺ T cells have been shown to directly injure axons through MHCI, upregulated via IFN γ , and granzyme-B dependent mechanisms (Sauer et al., 2013). Together, this evidence supports a role of MHCI and CD8⁺ T cell-induced changes in neuronal function and death that may play a role in mediating cognitive symptoms of neurodegenerative disease that may be revealed with further investigation.

Work in models of brain-targeted autoimmunity have led to greater understanding of the role that T cells play in neurodegenerative diseases, as well as the mechanisms of T

cell recruitment to the brain including role of regional expression of vascular adhesion molecules (reviewed here (Engelhardt and Ransohoff, 2005)). Inflammatory T cells have been shown to initially enter at the choroid plexus in a CCR6-dependent manner; however, following initiation of inflammation, a second wave of trafficking T cells are also able to enter in a CCR6-independent manner following the development of inflammation in an EAE (experimental autoimmune encephalomyelitis) model (Axtell and Steinman, 2009). In a model of EAE, pathogenic T cells (specific to myelin basic protein) have been shown to first accumulate in the leptomeninges and CSF, where they are rapidly turned over; within the CSF pathogenic T cells were less activated than within the leptomeninges and parenchyma and pathogenic T cells were shown to upregulate CCR5, CXCR3, and CXCR4 before entering CNS. (Schlager et al., 2016). Pathogenic T cells targeting a non-brain protein (OVA) increased trafficking to the leptomeninges and parenchyma when co-transferred with pathogenic T cells, however they showed significant differences in their migration pattern (Schlager et al., 2016). Blockade of VLA-4 (very late antigen-4; $\alpha 4\beta 1$ -integrin), via long-term treatment with natalizumab in multiple sclerosis patients, induces upregulation of P-selectin glycoprotein ligand-1 (PSGL-1) on CD4⁺ and CD8⁺ T cells; P-selectin expression was restricted to the choroid plexus and more pronounced. Firm adhesion, but not rolling, of T cells was blocked in these patient samples (Schneider-Hohendorf et al., 2014). Blockade of VLA-4, in a mouse model, reduced infiltration of CD8⁺ T cells and microglial activation in the CNS; while blockade of VCAM-1 only partially block CD8⁺ T cell infiltration and does not protect development of CNS tissue damage. Suggesting CD8⁺ T cells use $\alpha 4\beta 1$ -integrin to traffic into the CNS via VCAM-1 and additional vascular ligands (Martin-Blondel et al., 2015). Understanding not only the

mechanisms of trafficking under homeostatic conditions, but also under inflammatory conditions, as well as phenotypic changes in trafficking leukocytes is crucial to determining how the peripheral immune system contributes to neurodegenerative disease.

1.2.4 Astrocytes

Astrocytes are a heterogeneous population of glial cells derived from radial glia in the ventricular zone during development in a regionally and temporally distinct manner (Bayraktar et al., 2015). Astrocytes are the most abundant glial cell in the brain and participate in many aspects of brain health, including modulation of synaptic formation and removal, synaptic function, and neuronal survival (Allen, 2014). Astrocytes also play a supportive role for the neuroinflammatory response in the CNS, and they divide in response to inflammatory stimuli such as TNF (Barna et al., 1990). Astrocytes not only form an integral part the BBB that blocks potential pathogens from entering the brain (Goldstein, 1988), but they also function as APCs (Fontana et al., 1984). APCs, in both the brain and periphery, can communicate with antigen-specific T cells of the adaptive immune system via peptide presentation on the major histocompatibility complex (MHC). Astrocyte function can be regulated in an autocrine manner through immunomodulatory signaling produced by astrocytes as well as other cells in the brain. Astrocytes can produce many immune factors in response to stimulation (CXCL12, CCL2, CD40, IL15, CCL8, and CXCL1) and they can upregulate receptors to immune signaling molecules such as IL-1 β , IL-6, INF γ , TNF, TGF β , and lipopolysaccharide (LPS). These factors are known to modulate astrocyte function with regard to cell morphology, cell growth, cell proliferation,

glutamate regulation, antigen presentation, and pro- and anti-inflammatory cytokine production (Sofroniew, 2014).

Recent work has shown that activation of astrocytes leads to a decrease in their protective function and can also lead to neuronal death by soluble factors. LUHMES-IMA (Immortalized post-mitotic human neuron cell line – immortalized mouse astrocyte) co-cultures protected LUHMES neurons from MPP⁺ and NO-induced death (Efremova et al., 2016). LUHMES cells, derived from mesencephalic neurons, when differentiated serve as a dopaminergic cell model that has been shown to be susceptible to the parkinsonian toxin MPP⁺, similar to primary dopaminergic cells (Scholz et al., 2011). However, pretreatment for 6 days with either TNF or IL-1 β or both, but not IFN γ that selectively activated IMA but not LUHMES cells, lead to significant neuronal degeneration without the need for additional toxicants (Efremova et al., 2016). Similar responses were seen with cultures of human astrocytes; after 4 days of stimulation, evidence of morphological changes as well as neurodegeneration was observed, indicating these are not cross-species effects. In addition, it was determined that stimulated IMA conditioned media induced LUHMES cell death, not due to increased extracellular glutamate, suggesting that soluble factors are responsible for neuronal death in response to astrocyte activation (Efremova et al., 2016).

Astrocyte-enriched human cultures treated with IFN γ , IL-1 β , TNF α , but not TGF β showed increased MHCII and MHCI as well as the cellular adhesion molecules, ICAM and VCAM (Aloisi et al., 1995). This upregulation in MHC enables astrocytes to present antigen to CD4⁺ and CD8⁺ T cells, and is known to play a role in models of neurodegeneration (Engelhardt and Ransohoff, 2012a; Cebrian et al., 2014a). Astrocyte MHCII expression is down-regulated through direct functional neuronal contact and acts

to prevent the astrocytes from inducing T cell activation (Tontsch and Rott, 1993). Upregulation in ICAM and VCAM suggest that trafficking of peripheral immune cells, such as macrophages and T cells, into the parenchyma may be facilitated during astrocyte stimulation. Astrocyte-macrophage crosstalk has been shown to alter astrocyte proliferation and inflammatory responses. Conditioned media (CM) from pro-inflammatory M1 macrophage cultures, but not anti-inflammatory homeostatic M2 macrophage cultures, induced astrocyte proliferation (Haan et al., 2015). A history of exposure to either pro- or anti-inflammatory peripheral macrophages can alter the secretory profile of astrocytes and can include either an enhanced or diminished response (Haan et al., 2015). CM from astrocytes incubated with M2 CM decreased proliferation and TNF production in M1 macrophages, while CM from astrocytes incubated with M1 CM increased TNF production in M1 macrophages (Haan et al., 2015). These results suggest that a history of exposure can influence how astrocytes contribute to the local inflammatory environment, and may play an important role in chronic neuroinflammation. In many neuroinflammatory diseases there is also the presence of peripheral inflammation in human populations that may further alter the inflammatory profile of infiltrating macrophages into the CNS that participate in crosstalk with astrocytes and can thus contribute to chronic neuroinflammation.

Together, these non-neuronal cell types mediate and regulate the inflammatory environment of the brain and contribute to overall brain health and function. When regulatory mechanisms are altered due to either acute or chronic inflammation, these cells work together to mediate neuroinflammatory disease. Understanding how each

population is altered by inflammatory disease conditions can help to elucidate the broader network of immune crosstalk among these cell types that potentially mediates disease. Conditions that result in chronic peripheral inflammation have been shown to increase the risk for AD (Perry et al., 2007; Cunningham et al., 2009; Walker and Harrison, 2015), and investigation into how these conditions impact these immune cell populations as well as the CNS disease state may yield new strategies for therapeutic intervention.

1.3 REGULATION OF NEUROINFLAMMATION

As discussed in the previous section, the immune system is an integral player both in brain health and function, and it actively communicates with the peripheral immune system. The inflammatory response, especially microglial activation, is tightly regulated both through neuroimmune mechanisms, discussed above, as well as peripheral input; regulation of peripheral immune cell traffic at the BBB, surveillance at the deep cervical lymph nodes, as well as regulation of inflammatory signaling from inflamed tissue. To avoid immunodeficiency and chronic systemic inflammation, precise regulation of the inflammatory response is achieved in part through brain-derived immunoregulatory output via the autonomic nervous system and the vagus nerve that mediates bi-directional communication between the peripheral immune system and the brain (Pavlov and Tracey, 2015). Stimulation of the vagus nerve above the celiac ganglion, the location of neural cell bodies that project axons via the splenic nerve to innervate the spleen, inhibits cytokine release. This inflammatory reflex has been shown to be dependent on acetylcholine-producing T cells residing in the spleen. The released acetylcholine inhibits cytokine-producing macrophages via $\alpha 7$ nicotinic acetylcholine receptors, limiting systemic levels

of cytokines such as TNF (Rosas-Ballina et al., 2011). Input to the brain via vagal input as well as cytokine signaling across the BBB and leukocyte trafficking through the lymphatic systems all play an integral role in the regulation of neuroinflammation.

1.3.1 Lymphatics and Deep Cervical Lymph Nodes (DCLNs)

To provide immunological support for the CNS, the peripheral immune system must be able to survey for foreign antigens, which occurs via cellular surveillance of the CSF and perivascular spaces and through antigen drainage to the deep cervical lymph nodes (DCLNs). Brain derived antigens drain via the CSF through the nasal mucosa and into the DCLNs; thus the CSF is thought to act as the functional equivalent of lymph (Ransohoff and Engelhardt, 2012). To show that specific antibody producing cells form in the lymphoid tissues following inoculation in the brain, Walter and colleagues used a FITC labeled antigen to track antigen movement as well and anti-FITC antibody forming cell localization. Two hours following antigen injection into the subarachnoid space, FITC was observed in the nasal mucosa, subcapsular sinus, and DCLNs. Four days following injection of antigen, specific antibody forming cells were found in the deep cervical lymph nodes, peaking 6-8 days following injection, fewer in superficial lymph nodes, but none within axillary lymph nodes (Walter et al., 2006).

Solutes from the interstitial fluid are eliminated from the brain along basement membranes through the walls of capillaries and arteries. Dextran (3-kDa) was found to have diffused through the parenchyma and was located within phagocytic myeloid cells in blood vessels and capillary walls 5 minutes and 24 hours following injection into the

striatum. FluoSpheres have also been reported to be phagocytosed by perivascular macrophages located in the perivascular space. After intraventricular injection of 0.02 μ m and 1 μ m FluoSpheres, but not dextran, the tracer was found within the cervical lymph nodes (Carare et al., 2008). While it is clear from these data that solutes are able to drain from the brain to the DCLNs, the authors suggest that there is little evidence to support the drainage of cells along this perivascular route. There is, however, evidence to support the view that cells are able to drain via the subarachnoid space to the nasal mucosa and cervical lymph nodes, which have been shown to play a crucial role in mediating neuroinflammatory disease (reviewed here (Laman and Weller, 2013)).

When considering what drains to the DCLNs, context matters; therefore, it may be important to consider the inflammatory state of the CNS. While microglia are highly motile cells that can traffic to the site of injury within the brain (Davalos et al., 2005; Gyoneva et al., 2014), there is no evidence to suggest that microglia leave the CNS to enter the periphery. Under homeostatic conditions, where there is minimal peripheral immune cell traffic to the brain, there may be little cellular drainage to the DCLNs. However, under chronic inflammatory conditions such as occurs in neurodegenerative disease where increased evidence of peripheral immune cell trafficking into the CNS has been implicated, the cellular drainage into DCLNs may be increased or altered in response to ongoing neuroinflammation. T cells as well as myeloid cells have been found to drain to the DCLNs when injected into the parenchyma (Goldmann et al., 2006; Hatterer et al., 2006), suggesting that these cell types are capable of trafficking into the brain parenchyma in response to inflammation and then trafficking to the DCLNs where they may play a role in mediating neuroinflammatory disease. Recently, an alternative route, the lymphatic system

in the brain, which drains cerebrospinal fluid to the deep cervical lymph nodes and contains CD3⁺ T cells as well as CD11c⁺ and B220⁺ cells, has been visualized in the rodent localized in the dura matter at the base of the skull; however the presence of this tissue is not yet confirmed in humans (Aspelund et al., 2015; Louveau et al., 2015). Dye placed within the parenchyma has been shown to drain to the DCLNs, but not the superficial lymph nodes (Aspelund et al., 2015). This significant finding offers a new route through which CSF as well as antigen-presenting cells can drain to the lymphatic system and mediate immune surveillance of the brain.

1.3.2 Blood-brain Barrier

The BBB is comprised of tight junctions (TJ) and adherens junction (AJ) between the brain endothelial cells, and its overall function is to limit the entry of plasma components, red blood cells, and leukocytes into the brain (Zlokovic, 2008). The changes in the expression level of junctional proteins, such as occludins, ZO-1, claudin-5, VE-cadherin, and β -catenin have been implicated in increased BBB permeability and neuroinflammatory disease (Zlokovic, 2008). The outer wall of the BBB can be crossed by immune cells that then remain in the CSF-drained perivascular spaces separated from the CNS parenchyma by the glia limitans, where immune surveillance is carried out (Engelhardt and Ransohoff, 2012a). Different sets of adhesion molecules and cytokine signals are used to regulate traffic across the BBB and the glia limitans (Engelhardt, 2008). CCL2 induces recruitment of immune cells across the BBB, but induction of MMP-2 and MMP-9, up-regulated by TNF, are required to cross the glia limitans to access the parenchyma (Engelhardt and Ransohoff, 2012b). TNF may be a key mediator of BBB

permeability during disease, as an elevated plasma level of TNF is associated with increased risk for dementia and acceleration of AD pathology (Engelhart et al., 2004; Holmes et al., 2009). Evidence supports a role for TNF as an inflammatory mediator of BBB permeability that enables peripheral immune cells to more readily cross into the CNS (Rezai-Zadeh et al., 2009).

Changes in BBB transport systems have been strongly implicated in cognitive dysfunction and neurodegenerative disease (reviewed here (Zlokovic, 2008; Erickson and Banks, 2013)). The choroid plexus, a highly permeable region of the BBB, has been shown to play a role in mediating neuroinflammatory disease. As discussed in the sections above, recent studies have shown that the population of macrophages that reside in the choroid plexus are derived from blood populations (Goldmann et al., 2016). This alternative origin may assist these more permeable regions with combating pathogens and/or make these regions more susceptible to neuroinflammation. Dysfunction of the choroid plexus has been shown to play a role in mediating AD-like pathology. One month following transplantation of choroid plexus epithelial cells into the brains of 9-month-old APP/PS1 mice, A β accumulation, astrogliosis, and cognitive deterioration was significantly attenuated (Bolos et al., 2014). The authors suggest a role of secretion of A β degradation enzymes to account for this improvement in AD-like pathology (Bolos et al., 2014), however an additional mechanism may be the renewed regulation of immune cell trafficking at the choroid plexus. Indeed CD4⁺ T cells have been shown to play a role at the choroid plexus in mediating cognition and AD-like pathology (Baruch et al., 2015). Changes in leukocyte trafficking across the BBB may have disease-mediating

consequences as well as serve as potential therapeutic targets to modulate disease progression.

1.3.3 Cytokine signaling – focus on tumor necrosis factor (TNF)

The cytokine and chemokine signals that mediate recruitment of peripheral immune cells to the CNS have become popular targets of investigation, and new models and pharmacological tools provide us with new ways to modulate immune cell recruitment to the CNS to investigate how peripheral immune populations impact brain health and disease. Tumor necrosis factor (TNF) is produced by both microglia and macrophages and is a key modulator of pro-inflammatory cytokine cascades and immune cell activation (MacEwan, 2002). TNF exists in two functional forms: soluble TNF (sTNF) and transmembrane TNF (tmTNF), each with distinct functional bioactivities. sTNF signaling via TNFR1, results in pro-inflammatory actions, while tmTNF signaling via TNFR2 results in pro-survival signaling and plays an important role in immune system development (McCoy and Tansey, 2008). While the exact role of TNF in brain function is not well understood, elevations in systemic sTNF are associated with accelerated cognitive decline and increased conversion of mild cognitive impairment (MCI) to AD in elderly populations (Holmes et al., 2009).

A recent study demonstrated that a single systemic TNF challenge induced a transient working memory deficit and significant increase in hippocampal and hypothalamic inflammation in prion-injected mice as compared to controls; however, this manipulation alone was unable to exacerbate brain pathology (Hennessy et al., 2016).

These data suggest that, because there are no acute effects on pathology, TNF levels need to be chronically rather than acutely elevated or that TNF is not the sole mediator of brain pathology in that model. This idea is supported by evidence that acute systemic LPS, but not TNF, is able to increase the number of apoptotic cells in the hippocampus independent of sTNF in a prion model (Hennessy et al., 2016). Peripheral administration of LPS increases TNF expression in the CNS detectable 10 months after the initial insult in a TNF receptor-dependent signaling fashion (Qin et al., 2007). However, TNF is not the only inflammatory factor elicited by LPS treatment, and chronic and acute treatment of LPS produce different cytokine profiles in the serum and brain; TNF levels are significantly increased in the brain following repeated administration as compared to a single administration (Erickson and Banks, 2011), suggesting that chronic peripheral inflammation rather than acute inflammation increased brain TNF levels. TNF is at the apex of a wider network of pro-inflammatory mediators that have been implicated in neuroinflammatory disease (Steinman, 2013b). Therefore, understanding how TNF acts to modulate the pro-inflammatory environment and how it contributes to AD-like pathology will help us understand the CNS global network of inflammatory changes that occur with AD pathology.

Both TNF and LPS act at the BBB to modulate BBB permeability. Peripheral LPS increases TNF receptor expression at the BBB, particularly the expression of TNFR1, leading to up-regulation of factors that increase BBB permeability and allow infiltrating cells and other factors that are normally excluded from the brain parenchyma to enter it (Mackay et al., 1993; Nadeau and Rivest, 1999). Evidence of increased BBB permeability is present in brains of AD patients: increased CSF:serum albumin ratios, microvascular

pathology, and up-regulation of factors that regulate immune cell infiltration across the BBB have been reported (Sharma et al., 2012). Within the CNS, TNF can also contribute to neuroinflammation through activation of resident immune cells and recruitment of peripheral immune cells (Qin et al., 2007). Specific regulation of peripheral immune cell traffic across the BBB is crucial to maintaining the highly controlled immunological responses of the CNS.

Examining changes in these regulatory structures and pathways in response to central or peripheral inflammation can shed light on how regulation and activation of infiltrating populations is changing over the course of disease. TNF is shown to play an active role in modulation of the BBB and to contribute to activation of peripheral immune cell populations; thus, TNF may represent a valid target for modulation of immune cell traffic to the CNS to ameliorate chronic neuroinflammation in neurodegenerative diseases. Modulation of signaling at barrier structures may renew regulation of trafficking populations and boosts the brain's natural ability to combat neuroinflammatory disease.

1.4 ROLE OF PERIPHERAL INFLAMMATION IN ALZHEIMER'S DISEASE

Conditions of increased peripheral inflammation, including acute infections and chronic inflammatory disease, are associated with development of dementia and delirium in elderly patients, and have been reported as risk factors for development of AD (Holmes et al., 2003; Biessels et al., 2006; Kamer et al., 2008; Misiak et al., 2012; Murray et al., 2012). Epidemiological data suggest that chronic use of NSAIDs reduces the risk for AD, but clinical and animals studies have not found promising results for the use of NSAIDs to

treat AD (McGeer and McGeer, 2007), thus suggesting that a more targeted anti-inflammatory treatment is warranted. The peripheral immune system plays an active role in surveying the CNS for immunological threats, and evidence suggests that it may also play a role in neurodegenerative disease, as discussed in the sections above. However, it is still unclear how changes in peripheral immune cell populations over the course of AD pathology affect disease outcome, and how chronic peripheral inflammation modulates these mechanisms.

1.4.1. Inflammatory Risk factors for AD

Mutations within the APP, PSEN1, and PSEN2 genes are known to confer early onset AD (Tanzi, 2012); however, genetic variants have been found to associate with sporadic late onset AD, most strongly APOE, and many of these identified genes are expressed in the immune system and play a role in immune function, such as *CRI*, *CLU*, and *EPHA1* (reviewed here (Tanzi, 2012)). The *CD33* allele SNP re3865444 has been identified as protective against AD and is associated with reduction in CD33 protein expression and insoluble A β 42 (Griciuc et al., 2013). CD33 plays a role in regulation of the innate immune system (Crocker, 2005) and has been shown to inhibit microglial clearance of A β 42 in vitro (Griciuc et al., 2013). Variants in *TREM2* have been shown to be increased in AD populations and to increase AD susceptibility (Guerreiro et al., 2013). Increased levels of TREM2 were associated with increased levels of A β , and in mouse models TREM2 is increased in myeloid cells surrounding A β plaques (Guerreiro et al., 2013). Recent meta-analysis of 4 GWAS studies of people of European ancestry revealed 5 newly associated genomic regions: HLA-DRB5-HLA-DRB1, PTK2B, SORL1,

SLC24A4-RIN3 and DSG2 (Lambert et al., 2013). Associations with AD and CD33 were not replicated, of these newly identified risk genes, HLA-DRB5-HLA-DRB1 is associated with immunocompetence and histocompatibility. Together these data indicate that changes in regulation and function of the immune system increase the risk for AD.

1.4.2 Alterations in trafficking of peripheral immune cells to brain

Increased numbers of T cells have been found in the brain in AD patients as well as animal models of AD-like pathology (Togo et al., 2002), while markers of myeloid activation are increased, suggestive of increased microglial activation and peripheral macrophage infiltration with aging or AD-like pathology (Martin et al., 2016). Together these data support a role for peripheral immune cells in AD progression. While some studies suggest that these populations mediate disease, others suggest that they are not significant contributors (Prokop et al., 2015; Varvel et al., 2015), and even play a protective role. TREM2 expression was increased on CD11b⁺CD45^{high} myeloid cells that associated with A β deposits in an age-dependent manner, and these cells were found to also express Ly6C, suggesting that they were peripherally derived macrophages. Loss of TREM2 significantly reduced this population myeloid cells surrounding plaques, as well as A β accumulation, while not reducing microglial populations, suggesting that TREM2 and peripheral macrophages may be contributing to AD-like pathology (Jay et al., 2015). However, studies in a model of brain microglial depletion followed by rapid repopulation by peripheral myeloid cells have shown that peripheral myeloid cells were not recruited to A β plaques, nor did they alter A β pathology, even following treatment with A β -specific antibodies (Prokop et al., 2015). These studies suggest that the actions of peripheral

macrophages mediating disease may only be relevant in the context of interactions with brain-resident microglia. However, studies examining overexpression of CCL2, a chemokine that recruits peripheral macrophages to the CNS, or the loss of its receptor CCR2, have shown that loss of CCL2:CCR2 signaling accelerated memory impairments, synaptic impairment, and A β deposition, supporting a role for peripheral macrophage recruitment in the suppression of AD-like pathology (El Khoury et al., 2007; Kiyota et al., 2009). Combined, these studies suggest that there is potentially an optimal level of peripheral macrophage infiltration to maintain brain health, and deviations from this level may contribute to AD-like pathology.

Macrophages are not the only peripheral immune cells shown to provide protective effects against AD-like pathology. Mice lacking functional B and T cells have increased levels of A β and neuroinflammation that are reduced upon replacement of missing B and T cell populations (Marsh et al., 2016). However, some reports indicate that not all T cell subsets are protective under every circumstance. As discussed above, Treg populations have been shown to have a suppressive effect on peripheral immune cell recruitment that, when removed, mitigated AD-like pathology (Baruch et al., 2015). Increased levels of T cells have also been found in post-mortem AD brains as well as animal models of AD (Togo et al., 2002; Ferretti et al., 2016). Thus, optimal T cell trafficking and activation state may have to be paired with optimal macrophage trafficking and activation state to maintain brain health, especially during the conditions of neuroinflammatory disease. The timing of immune cell trafficking to the brain may play a role in the determination of whether the contributions are protective or pathogenic, and may be altered by chronic peripheral inflammation.

1.5 DISSERTATION OVERVIEW

This dissertation will focus on further examining the trafficking patterns of immune cells during the course of AD-like pathology in the 5xFAD mouse model of AD. I will build upon the current knowledge of macrophage and T cell trafficking by assessing multiple subsets of peripheral immune cell populations, not only in the brain, but also within the draining DCLNs and spleen at several stages of disease progression. Further knowledge of how trafficking patterns of these populations respond to increasing levels of AD-like pathology and neuroinflammation will enable us to better understand how the adaptive and innate immune systems in the brain and in the periphery network to mediate disease. Through modulation of inflammation, dampening of sTNF signaling and utilization of diet-induced peripheral inflammation, I will show how this network is altered in conditions that associate with changes in AD-like pathology. I hypothesize that sTNF signaling mediates immune cell trafficking to the brain, contributing to AD-like pathology. Chronic low-grade peripheral inflammation, including increased systemic sTNF levels, will further modulate trafficking immune cell populations and accelerate disease progression. I hypothesize that blocking sTNF signaling will re-establish immune cell trafficking patterns into the CNS and decelerate the effects of AD-like pathology on neuronal dysfunction and neuroinflammation, **figure 1.1**.

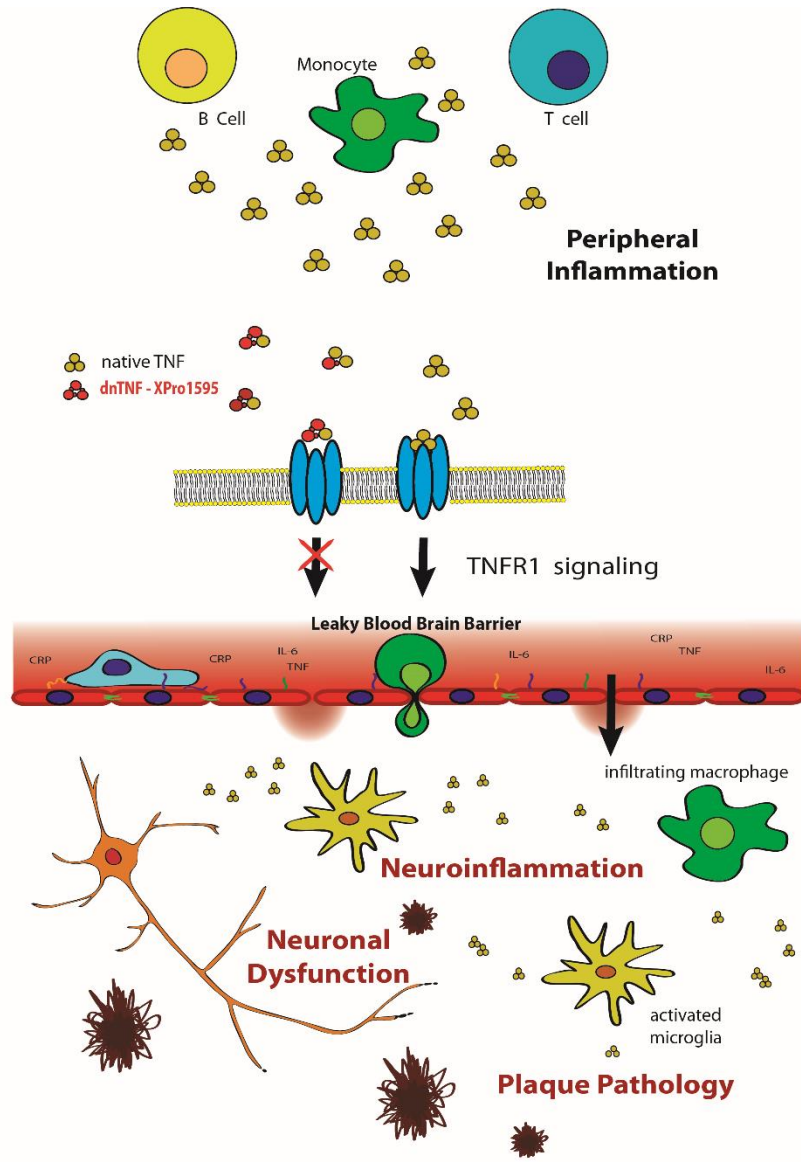


Figure 1.1: Modeling the effects of peripheral inflammation and soluble TNF signaling on peripheral immune cell traffic to the brain and AD-like pathology.

Chronic peripheral inflammation leads to systemic increase in cytokines and other inflammatory factors, such as soluble TNF (sTNF). Systemic sTNF, signaling via the TNFR1 receptor, leads to blood-brain barrier (BBB) breakdown, altered peripheral immune cell trafficking to the brain, and neuroinflammation that together contribute to neuronal dysfunction and the progression of AD-like pathology. Selective inhibition of sTNF signaling, via XPro1595, will enable the BBB to re-establish regulation of immune cell traffic to the brain as well as dampen neuroinflammation, restore synaptic function, and slow the progression of AD-like pathology.

Chapter 2:

Peripheral administration of the soluble TNF inhibitor XPro1595 modifies brain immune cell profiles, decreases beta-amyloid plaque load, and rescues impaired long-term potentiation in 5xFAD mice

2.1 Context, Author's Contribution, and Acknowledgement of Reproduction

The following chapter describes the effects of AD-like pathology and sTNF signaling on trafficking populations of peripheral immune cells into the brain. This work was conceptualized by the dissertation author and Dr. Malú Tansey. Research was conducted by the dissertation author, Dr. Pradoldej Sompol, Dr. George T. Kannarkat, Jianjun Chang, Lindsey Sniffen, and Mary E. Wildner. The document was written by the dissertation author, Dr. Malú Tansey, and Dr. Christopher M. Norris. This chapter is reproduced with minor edits from MacPherson, K.P., Sompol, P., Kannarkat, G.T., Chang, J., Sniffen, L., Wildner, M.E., Norris, C.M., Tansey, M.G. Inhibition of soluble TNF modifies brain immune cell profiles, rescues impaired long-term potentiation, and decreases beta-amyloid plaque load in the subiculum of 5xFAD mice, *Neurobiology of Disease* (2017) PMID: 28237313

2.2 Abstract

Clinical and animal model studies have implicated inflammation and peripheral immune cell responses in the pathophysiology of Alzheimer's disease (AD). Peripheral immune cells including T cells circulate in the cerebrospinal fluid (CSF) of healthy adults and are found in the brains of AD patients and AD rodent models. Blocking entry of peripheral macrophages into the CNS was reported to increase amyloid burden in an AD mouse model. To assess inflammation in the 5xFAD (Tg) mouse model, we first quantified central and immune cell profiles in the deep cervical lymph nodes and spleen. In the brains of Tg mice, activated (MHCII⁺, CD45^{high}, and Ly6C^{high}) myeloid-derived CD11b⁺ immune cells are decreased while CD3⁺ T cells are increased as a function of age relative to non-Tg mice. These immunological changes along with evidence of increased mRNA levels for several cytokines suggest that immune regulation and trafficking

patterns are altered in Tg mice. Levels of soluble Tumor Necrosis Factor (sTNF) modulate blood-brain barrier (BBB) permeability and are increased in CSF and brain parenchyma post-mortem in AD subjects and Tg mice. We report here that *in vivo* peripheral administration of XPro1595, a novel biologic that sequesters sTNF into inactive heterotrimers, reduced the age-dependent increase in activated immune cells in Tg mice, while decreasing the overall number of CD4⁺ T cells. In addition, XPro1595 treatment *in vivo* rescued impaired long-term potentiation (LTP) measured in brain slices in association with decreased A β plaques in the subiculum. Selective targeting of sTNF may modulate brain immune cell infiltration, and prevent or delay neuronal dysfunction in AD.

2.3 Significance Statement

Immune cells and cytokines perform specialized functions inside and outside the brain to maintain optimal brain health; but the extent to which their activities change in response to neuronal dysfunction and degeneration is not well understood. Our findings indicate that neutralization of sTNF reduced the age-dependent increase in activated immune cells in Tg mice, while decreasing the overall number of CD4⁺ T cells. In addition, impaired long-term potentiation (LTP) was rescued by XPro1595 in association with decreased hippocampal A β plaques. Selective targeting of sTNF holds translational potential to modulate brain immune cell infiltration, dampen neuroinflammation, and prevent or delay neuronal dysfunction in AD.

2.4 Introduction

Inflammation as a hallmark of Alzheimer's disease (AD) is well established. However, the mechanisms by which the peripheral immune system contributes to the etiology or progression of AD are not yet elucidated. The pro-inflammatory response of brain-resident immune cells to AD pathophysiology leads to increased local production of cytokines and chemokines, and recruitment of peripheral immune cells (Akiyama et al., 2000; Heneka et al., 2015). The chemoattractant CCL2/MCP-1, plays an important role in recruitment of phagocytic macrophages to the inflamed CNS (Hickman and El Khoury, 2010), and is upregulated in CSF, but not plasma, of MCI and early stage AD patients (Brosseron et al., 2014). These observations suggest peripheral immune cells respond to signals generated in the CNS and traffic across the blood-brain barrier (BBB) to play an important role in early AD. T cells are also found in increasing frequency in postmortem brain of aged individuals and patients with AD (Togo et al., 2002). Recently identified lymphatic vessels in the rodent brain regulate neuroimmune responses by connecting to deep cervical lymph nodes (DCLNs) where they drain antigens from the brain parenchyma (Ransohoff and Engelhardt, 2012; Laman and Weller, 2013; Aspelund et al., 2015; Louveau et al., 2015). The extent to which alterations in immune cell trafficking to the brain occur during the course of AD and whether these are beneficial or maladaptive remains unknown.

At the pinnacle of inflammatory cascades, elevations in TNF are associated not only with induction of the inflammatory response but also with chronic inflammation (MacEwan, 2002; Steinman, 2013a). TNF exists in two functional forms: soluble TNF (sTNF) and transmembrane TNF (tmTNF), each with distinct functional bioactivities. sTNF signaling, primarily via TNFR1, results in pro-inflammatory actions while tmTNF signaling, primarily via TNFR2 results in pro-survival signaling and plays an important role in immune system development (McCoy and

Tansey, 2008). TNF elevations are reported in AD patient plasma, and an acute increase in serum TNF, as well as higher baseline TNF level, has been associated with greater cognitive decline in elderly populations (Holmes et al., 2009; Swardfager et al., 2010). Results from non-selective TNF blockade in pre-clinical animal models of AD-like pathology call into question the validity of the therapeutic benefit of targeting TNF in AD (Montgomery et al., 2011); however studies specifically targeting sTNF/TNFR1 axis in the CNS are promising (McAlpine et al., 2009). Neuronal ablation of TNFR2, but not TNFR1, increased extracellular A β (Montgomery et al., 2013), a hallmark of AD pathology, while ablation of TNFR1 increased Iba1 (microglial) reactivity in the hippocampus of 12-month old 3xTg-AD mice (Montgomery et al., 2013), a potentially beneficial response as microglia have a complex role in brain health and disease (Mandrekar-Colucci and Landreth, 2010). Together, these data provide rationale for the specific targeting of sTNF while sparing tmTNF/TNFR2 signaling. Moreover, loss of BBB integrity establishes an environment susceptible to dysregulated interactions with the peripheral immune system. TNF downregulates the BBB phenotype in human brain microvascular endothelial cells at 1ng/ml TNF (Rochfort et al., 2014). While plasma and CSF TNF levels in AD patients are typically 10 fold lower than this, the permeability of the BBB increases as a function of age and these sTNF levels may be sufficient for further BBB disruption in subjects with MCI, promoting faster conversion to AD (Swardfager et al., 2010; Montagne et al., 2015).

Here, we measure populations of peripheral immune cells found in the CNS of 5xFAD (Tg) mice and assess the role of sTNF in recruiting these populations to the brain. We investigated whether inhibition of sTNF, with XPro1595 (Steed et al., 2003; McCoy et al., 2006; Brambilla et al., 2011) would mitigate the AD-like pathology found in Tg mice and evaluated the extent to which these effects occur in association with alterations in central and peripheral immune cell

population profiles. Our results showed that neutralization of sTNF reduces proinflammatory immune cell markers and gene expression, and rescues impaired LTP within the Tg brain.

2.5 Methods

2.5.1 *Animals*

The 5xFAD (Tg) mouse model displays key pathological hallmarks of AD including synaptic dysfunction, plaque accumulations, and neuronal degeneration (Oakley et al., 2006). While amyloid deposition begins early in this model, around 2 months, spatial working memory deficits in Y-maze are not detected until 4-5 months of age (Oakley et al., 2006). Our own group has not found significant deficits in 8-arm radial water maze until 8-10 months (unpublished observations). Female 5xFAD mice, on a congenic C57BL/6J background, were used for all flow cytometry, XPro1595, and electrophysiology experiments to assess the role of sTNF and trafficking immune cell populations in AD-like pathology. Female mice were used because they show accelerated AD-like pathology when compared to male 5xFAD mice (Oakley et al., 2006). For all XPro1595 studies mice were randomly assigned to treatment group based on genotype, and investigators involved in quantification of outcome measures were blinded to genotype and treatment history. For measurements of cytokines in CSF by multiplexed immunoassay and inflammatory mRNA analysis by qPCR, we used both male and female mice at 2-, 4-, and 6-months of age to assess baseline level of inflammation in the periphery and within the brain, **Table 1**. Specifics on age and group size are detailed in each specific methods section. Tg mice, generously provided by Vassar lab, were co-housed in a vivarium at Emory University, or University of Kentucky for electrophysiology studies, with *ad libitum* access to food and water on

a 12hr light/dark cycle. All experimental procedures were approved by the Institutional Animal Care and Use Committee of Emory University or University of Kentucky and comply with the National Institutes of Health guide for the care and use of Laboratory animals.

2.5.2 *Multiplexed Immunoassays*

Serum and CSF samples were analyzed for cytokines and chemokines that play key roles in pro-inflammatory and anti-inflammatory pathways (IFN- γ , IL-1 β , IL-6, IL-10, IL-12p70, mKC/CXCL1, and TNF) using a V-PLEX multiplexed immunoassay per the manufacturer's instructions (Meso Scale Discovery, Gaithersburg, MD). XPro1595 levels in serum and brain were measured using an anti-human TNF ultrasensitive (Cat # K151BHC-1) singleplex immunoassay and quantified using the Meso Scale Discovery SECTOR Imager 2400-A (Meso Scale Diagnostics, LLC, Rockville, MD). To measure XPro1595, the supplied human TNF protein used to generate a calibrator/standard protein was replaced by the XPro1595 protein, which increases the sensitivity of the assay substantially. Signals from the linear standard curve range from 3000 (at 0 XPro1595) to 1 million counts (at 250ng/mL). All samples were assayed in duplicate by an experimentalist blinded to treatment history. The data were analyzed and converted to pg/mL values using the Meso Scale Discovery integrated data analysis software. Mice used: 2 months of age Tg: 4 male and 3 female samples pooled – 30 μ l total; non-Tg: 1 male and 7 female samples pooled – 20 μ l total; 4 months of age Tg: 2 male and 3 female samples pooled – 20 μ l total; non-Tg: 5 male and 3 female samples pooled – 50 μ l total; 6 months of age Tg: 5 male and 3 female samples pooled – 30 μ l total; non-Tg: 3 male and 2 female samples pooled – 40 μ l total. Samples were run in replicates of 10 μ l. Samples were pooled for analysis of CSF cytokines and chemokines due to the very low volume yield per animal.

2.5.3 Brain Dissociation for Immune Cell Isolation

5xFAD mice were anesthetized with isoflurane and whole brain, deep cervical lymph nodes, and spleen were removed. Rapid removal of the brain ensured high immune cell yield and viability needed to run two multi-channel flow panels on the harvested immune cells. In pilot studies, we compared the yield, viability, and brain immune subset frequencies between perfused and non-perfused mice and confirmed that this method of harvest did not result in contamination from blood vessels as there were no differences across the non-brain tissues (spleen and deep cervical lymph nodes) in CD4⁺ and CD8⁺ T cell subsets, or in the number of viable cells (data not shown). More importantly, we found no significant differences in the frequency of total CD3⁺ T cell or within the CD4⁺ and CD8⁺ T cell subset populations in the brains of non-perfused as compared to perfused mice. Given that the frequency of T cell populations is much higher in the blood than in the brain, contamination from blood PBMC populations would have resulted in an increase in the frequency of T cells in non-perfused animals as compared to perfused animals. Whole brain tissue was finely minced in 1xHBSS (without Calcium, Magnesium, and phenol red, Invitrogen, 14175) and transferred to an enzymatic DDP solution (DMEM/F12 media containing 1mg/ml papain from papaya latex (P4762 Sigma Aldrich, St. Louis, MO), 1.2U/mL dispase II (4942078001 Roche diagnostics, Risch-Rotkreuz, Switzerland), and 220U/mL DNase I (18047-019 Invitrogen, Carlsbad, CA)). The minced tissue and DDP was incubated at 37°C for 20 minutes before being neutralized with 10% FBS (heat inactivated, Atlanta Biologicals, S11150). The tissue pellet was homogenized in ice-cold 1xHBSS using a fine-tip glass pipette. The homogenate was filtered through a 70µM cell strainer. The pellet was resuspended in 37% Percoll (Percoll pH8.5-9.5; Sigma Aldrich Co, P1644) and 70% Percoll layered below, and 30% Percoll layered above, with 1xHBSS layered on the top. The Percoll gradient was centrifuged and immune cells were

collected from the cell cloud between the 70% and 37% Percoll layer, washed with 4x volume of 1xHBSS. Cells were split in half and stained with separate antibody panels for flow cytometry; approximately 1×10^6 cells were used per panel.

2.5.4 Spleen Dissociation for Immune Cell Isolation

The spleen was removed and placed into 1xHBSS with 5% FBS. A single cell solution was made by passing tissue through a $70 \mu\text{M}$ cell strainer. Cells were counted on a hemocytometer at a 1 to 10 dilution, and 1×10^6 cells were stained per animal.

2.5.5 Deep Cervical Lymph Node Dissociation for Immune Cell Isolation

Both the right and left deep cervical lymph nodes were removed and placed into 1xHBSS with 5% FBS. A single cell solution was made by passing tissue through a $70 \mu\text{M}$ cell strainer. Cells were counted on a hemocytometer at a 1 to 1 dilution, and 1×10^6 cells were stained per animal.

2.5.6 Multi-color Flow Cytometry

All cells were stained with Live/Dead Fixable Aqua (1:2000, L34957 Invitrogen) and incubated with anti-mouse CD16/CD32 (1:100, 14-0161085 eBioscience). 1×10^6 cells from the spleen, deep cervical lymph nodes, and brain were stained with panel 1: anti-mouse CD3 PE eFluor 610 (1:100, 61-0031 eBioscience), anti-mouse CD4 Alexa Fluor 488 (1:100, 53-0041 eBioscience), anti-mouse CD8b APC-eFluor780 (1:100, 47-0083 eBioscience), anti-mouse

CD62L PE-Cy7 (1:200, 25-0621 eBioscience), anti-mouse CD44 Alexa Fluor 700 (1:100, 130326 BioLegend) in FACS buffer. One million cells from the brain were stained with panel 2: anti-mouse Ly6G PacBlue (1:100, 127611 BioLegend), anti-mouse CD11b FITC (1:100, 11-0112 eBioscience), anti-mouse CD19 PE (1:100, 561736 BD Bioscience), anti-mouse MHCII Pe-Cy7 (1:100, 25-5321 eBioscience), anti-mouse CD45 PerCP-Cy5.5 (1:100, 45-0451 eBioscience), anti-mouse CD3 PE eFluor610 (1:100, 61-0031 eBioscience), anti-mouse CD11c Alexa Fluor 700 (1:50, 117320 BioLegend), anti-mouse Ly6C APC-Cy7 (1:100, 128026 BioLegend) in FACS buffer. Samples were run on an LSRII (BD Biosciences) and analyzed with FlowJo_V10.

Single cell lymphocytes were gated based on Forward Scatter Height (FSH) (Size) and Side Scatter Height (SSH) (granularity) and then by FSH by FHA (Forward Scatter Area). Live cells were then selected as the Fixable Aqua negative population. In the samples stained with panel 1: CD3⁺ cells were selected and then gated for CD4⁺ and CD8⁺. Each of the CD4⁺ and CD8⁺ gated populations were gated by CD44 vs CD62L. In samples stained with panel 2: CD45⁺ cells were selected and then gated by CD3 (T cells) vs Ly6G (Neutrophils). The CD3⁻Ly6G⁻ population was gated CD19 vs CD11b and the CD11b⁺CD19⁻ population was gated for CD45^{high} and CD45^{low} populations. Those populations were gated for MHCII⁺ and MHCII⁻ and Ly6C^{high} and Ly6C^{low} from histogram distribution. The CD11b⁺CD19⁻ population was also gated for CD11c, a marker of dendritic cells and potentially of a subpopulation of antigen presenting microglia (Włodarczyk et al., 2014). From every sample counting beads (AccuCheck Counting Beads, Invitrogen PCB100, 10µl were added to each sample before running on the LSRII) were selected on size from the FSH vs FHA plot and then again from FSH vs FHA. Sample counts of all target populations were calculated in FlowJo and from these counts total tissue counts were obtained: ((population

count/bead count) x bead concentration in sample run) x run volume x (whole sample volume/volume processed for 1×10^6 cells).

For assessment of immune cells populations at 3.5, 5, 7, and 12 months the following group sizes of female 5xFAD were used: 3.5 months: non-Tg n = 8, Tg n = 9; 5 months: non-Tg n = 11, Tg n = 11; 7 months: non-Tg n = 11, Tg n = 13; 12 months: non-Tg n = 10, Tg n = 9. Within these groups, subsets with robust MHCII and Ly6C staining were used for analysis of these markers in the brain, non-robust staining was determined as antibody or experimental error and not specific to treatment group or genotype: 3.5 months: non-Tg n= 8 (MHCII)/5 (Ly6C), Tg n = 9/4; 5 months: non-Tg n = 4/7, Tg n = 7/8; 7 months: non-Tg n = 8/6, Tg n = 11/7; 12 months: non-Tg n = 9/10, Tg n = 8/4. From the overall group, a subset of samples had robust CD44 and CD62L staining and were used for analyses of those markers in brain 3.5 months non-Tg n = 5, Tg n = 3; 5 months: non-Tg n = 4, Tg n = 4; 7 months: non-Tg n = 5, Tg n = 5; 12 months: non-Tg n = 6, Tg n = 4

2.5.7 XPro1595 Administration

XPro1595 is a PEG-ylated human TNF variant devoid of TNF receptor-binding activity that forms heterotrimers with native sTNF (but not membrane-bound TNF), thereby sequestering sTNF away from TNF receptors (Steed et al., 2003; Barnum et al., 2014). To assess the role of sTNF in AD-like pathology and immune cell trafficking to the CNS, Tg female mice were divided into two cohorts each with two treatment groups. Mice received either subcutaneous (s.c.) saline vehicle control or s.c. XPro1595 (10mg/kg) twice weekly for two months. This dose was selected on the basis of PK/PD studies and its efficacy in reducing dopaminergic neuron loss and glial activation in a rat model of nigral degeneration (Barnum et al., 2014). When administered

peripherally XPro1595 is detectable in the brain (**Supplementary figure S2.1**) which is sufficient to neutralize the native soluble homotrimer TNF through soluble heterotrimer formation. To assess the role of sTNF on trafficking immune cell population one cohort of female mice was treated between 5 and 7 months of age (Saline n =9, XPro1595 n = 10); within this group, n = 9 saline and n = 7 XPro1595 were used for analysis of the Ly6C marker within the myeloid panel, and n = 5 saline and n = 6 XPro1595 were used for analysis of CNS T cell panel in addition to the CNS myeloid panel). The other cohort was treated with XPro1595 or saline between 2 and 4 months of age (Saline n = 8 and XPro1595 n = 7). XPro1595 (generously provided by Dr. David Szymkowski at Xencor, Inc.) was diluted with sterile saline to 2mg/ml concentration to be dosed in mice at 10mg/kg. To assess the role of sTNF on AD-like amyloid accumulation and mRNA associated with inflammatory markers female Tg and non-Tg mice treated with either saline or XPro1595 from 5 to 7 months of age (non-Tg saline n = 8, non-Tg XPro1595 n = 6, Tg saline n = 3, Tg XPro1595 n = 5).

2.5.8 *Electrophysiology*

Brain slice electrophysiology methods were performed as previously published (Mathis et al., 2011; Bachstetter et al., 2012; Furman et al., 2012). The study design was the same as for the mice used for immunological and histological outcome measures. After eight weeks of i.p. injections, mice were deeply anesthetized with CO₂ and decapitated. Brains were removed and stored briefly in ice-cold, Ca²⁺-free artificial cerebrospinal fluid (ACSF) containing (in mM) 124 NaCl, 2 KCl, 1.25 KH₂PO₄, 2 MgSO₄, 26 NaHCO₃, 10 dextrose (pH=7.4), and saturated with 95% O₂ and 5% CO₂. 400 µm-thick sections were cut on a Vibratome® 1000 vibrating microtome (Leica Biosystems, Buffalo Grove, IL). Slices were then transferred to a custom holding chamber (Mathis

et al., 2011) and maintained in CaCl₂-containing (2mM)-ACSF at an interface with warm (32°C), humidified air. Slices were permitted to equilibrate for at least 1.5 hr before beginning electrophysiological analysis. Investigators were blinded to treatment history.

Slices were transferred to an RC-27 recording chamber (Warner Instruments, Hamden, CT) and perfused with oxygenated ACSF (32°C) at a rate of 1–2 mL/min for 15–20 min before the start of each recording session. CA3 Schaffer collaterals were activated with a bipolar platinum-iridium electrode located in *stratum radiatum* near the CA3 border. Stimulus intensity was controlled by a constant current stimulus isolation unit (World Precision Instruments, Sarasota, FL), and stimulus timing was controlled by Clampex 9.2 software (Molecular Devices, Sunnyvale, CA). Field EPSPs were recorded using a glass micropipette (1–6 MΩ), filled with ACSF and containing an Ag-AgCl wire, positioned in *stratum radiatum* of CA1, approximately 1-2 mm away from the point of stimulation. Field potentials were amplified 100X, Bessel-filtered at 1 kHz, and digitized at 10 kHz using a Multiclamp 700B amplifier and a Digidata 1320 digitizer (Molecular Devices).

To assess basal synaptic strength, twin stimulus pulses (S1 and S2, 100 μs pulse duration, 50 msec interpulse interval) were given at 12 intensity levels (range 25–500 μA) at a rate of 0.1Hz. Five field potentials at each level were averaged, and measurements of fiber volley (FV) amplitude (in mV) and excitatory postsynaptic potential (EPSP) slope (mV/ms) for S1 were performed offline using ClampFit software (Molecular Devices). Synaptic strength curves were constructed by plotting the EPSP slope against the FV amplitude at each stimulus intensity. Maximal synaptic strength for each slice was estimated by taking the maximal EPSP slope amplitude during the input/output curve and dividing by the corresponding FV amplitude. Paired-pulse facilitation (PPF) was calculated by dividing the S2 EPSP slope by the S1 EPSP (taken from the linear portion of the synaptic strength curve) and multiplying by 100. To estimate population spike (PS)

threshold, the EPSP slope amplitude at which a population spike first appeared in the ascending phase of the field potential was calculated and averaged across five successive trials at the spike threshold stimulation level.

After synaptic strength curves were constructed, the stimulus intensity was readjusted to elicit an EPSP of ~1 mV, and stimulus pulses were delivered at 0.033 Hz until a stable 20 min baseline was established. High-frequency stimulation (two 100 Hz trains, 1 sec each, 10 sec inter-train interval) was then delivered at the baseline stimulation intensity to induce LTP, followed by an additional 60 min baseline. Within each group, EPSP slope measures from the last 10 min of the post-LTP baseline were averaged across slices within each animal and compared to the pre-LTP baseline slope average. Electrophysiological parameters were averaged across all slices within each animal (one to three slices), and the *n* used for statistical comparisons reflects the number of animals per genotype and treatment group.

2.5.9 Brain dissection for RNA Extraction

Mice were rapidly decapitated under isoflurane and the brain was removed. Half of the brain was post fixed for immunohistochemistry (see below). From the other half, the cerebellum, midbrain, hippocampus, and cortex were dissected out on a cold glass petri dish. Tissue was fast cooled in liquid nitrogen and stored at -80C° until processing. Tissue was processed by first homogenizing in Trizol (Life Technologies, 1596018) with a Tissue LyserII (Retsch). mRNA was isolated with RNeasy kit (Qiagen, 74106) and treated with DNAase1 (Invitrogen, 18068).

2.5.10 *Real-time PCR (qPCR)*

To assess baseline inflammation at 2, 4 and 6 months of age, tissue was collected from the same mice used for the CSF collection (2 months: Tg 4 Male and 4 Female, non-Tg 5 Male and 9 Female; 4 months: Tg 4 Male and 6 Female, non-Tg 6 Male and 4 Female; 6 months: Tg 3 Male and 4 Female, non-Tg 7 Male and 7 Female) and assessed for expression of mRNA associated with pro-inflammatory cytokines. To assess hippocampal inflammation and the role of sTNF tissue was collected from female Tg and non-Tg mice treated with either saline or XPro1595 from 5 to 7 months of age (non-Tg saline n = 8, non-Tg XPro1595 n = 6, Tg saline n = 3, Tg XPro1595 n = 5), only half of the brain was use the other half was post fixed for immunohistochemistry, below. Power analysis (75%) to determine significant effect of TNF mRNA in hippocampus due to genotype (Tg mean = 5.390, Non-Tg mean = 1.103, SD = 1.992) determined a samples size = 3 is sufficient.

Reverse transcription was preformed to make cDNA as published previously (Kannarkat et al., 2015). Briefly, cDNA was used with the following primer sets for qPCR, with TATA binding protein used as a housekeeping control to normalize samples: TNF – Forward 5' CTG AGG TCA ATC TGC CCA AGT AC 3' Reverse 5' CTT CAC AGA GCA ATG ACT CCA AAG 3' ; CCL2 – Forward 5' CTT CCT CCA CCA CCA TGC A 3' Reverse 5' CCA GCC GGC AAC TGT GA 3' ; TGF β – Forward 5' GCA GTG GCT GAA CCA AGG A 3' Reverse 5' AGA GCA GTG AGC GCT GAA TC 3' ; IL-1 β – Forward 5' CAA CCA ACA AGT GAT ATT CTC CAT G 3' Reverse 5' GAT CCA CAC TCT CCA GCT GCA 3' ; TATA binding protein – Forward 5' GTA TCT GCT GGC GGT TTG G 3' Reverse 5' GGC ACT GCG GAG AAA ATG A 3' ; CD45 – Forward 5' TCA TGG TCA CAC GAT GTG AAG A 3' Reverse 5'AGC CCG AGT GCC TTC CT 3' ; TNFR1– Forward 5' GTC CAT TCT AAG AAC AAT TCC ATC TG 3' Reverse 5'GCT CGG

ACA GTC ACT CAC CAA 3'; TNFR2– Forward 5' CTA TGA CAG GAA GGC TCA GAT GTG
3' Reverse 5'GTG TCC GAG GTC TTG TTG CA 3'; IFN γ R– Forward 5' GAC GTC TGT ATC
CCT CCT TTC C 3' Reverse 5' GTA AGA GGA GCA ACC ACC AGA A 3'.

2.5.11 *Brain Dissection for Immunohistochemistry and Histological Analysis*

Female Tg and Non-Tg mice treated with XPro1595 or saline from 5 to 7 months of age (non-Tg saline n = 8, non-Tg XPro1595 n = 6, Tg saline n = 3, Tg XPro1595 n = 5) were rapidly decapitated under isoflurane and the brain was removed. Half of the brain was post fixed for immunohistochemistry in 4% PFA for 24 hours and then transferred to 30% sucrose in 1xPBS. Brains (n=4 per treatment group) were embedded and sectioned at 35 μ M; serial sections were stained with anti-Amyloid- β (6e10), counterstained with thionine, and Amino Cupric Silver staining for to measure disintegration of multiple neuronal elements including cell bodies, axons, dendrites, and synaptic terminals, and counterstained with Nissl red by NeuroScience Associates (Knoxville, TN). Slides were scanned using the Aperio System (Leica Biosystems). Regions of interest were outlined and analyzed in ImageScope (Leica Biosystems). Sections stained with 6e10 were analyzed with the algorithm (positive pixel count), positive and strong positive pixels were used to measure amyloid density. Sections stained with amino cupric silver were analyzed with a modified algorithm with the following settings: Hue value 0.1, Hue width 0.8, CST 0.04, Iwp (high) 200, Iwp (low) 175, Ip (low) 110, Isp (low) 0, Inp (high) -0.8. Only strong positive pixels were used to measure early cellular degradation.

2.5.12 Statistical Analysis

Synaptic strength parameters and LTP values were compared across genotypes and drug treatment conditions with two-way analysis of variance (ANOVA) using GraphPad Prism 6 software (La Jolla, CA). Fisher's PLSD was used for *post hoc* comparisons. Cytokine protein values from multiplexed immunoassay analyses were compared across genotypes within each age using non-parametric T test using GraphPad Prism 6 software. qPCR data for aging evaluation of inflammatory mRNA data was normalized to 2mo non-Tg and were compared across genotypes and age with two-way ANOVA. Sidak's multiple comparisons test was used for *post hoc* comparisons within each age. Data from immunophenotyping studies across age was compared across genotypes and age with two-way ANOVA. Sidak's multiple comparisons test was used for *post hoc* comparisons within each age. Effects of XPro1595 on Tg immune cell populations, 6E10, and immune cupric Ag reactivity were determined across treatment using non-parametric T test using GraphPad Prism 6 software. XPro1595 effects on mRNA expression were normalized to non-tg saline and analyzed across genotypes and drug treatment conditions with two-way ANOVA. Sidak's multiple comparisons test was used for *post hoc* comparisons within genotype. Significance for all statistical comparisons was set at $p \leq 0.05$. All data are presented as mean \pm SEM.

2.6 Results

2.6.1 Age-dependent pro-inflammatory cytokine expression in 5xFAD mice

The 5xFAD (Tg) mouse model of Alzheimer's disease displays progressive amyloid beta plaque accumulation before 3 months of age, progressive synaptic protein loss as well as later neuronal degeneration, and cognitive deficits by 5 months of age (Oakley et al., 2006). In this

model we found age-dependent and region-specific increases in inflammatory mRNAs within the CNS but minimal evidence of inflammation in the CSF, as measured by multiplexed immunoassay. Tg mice, male and female, were not found to express significantly different levels of several cytokines in CSF at 2, 4, or 6 months of age. Levels of mKC/CXCL1 protein are significantly lower in Tg mice at 6 months of age (non-Tg mean 7.962 ± 0.438 pg/mL; Tg mean 4.3033 ± 1.481 pg/mL $df = 5$ $t = 2.724$ $p < 0.05$ *, **table 2.1A**; CSF levels of INF γ , IL-10, IL-1 β , IL-6 and IL-12 p70 protein levels undetectable). TNF protein levels are not detectable at 2 month of age and no significant differences were found at 4 and 6 months of age. Within the cortex, there was a significant increase in expression of CD45 mRNA at 6 months Tg mice as compared to non-Tg mice, male and female, (non-Tg mean = 1.188 ± 0.138 fold change, Tg mean = 2.901 ± 0.415 fold change from 2 month non-Tg baseline by 2-way ANOVA $df = 58$ $t = 7.107$ $p < 0.0001$, **table 2.1B**). Within the midbrain, expression of CD45 and TNF mRNA was significantly increased at 6 months in Tg mice as compared to non-Tg mice (TNF: non-Tg = 1.21 ± 0.147 , Tg = 3.325 ± 0.731 fold change from 2 month non-Tg baseline by 2-way ANOVA $df = 57$, $t = 5.560$, $p < 0.05$; CD45: non-Tg = 1.122 ± 0.074 , Tg = 3.276 ± 0.586 fold change from 2 month non-Tg baseline by 2-way ANOVA $df = 58$ $t = 7.895$ $p < 0.0001$, **table 2.1B**).

2.6.2 *Altered peripheral immune cell populations in the pro-inflammatory Tg CNS environment*

Immune cells were isolated from the CNS of Tg and non-Tg mice at 3.5, 5, 7, and 12 months of age. These ages correspond to early stages of amyloid deposition (3.5 months), onset of cognitive impairment (5 months), and aggressive amyloid burden (7 and 12 months) (Oakley et al., 2006). Here, we show that populations of immune cells trafficking into the brain were altered between Tg and non-Tg mice as a function of age. Peripheral macrophages that have trafficked

into the brain are CD11b⁺ and CD45^{high}. CD45^{high}CD11b⁺ cells historically have been identified solely as peripheral macrophages however microglia, while they are in majority CD45^{Low}, have been shown to be capable of expression CD45 at high levels when activated (Sedgwick et al., 1991). Thus our CD45^{high}CD11b⁺ population was not purely peripheral macrophages but also contained activated microglia and dendritic cells, which also express CD11b and CD45 at high level; neutrophils were gated out of this population using the marker Ly6G (Rose et al., 2012). Within the brain, there was no effect of genotype or age on the number of CD11b⁺CD45^{high} cells (data not shown), however within this population there was a significant decrease in the frequency of CD11b⁺CD45^{high}MHCII⁺ cells in Tg mice as compared to non-Tg at 7 months of age, (non-Tg = $4.240 \pm 0.213\%$, Tg = $2.601 \pm 0.316\%$ by 2-way ANOVA df = 53 t = 5.061 p < 0.0001, **figure 2.1B**). MHCII is used by antigen presenting cells, such as macrophage and microglia of the innate immune system, activate CD4⁺ T cells of the adaptive immune system (Neefjes et al., 2011). In Tg mice, there was a significant increase in the ratio of CD11b⁺Ly6C^{high}:Ly6C^{low} at 5 months in the brain as compared to non-Tg mice, (non-Tg = 0.098 ± 0.004 , Tg = 0.171 ± 0.018 by 2-way ANOVA df = 38 t = 2.722 p < 0.05, **figure 2.1B**).

Immune cells, including T cells, neutrophils, and dendritic cells, will traffic to tissues including the brain to conduct immune surveillance and respond to inflammation (Ransohoff and Brown, 2012; Ransohoff and Engelhardt, 2012). In the brain of Tg and non-Tg mice, there were no significant differences in the frequency or number of neutrophils (CD3⁻Ly6G⁺), B cells (CD3⁻Ly6G⁻CD11b⁻CD19⁺), or dendritic cells (CD3⁻Ly6G⁻CD11b⁺CD11c⁺), (data not shown). At 12 months of age, the frequency of CD3⁺ T cells in all CD45⁺ brain cells was significantly increased in Tg mice as compared to non-Tg mice (non-Tg = $20.822 \pm 2.919\%$ Tg = $34.000 \pm 3.506\%$ by 2-way ANOVA df = 72 t = 3.636 p < 0.01, **figure 2.1C**). Within this population, CD4⁺ and CD8⁺ T

cells were measured (**figure 2.1C**). The number of CD4⁺ T cells was not significantly different between Tg and non-Tg mice, however, at 12 months of age, there was a significant increase in the number of CD8⁺ T cells in the brains of Tg mice as compared to non-Tg mice (non-Tg = 5622.937 ± 1238.101 Tg = 13098.990 ± 2637.522 by 2-way ANOVA df = 67 t = 3.903 p < 0.001, **figure 2.1D**). Within the CD8⁺ T cell population, naïve, effector, and memory subtypes were assessed via expression of CD62L and CD44 expression level. Tg mice show alterations of the CD8⁺ effector (CD62L⁻CD44⁺) T cell population as compared to non-Tg. At 3.5 months of age, there was a significant decrease in the frequency of CD8⁺ effectors (non-Tg = $73.125 \pm 3.744\%$ Tg = $42.978 \pm 14.773\%$ by 2-way ANOVA df = 37 t = 2.692 p < 0.05, **figure 2.1E**), and at 5 months of age, there was a significant increase in the number of CD8⁺ effectors (non-Tg = 3166.673 ± 661.671 Tg = 5604.624 ± 902.898 by 2-way ANOVA df = 36 t = 2.979 p < 0.05, **figure 2.1E**). No significant changes were detected in the other subpopulations of CD8⁺ or CD4⁺ T cells (data not shown).

2.6.3 Altered naïve and effector T cell populations in deep cervical lymph node of Tg mice

No significant differences in the number of CD4⁺ or CD8⁺ T cells were found in the DCLNs or spleen between Tg and non-Tg mice (data not shown). However, within the CD4⁺ and CD8⁺ T cell populations in the DCLN, but not spleen (data not shown), Tg mice showed increased frequency of CD4⁺ and CD8⁺ naïve (CD62L⁺CD44^{low}) T cells, and decreased frequency of effector T cells, at 5 months (CD4⁺ Naïve non-Tg = $55.825 \pm 5.198\%$ Tg = $75.425 \pm 3.123\%$ by 2-way ANOVA df = 29 t = 2.927 p < 0.05, CD4⁺ Effector non-Tg = $36.375 \pm 5.344\%$ Tg = $15.450 \pm 1.023\%$ by 2-way ANOVA df = 28 t = 3.796 p < 0.01, **figure 2.2A**; CD8⁺ Naïve non-Tg = $51.000 \pm 3.143\%$ Tg = $70.025 \pm 2.885\%$ by 2-way ANOVA df = 29 t = 3.123 p < 0.05, CD8⁺ Effector

non-Tg = $38.650 \pm 3.847\%$ Tg = $22.075 \pm 2.893\%$ by 2-way ANOVA df = 28 t = 2.841 p < 0.05, **figure 2.2B**). In the DCLN, CD4⁺ and CD8⁺ T cell subsets shifted with age towards memory phenotypes. Frequency of both central and effector memory CD4⁺ T cells subsets was significantly increased at 12 months in both genotypes from all other time points in both spleen and DCLNs (data not shown). Frequency of central memory CD8⁺ T cells was significantly increased at 12 months in both genotypes from all other time points in both spleen and DCLNs (data not shown). Frequency of effector memory CD8⁺ T cells was significantly decreased in the DCLNs in Tg mice as compared to non-Tg mice at 12 months of age, (non-Tg = $7.598 \pm 0.518\%$ Tg = $4.473 \pm 1.197\%$ by 2-way ANOVA df = 29 t = 3.111 p < 0.05 (data not shown)).

2.6.4 *Inhibition of soluble TNF decreases brain populations of activated CD11b⁺ immune cells and CD4⁺ T cells*

Tg mice were treated with s.c. XPro1595 (10mg/kg) twice weekly for two months starting at 5 months of age or starting at 2 months of age to assess the role of sTNF on AD-like pathology after significant plaque deposition or as plaque deposition begins to build up, respectively. Inhibition of soluble TNF with XPro1595 between 5 and 7 months of age decreased MHCII⁺ microglia/macrophages within both populations of activated microglia/peripheral cells (CD11b⁺CD45^{high}; frequency but not number) and quiescent/homeostatic resident microglia (CD11b⁺CD45^{low}; frequency and number) immune cells (activated/peripheral MHCII⁺: frequency - non-Tg = $5.811 \pm 0.5256\%$ Tg = $3.843 \pm 0.2614\%$ by unpaired T test df = 16 t = 3.352 p < 0.01, number - non-Tg = 1676 ± 186.7 Tg = 1334 ± 174.7 by unpaired T test df = 16 t = 1.331 p = 0.2020; quiescent/homeostatic MHCII⁺: frequency - non-Tg = $4.440 \pm 0.4430\%$ Tg = $2.678 \pm 0.3250\%$ by unpaired T test df = 17 t = 3.252 p < 0.01, number - non-Tg = 1309 ± 233.0 Tg =

744.2 \pm 113.6 by unpaired T test df = 15 t = 2.260 p < 0.05, **figure 2.3A**). While these effects on MHCII⁺ populations were not observed in Tg mice dosed between 2 and 4 months of age, there was an overall decrease in the frequency of CD11b⁺CD45^{high} populations and an increase in CD11b⁺CD45^{low} populations (CD45^{high} - non-Tg = 15.44 \pm 1.633% Tg = 10.53 \pm 1.14% by unpaired T test df = 12 t = 2.293 p < 0.05; CD45^{low} - non-Tg = 84.51 \pm 1.639% Tg = 89.43 \pm 1.147% by unpaired T test df = 12 t = 2.290 p < 0.05, **figure 2.3F**).

Xpro1595 from 5 to 7 months in Tg mice decreased the ratio of Ly6C^{high}:Ly6C^{low} CD11b⁺ immune cells however the individual cell counts of Ly6C^{high} and Ly6C^{low} populations were not significantly different with XPro1595 treatment (Ly6C^{high}:Ly6C^{low} - non-Tg = 0.2133 \pm 0.02147 Tg = 0.1335 \pm 0.02178 by unpaired T test df = 14 t = 2.571 p < 0.05; Ly6C^{high} count - Non-Tg = 822.1 \pm 163.3 Tg = 630.5 \pm 125.5 by unpaired T test df = 14 t = 0.8855, p = n.s., Ly6C^{low} count - non-Tg = 4084 \pm 741.1 Tg = 5921 \pm 1625 by unpaired T test df = 14 t = 1.112 p = n.s., **figure 2.3B**). When mice were dosed between 2 and 4 months of age, there was a trend for a decreased ratio of Ly6C^{high}:Ly6C^{low} of CD11b⁺ immune cells in Tg mice (Ly6C^{high}:Ly6C^{low} - non-Tg = 0.1225 \pm 0.01449 Tg = 0.08311 \pm 0.01334 by unpaired T test df = 12 t = 1.933 p = 0.0772, **figure 2.3G**).

Among the other immune cell populations in the brain, no changes were detected in frequency or number of B cells or neutrophils when XPro1595 was dosed from 5 to 7 months of age in Tg mice (data not shown). Within the dendritic cell population, there was a significant increase in frequency of CD11c⁺ cell population in the brain (CD11b⁺CD11c⁺ Frequency - non-Tg = 10.12 \pm 0.8053% Tg = 16.78 \pm 12.116% by unpaired T test df = 14 t = 3.229 p < 0.001); however, there was no significant increase in cell number (data not shown). When mice were dosed with XPro1595 between 2 and 4 months of age, there was no significant increase in the number or

frequency of CD11c⁺ cells within the CD11b⁺ population (data not shown). Within this population, only when XPro1595 was dosed between 2 and 4 month of age but not when dosed between 5 and 7 months of age, there was a significant decrease in the frequency of a MHCII⁺ populations (CD11b⁺CD11c⁺MHCII⁺ 2-4 months XPro1595: non-Tg = $5.775 \pm 0.7116\%$ Tg = $3.113 \pm 0.2031\%$ by unpaired T test df = 12 t = 3.138 p < 0.01).

In Tg mice treated with XPro1595 from 5 to 7 months, CD3⁺ T cell populations were decreased by XPro1595 treatment in frequency but not in number (CD3⁺ Frequency - non-Tg = $24.64 \pm 1.817\%$ Tg = $18.88 \pm 1.349\%$ by unpaired T test df = 16 t = 2.548 p < 0.05, Count - non-Tg = 14427 ± 1390 Tg = 11963 ± 1829 by unpaired T test df = 17 t = 1.054 p = n.s., **figure 2.3C**). Within the T cell population, inhibition of sTNF did not induce any significant changes within the CD8⁺ T cell population (CD8⁺ T cell count non-Tg = 9333 ± 2233 Tg = 6811 ± 1572 by unpaired T test df = 11 t = 0.9509 p = n.s.; CD8⁺ Effector T cell count non-Tg = 7536 ± 1876 Tg = 4234 ± 786.1 by unpaired T test df = 8 t = 1.623 p = n.s. **figure 2.3E**); however, there was a significant decrease in the number of CD4⁺ T cells and a trend for decreased number of CD4⁺ effector T cells in Tg mice treated with XPro1595 between 5 and 7 months of age (CD4⁺ T cell count - non-Tg = 4244 ± 725.7 Tg = 2369 ± 305.9 by unpaired T test df = 11 t = 2.746 p < 0.05, CD4⁺ Effector T cell Count - non-Tg = 4151 ± 734.9 Tg = 2263 ± 427.5 by unpaired T test df = 8 t = 2.221 p = 0.0571, **figure 2.3D**). Inhibition of sTNF from 2 to 4 months did not produce any significant effects in T cells populations in Tg mice (CD8⁺ T cell count - non-Tg = 3010 ± 508.8 Tg = 7872 ± 3025 by unpaired T test df = 12 t = 1.834 p = n.s., CD4⁺ T cell Count - non-Tg = 1886 ± 308.9 Tg = 2701 ± 238.7 by unpaired T test df = 11 t = 1.862 p = n.s., **figure 2.3H**.)

2.6.5 *Inhibition of soluble TNF increases the naïve T cell populations in the DCLNs of Tg mice*

In mice treated with XPro1595 between 5 and 7 months of age in Tg mice, no significant changes were seen in the number of total CD8⁺ or CD4⁺ T cells in DCLN (CD4⁺ T cell count - non-Tg = 43112 ± 8847 Tg = 100768 ± 29891 by unpaired T test df = 16 t = 1.670 p = n.s. **figure 2.4A**; CD8⁺ T cell Count - non-Tg = 43901 ± 10246 Tg = 71747 ± 17832 by unpaired T test df = 15 t = 1.308 p = n.s., **figure 2.4D**); however, within the CD4⁺ and CD8⁺ populations, there were significant changes in the effector and naïve populations. Within the CD4⁺ T cells, there was a trend for an increase in the frequency and a significant increase in the number of naïve T cells in in XPro1595-treated Tg mice (CD4⁺ naïve Frequency - non-Tg = 46.01 ± 5.005% Tg = 61.00 ± 5.962% by unpaired T test df = 13 t = 1.940 p = n.s.; CD4⁺ naïve Count - non-Tg = 18548 ± 4598 Tg = 73129 ± 23124 by unpaired T test df = 13 t = 2.473 p < 0.05, **figure 2.4B**); however, no significant changes were found in the CD4⁺ effector T cells (CD4⁺ effector Frequency - non-Tg = 42.36 ± 5.331% Tg = 27.46 ± 6.335% by unpaired T test df = 13 t = 1.814 p = n.s.; CD4⁺ effector Count - non-Tg = 17979 ± 4168 Tg = 24819 ± 10240 by unpaired T test df = 16 t = 0.5654 p = n.s., **figure 2.4C**). Within the CD8⁺ T cells, there was a significant increase in the frequency and number of naïve T cells (CD8⁺ naïve Frequency - non-Tg = 46.35 ± 5.793% Tg = 65.76 ± 6.619% by unpaired T test df = 13 t = 2.217 p < 0.05; CD8⁺ naïve Count - non-Tg = 19948 ± 5588 Tg = 80549 ± 28025 by unpaired T test df = 13 t = 2.265 p < 0.05, **figure 2.4E**) and a significant decrease in the frequency, but not number, of effector T cells (CD8⁺ effector Frequency - non-Tg = 42.73 ± 5.339% Tg = 22.07 ± 5.048% by unpaired T test df = 13 t = 2.787 p < 0.05; CD8⁺ effector Count - non-Tg = 18953 ± 5212 Tg = 14172 ± 4231 by unpaired T test df = 12 t = 0.6760 p = n.s., **figure 2.4F**).

When dosed from 2 to 4 months of age, Tg mice showed an increase in the frequency, but not number, of CD8⁺ T cells and decrease in the frequency, but not number, of CD4⁺ T cells (CD8⁺ Frequency - non-Tg = $36.88 \pm 3.110\%$ Tg = $44.69 \pm 1.444\%$ by unpaired T test df = 13 t = 2.169 p < 0.05; CD4⁺ Frequency - non-Tg = $54.91 \pm 2.134\%$ Tg = $47.60 \pm 1.588\%$ by unpaired T test df = 13 t = 2.681 p < 0.05). Within the CD4⁺ T cell population there were no changes in measured subpopulations, however there was a trend for increased frequency of CD8⁺ central memory T cells (CD8⁺ central memory frequency - non-Tg = $4.326 \pm 0.3614\%$ Tg = $6.817 \pm 1.296\%$ by unpaired T test df = 13 t = 1.966 p < 0.05).

2.6.6 Inhibition of soluble TNF decreases amyloid β and cytokine expression in the hippocampus of Tg mice

Inhibition of sTNF significantly decreased the density (% of area) of amyloid- β in the subiculum, but not the entire hippocampus, of Tg mice (Subiculum - Tg Saline = $57.92 \pm 1.736\%$ Tg XPro1595 = $51.49 \pm 0.9899\%$ by unpaired T test df = 6 t = 3.216 p < 0.05; Hippocampus - Tg Saline = $27.67 \pm 1.556\%$ Tg XPro1595 = $26.51 \pm 1.543\%$ by unpaired T test df = 6 t = 0.5296 p = n.s., **figure 2.5A**). Specifically, within the subiculum, there was a significant decrease in amyloid- β density in the dorsal and posterior subiculum (when the dorsal and ventral subiculum come together anatomically) but not the ventral subiculum (Dorsal Subiculum - Tg Saline = $69.83 \pm 2.197\%$ Tg XPro1595 = $63.32 \pm 1.438\%$ by unpaired T test df = 6 t = 2.481 p < 0.05., **figure 2.5A**; Ventral Subiculum - Tg Saline = $37.76 \pm 1.730\%$ Tg XPro1595 = $32.16 \pm 2.951\%$ by unpaired T test df = 6 t = 1.897 p = n.s., **figure 2.5A** ; Posterior Subiculum - Tg Saline = $56.10 \pm 2.159\%$ Tg Xpro1595 = $47.93 \pm 1.178\%$ by unpaired T test df = 6 t = 3.322 p < 0.05, data not shown). No significant changes were seen in the hippocampus or subiculum in the density of amino cupric

silver stain which denotes disintegration of multiple neuronal elements including cell bodies, axons, dendrites, and synaptic terminals (Hippocampus - Tg Saline = $34.52 \pm 1.348\%$ Tg XPro1595 = $31.68 \pm 2.370\%$ by unpaired T test $df = 6$ $t = 1.037$ $p = \text{n.s.}$, **figure 2.5B**; Subiculum - Tg Saline = $60.96 \pm 1.873\%$ Tg XPro1595 = $57.18 \pm 1.816\%$ by unpaired T test $df = 6$ $t = 1.450$ $p = \text{n.s.}$, **figure 2.5B**; Dorsal Subiculum - Tg Saline = $66.11 \pm 1.694\%$ Tg XPro1595 = $62.45 \pm 1.734\%$ by unpaired T test $df = 6$ $t = 1.509$ $p = \text{n.s.}$, **figure 2.5B**; Ventral Subiculum - Tg Saline = $52.72 \pm 3.214\%$ Tg XPro1595 = $46.87 \pm 3.022\%$ by unpaired T test $df = 6$ $t = 1.325$ $p = \text{n.s.}$, **figure 2.5B**; Posterior Subiculum - Tg Saline = $61.49 \pm 1.689\%$ Tg XPro1595 = $57.50 \pm 1.381\%$ by unpaired T test $df = 6$ $t = 1.831$ $p = \text{n.s.}$, data not shown).

When the contralateral hemisphere was used to measure transcriptional changes in gene expression, gene expression associated with an inflammatory response and its resolution was found to be reduced by inhibition of sTNF with XPro1595. TGF β and CCL2 mRNA expression was significantly reduced in Tg mice, but not non-Tg mice, treated with XPro1595 from between 5 and 7 months of age. (CCL2 Tg saline = 6.713 ± 1.170 Tg XPro1595 = 4.055 ± 0.953 by 2-way ANOVA $df = 18$ $t = 2.858$ $p < 0.05$; TGF β Tg saline = 3.255 ± 0.257 Tg XPro1595 = 2.547 ± 0.201 by 2-way ANOVA $df = 18$ $t = 4.624$ $p < 0.01$, **table 2.2, figure 2.5C**).

2.6.7 *XPro1595 blocked LTP deficits in 5xFAD mice*

Deficits in hippocampal CA1 synaptic function have been reported in several mouse models of AD and are associated with cognitive deficits. To determine if *in vivo* peripheral administration of XPro1595 modulates synaptic function in Tg mice, brain slices were harvested for analysis of CA3-CA1 synaptic strength curves (**figure 2.6A-B**) and LTP levels (**figure 2.6F-H**). At four months of age, basal synaptic strength deficits were found to be relatively mild in

vehicle-treated Tg mice, characterized by a modest downward shift in the synaptic strength curve and a significant reduction ($p < 0.05$) in the maximal EPSP/FV ratio, relative to WT vehicle-treated mice (**figure 2.6C**). XPro1595 had minimal effect on synaptic strength (**figure 2.6A-B**), though it did slightly reduce and slightly increase the maximal EPSP/FV ratio in non-Tg and Tg mice, respectively (**figure 2.6C**). No genotype or XPro1595 treatment effects were observed for PPF measures or population spike threshold (**figure 2.6D-E**). LTP was induced in area CA1 using two 100 Hz-stimulus trains (one second duration) separated by 10 seconds. Consistent with PPF measures, post-tetanic EPSP values during the 5-10 min period after 100 Hz stimulation was similar across genotypes, indicating the absence of pre-synaptic deficits in 5xFAD mice at this age. However, relative to vehicle-treated non-Tg mice, the Tg group showed a significant reduction in LTP levels at 60 min post-100 Hz stimulation ($153.3 \pm 9.5\%$ vs $125.3 \pm 5.7\%$, $p < 0.05$) that was blocked by *in vivo* treatment with XPro1595 ($158.2 \pm 5.1\%$, $p < 0.05$ vs Tg vehicle group, **figure 2.6G**). In contrast, XPro1595 had minimal effect on LTP in non-Tg mice ($141.4 \pm 15.7\%$, **figure 2.6H**). Together, these results demonstrate that XPro1595 protects against age-dependent LTP deficits in Tg mice and does not disrupt LTP mechanisms in non-Tg mice.

2.7 Discussion

Chronic inflammation induced by metabolic syndrome and obesity is associated with increased risk for AD and may accelerate disease progression. While chronic anti-inflammatory usage has been associated epidemiologically with lower incidence of AD, global targeting of inflammatory pathways in clinical trials has had limited success in slowing cognitive decline, either because the targets are wrong or the intervention too late (McGeer and McGeer, 2007). Yet, global immunosuppression is not likely to be a viable therapeutic strategy to treat neuroinflammation in

AD. Our data support specific targeting of sTNF/TNFR1 signaling in regulating alterations in immune cell populations associated with AD-like synaptic deficits (**figure 2.7**). Specifically, Tg mice develop an age-dependent pro-inflammatory environment within the brain without evidence of robust CSF or peripheral inflammation; therefore, alterations observed in peripheral immune cells are in response solely to changes in brain inflammation and not additional peripheral inflammatory signals. Immune cells in Tg mouse brain display changes suggestive of altered communication between the innate and adaptive immune system arms. These observed changes appear at different ages suggesting these trafficking populations may play specific roles at specific points during the progression of the AD-like phenotype. As evidenced by a significant decrease in TGF β and CCL2 mRNA in hippocampus, this inflammation is partially mitigated by inhibition of sTNF (**Table 2**). Decreased CCL2 mRNA suggests that recruitment of peripheral immune cells is dampened with inhibition of sTNF. Decreased TGF β mRNA suggests TGF β -dependent regulation of inflammation is no longer occurring with sTNF inhibition. This selective response may be attributed to multiple inflammatory pathways also regulating expression of multiple inflammatory factors. Moreover, A β load in the subiculum and hippocampal LTP impairment are mitigated with *in vivo* treatment of XPro1595 in association with changes in brain and draining DCLNs.

The increase in cytokines in response to ongoing AD-like pathology at 6 and 7 months suggests that peripheral immune cells may be actively recruited to the pro-inflammatory environment of the brain in Tg mice, implicating the peripheral immune system in modulating progression of AD-like pathology. In support of this, studies have shown that the trafficking of peripheral macrophages to the CNS is necessary for mitigating plaque burden (El Khoury et al., 2007). However, a recent study reported that recruitment of peripheral macrophages is not

sufficient to clear accumulated plaque (Varvel et al., 2015). Taken together, these data suggest the CNS resident microglia must be working in concert with peripheral immune cells to combat the accumulation of aggregated A β and in modulating synaptic function.

Within the myeloid compartment of the innate immune system, overall changes in the frequency of CD45^{high}CD11b⁺ cells, a population that contains peripheral immune cells as well as activated microglia, was not increased in Tg mice with age. Here we surveyed total brain populations thus suggesting that while globally there are not changes in the CD45^{high}CD11b⁺ cell population that there may be regional changes that associated with increased pathology or response to experimental treatments. Inhibition of sTNF increased the frequency of CD11b⁺CD11c⁺ population in Tg mice. CD11c is used as a marker of dendritic cells, however a population of CD11b⁺CD11c⁺ cells within the brain parenchyma have been shown to display a microglial, rather than dendritic cells, phenotype based on surface marker expression as well as morphology (Dando et al., 2016). This population has been shown to expand in response to neuroinflammation and while increasing levels of MHCII equivalent to blood derived CD11c⁺ cells, express a different cytokine profile (Wlodarczyk et al., 2014). CD11c⁺ microglia that accumulate around amyloid plaques and increased anti-inflammatory genomic expression as compared to CD11b⁻ microglia (Kamphuis et al., 2016). The increase in CD11b⁺CD11c⁺ cells could thus be interpreted as an increased in CD11c⁺ microglia that perform a specific anti-inflammatory function within the inflamed brain. Our data revealed changes in activation status of recruited cells, high expression of Ly6C correlates with expression of CCR2 and higher capacity for phagocytosis while Ly6C^{low} expression correlates with expression of CX3CR1 and anti-inflammatory actions (Yang et al., 2014). The ratio of Ly6C expression can reveal shifts in the activation status of macrophage populations towards pro-inflammatory, phagocytic activation (higher ratio) or towards alternative

anti-inflammatory activation (lower ratio). Our data indicated the ratio of CD11b⁺Ly6C^{high} to Ly6C^{low} had shifted in Tg mice towards more towards more Ly6C^{high} cells. These changes in Ly6C suggest that the Ly6C⁺CD11b⁺ myeloid cells in the CNS of Tg mice, potentially infiltrating macrophages, may be more active than the infiltrating macrophages in non-Tg CNS. This may be an adaptive response to combat plaque accumulation, however peripheral macrophages from AD patients are less phagocytic as compared to healthy controls (Fiala et al., 2005), suggesting the phagocytic capabilities of these cells may be impeded.

A recent study reported in 5xFADxRAG mice lacking functional T cells, B cells, and some NK cells significantly increased amyloid β load, indicating that the adaptive immune system plays a key role in mitigating AD-like pathology (Marsh et al., 2016). In agreement with others (Bryson and Lynch, 2015), we found increased numbers of T cells in the brains of Tg mice at later stages. Specifically, we found increased CD8⁺ T cells but not CD4⁺ T cells. The frequency of CD8⁺ effector T cells is decreased in Tg mice at 3.5 months, without a change in number of CD8⁺ effector T cells, suggesting subtle changes in CD8⁺ naïve and memory subsets has decreased the proportion of CD8⁺ T cells that are effectors. At the following time point the decrease in CD8⁺ effector T cells is no longer seen in Tg mice, due to a significant increase in the number of CD8⁺ effector T cells. This response may be an adaptive response to the change in frequency seen at the earlier timepoint to return the frequency distribution of CD8⁺ T cell subsets to a homeostatic level seen in non-Tg mice. Cytotoxic CD8⁺ T cells are increased in the AD brain and likely have negative consequences for neuronal function and integrity (Togo et al., 2002). While CD8⁺ effector cells were not decreased in the brain with sTNF inhibition (potentially because the dosed time point is earlier than when we see significant differences in CD8⁺ T cells), the CD3⁺ T cell population was decreased due to a significantly decreased CD4⁺ T cell subpopulation and is likely to be due to a

trend in decreased CD4⁺ effector cells. Effector CD4⁺ T cells functions range from proinflammatory to regulatory, which may have very different consequences on AD-like pathology, specific regulation of T cell subsets has therapeutic potential yet the role of these subsets in AD needs further investigation.

Our findings also shed light on the potential role for antigen presentation in progression of AD-like pathology. Major histocompatibility complex II (MHCII) is used by antigen presenting cells (APCs), such as microglia and macrophage, to activate CD4⁺ T cells in an antigen specific manner. MHCII is important for crosstalk between the innate and adaptive immune systems and for presentation of antigens to activate CD4⁺ T cells (Neefjes et al., 2011). Decreases in MHCII frequency may suggest that cross talk between APCs and T cells is diminished and CD4⁺ T cell activation is decreased. We show that Tg mice have decreased frequency of CD11b⁺CD45^{high}MHCII⁺ brain immune cells. This is contrary to reports of increased MHCII reactivity around plaques in the human AD brain (Perlmutter et al., 1992). It is important to note, however, that animal models do not fully recapitulate human disease and in particular, our data were not derived from the most advanced stages of AD-like pathology in Tg mice. Levels of MHCII⁺ cells in the brain measured by flow cytometry reflect the net levels in the brain and region-specific differences certainly exist which can only be accurately captured using immunohistological approaches. Specifically, it is possible that MHCII⁺ cells are enriched around amyloid plaques while across the brain there may be overall decreases in the total CD11b⁺CD45^{high}MHCII⁺ population. Importantly, across all CD11b⁺ cells, there were no effects of genotype on MHCII expression only within this particular subset of CD45^{high} cells that contains peripheral macrophages as well as activated microglia. Therefore, the decreased MHCII observed in Tg mice suggests that communication and subsequent activation of brain CD4⁺ T cells by

infiltrating macrophages/activated microglia (CD11b⁺CD45^{high}) is impaired; this may or may not be an adaptive response. CD4⁺ T cells can have both pro-inflammatory and protective regulatory effects (Wan and Flavell, 2009). In our study, we found that primarily effector CD4⁺ T cells in the brain, which can be pro-inflammatory or regulatory, were decreased following XPro1595. One subset of CD4⁺ effector T cells, CD4⁺ regulator T cells (Treg), suppressors of immune responses, have been shown to be elevated in elderly populations, and shown to have increased suppressive activity in AD patients (Rosenkranz et al., 2007). In an AD mouse model removal of Treg suppressive effect on the immune system, via transient depletion or inhibition, increased leukocyte trafficking at the choroid plexus, increased brain CD45^{high}CD11b⁺ and Treg populations, as well as decreased plaque burden, pro-inflammatory cytokine mRNA expression, and improved on cognitive function (Baruch et al., 2015). Further investigation may reveal changes within effector CD4⁺ T cells, specifically Tregs, in the brain and will enhance our understanding of how changes in MHCII contribute to or protect against AD-like pathology.

T cells residing in the DCLNs have the opportunity to encounter antigens and other soluble factors draining from the brain. Our data revealed that Tg mice have populations of CD4⁺ and CD8⁺ T cells skewed towards significantly more naïve cells and fewer effector cells within the DCLNs. These T cells may then become primed to carry out their functions in the brain. While there were no significant differences in the overall number of T cells, fewer of these were effector cells in the DCLNs of Tg mice, suggesting they may be elsewhere (i.e. in the blood on route to the brain) or alternatively, that there is impaired crosstalk between the innate and adaptive immune system in Tg mice. The increased population of CD8⁺ effector cells that we see in the brain of Tg mice suggests the former; that these cells are trafficking from the DCLN where they may have first been exposed to brain antigen and have now moved into the brain where they will perform

their effector functions. In Tg mice the frequency of CD4⁺ and CD8⁺ effector T cells is decreased in the DCLNs, without corresponding changes in number of T cell subsets, these results may suggest that the localization of these T cells is altered by plaque pathology. The CD8⁺ effector T cell population is increased in the brain at 5 months of age suggesting that there may be increased trafficking from the DCLNs to the brain in Tg mice. Future studies will explore the soluble factors (including amyloid β) within the DCLNs that may be activating these T cells. With inhibition of sTNF, we observe an increased number of naïve CD4⁺ and CD8⁺ T cells within the DCLN. Despite the fact that we observe no change in the number of effector T cells within the DCLNs following sTNF inhibition, the cells within this population may be changed in function, given that sTNF can act as a regulator of effector T cell activation (Evangelidou et al., 2010). This and other possibilities will be explored in future studies that assess the profile of secreted cytokines along with histological markers of tissue inflammation.

The changes we observed in T cell profiles in the DCLNs and in immune cell profiles in the brain following XPro1595 are most likely due to direct inactivation of sTNF/TNFR1 signaling on immune cells. sTNF is an inflammatory mediator of BBB permeability activating cells along brain capillaries, leading to up-regulation of factors that facilitate immune cell entry across the BBB (Nadeau and Rivest, 1999; Rezai-Zadeh et al., 2009). Regulation of downstream factors of sTNF/TNFR1 signaling, such as Lipocalin 2 (Lcn2), may also be contributing to effects seen by XPro1595. Lcn2 expression is significantly increased in the AD brain, has been shown to impair neuroprotective TNFR2 signaling, and increase A β toxicity (Naude et al., 2012). As a measurement of pathology outcome, we also measured amyloid plaque via IHC. We found a small, yet significant decrease in amyloid (6E10) density indicating that sTNF may play a role in the

production or accumulation of amyloid pathology. Further investigation of the roll of soluble TNF inhibition on the mechanisms of plaque accumulation may be warranted based upon this data.

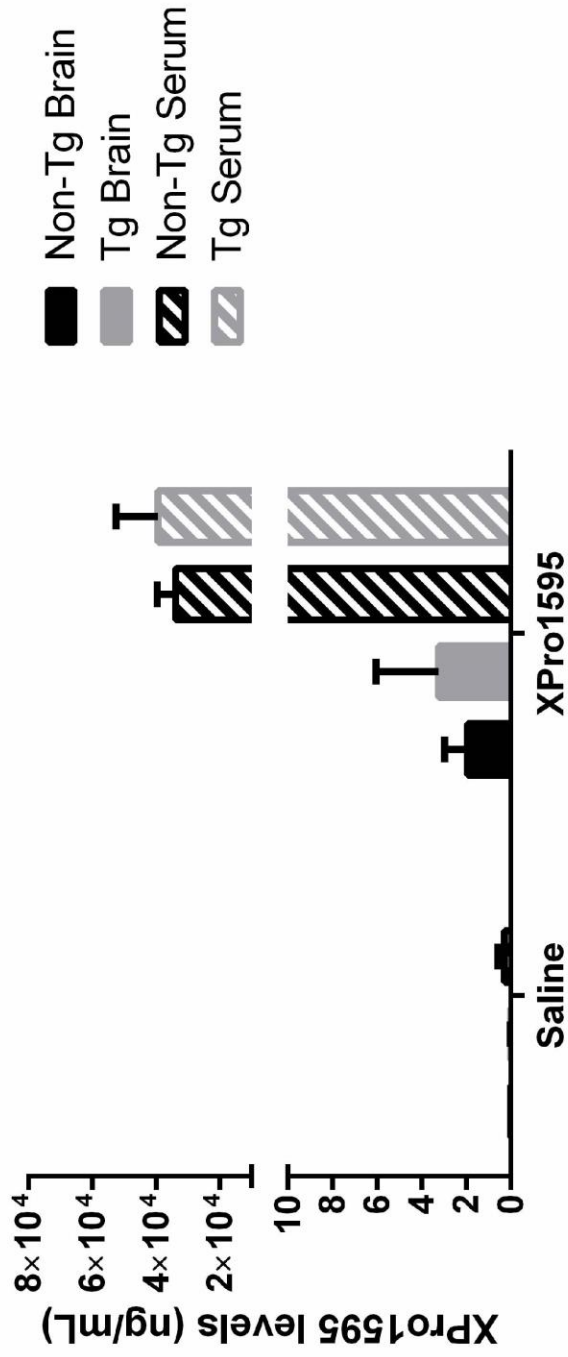
Finally, the most promising finding in our study is the ability of XPro1595 to restore LTP in Tg mice because it is clear that synaptic dysfunction is responsible for memory deficits and cognitive decline in AD. Future studies will be aimed at determining the extent to which the restoration of LTP resulting from sTNF signaling inhibition was due to decreased amyloid deposition in the hippocampus or via direct effect on synaptic physiology. However, given that TNF can inhibit LTP (Cunningham et al., 1996) and that sTNF promotes long-term depression (LTD) in aged rats (Sama et al., 2012), our findings with XPro1595 in 5xFAD mice strongly suggest that sTNF is likely to be directly mediating the LTP deficits in Tg mice. sTNF has been shown to play an important role in potentiating glutamate excitotoxicity, through direction activation of NMDA receptors and increasing AMPA receptor localization at the synapse, while transmembrane TNF/TNFR2 signaling has been implicated in protection against excitotoxicity (McCoy and Tansey, 2008). Inhibition of sTNF via XPro1595 may be modulating these direct mechanisms of sTNF at the synapse as well as modulating BBB permeability and immune cell activation. Further investigation may reveal that modulating these multiple mechanisms of sTNF may be contributing to the overall effects on LTP and immune cell trafficking. Our group has shown that peripherally administered XPro1595 gets across the BBB and is able to sequester the picomolar levels of sTNF within the brain (Barnum et al., 2014); however, a recent clinical study with a non-BBB crossing TNF inhibitor (Embril), implicates a TNF-dependent peripheral mechanisms in the cognitive decline associated with AD pathogenesis (Butchart et al., 2015). Together, these data suggest that TNF can have both direct effects on synaptic physiology as well as indirect effects on peripheral cytokines and immune cell traffic to the CNS and brain-resident

immune cells and thus, targeting sTNF centrally and peripherally may afford added advantage to improve functional outcomes in patients with AD.

2.8 Summary

Here we have shown that peripheral immune cell trafficking to the brain is altered with AD-like pathology and modulated through the inhibition of sTNF signaling. Increase in cytotoxic CD8⁺ T cells as well as peripheral macrophage populations were found in the brain in conjunction with decreased MHCII⁺ frequency on activated myeloid cells, suggesting impaired innate and adaptive cross talk. Evidence of the effect of AD-like pathology was also found within the draining DCLNs of the brain support the hypothesis for peripheral immune cell input on brain immune regulation. Trafficking to the brain in AD-like pathology of CD4⁺ T cells and active macrophages (Ly6C^{high}) cells is dampened with inhibition of sTNF signaling, while levels of CD4⁺ and CD8⁺ naïve T cells are increased in the DCLNs. We also have shown sTNF inhibition rescues impaired LTP in Tg mice suggesting these changes in trafficking patterns to the DCLNs and brain in response to sTNF inhibition are protective against AD-like pathology. While these results are significant and help the field understand the role of sTNF signaling in AD-like pathology and immune cell trafficking patterns, risk for AD has been associated with chronic peripheral inflammation. We found this model does not show signs of peripheral inflammation even at 6 months of age when AD-like pathology is advanced in this model. Thus to elucidate how changes in peripheral immune cell trafficking in populations with increased risk, chronic peripheral inflammation, impact disease progression a 2nd hit model needs to be developed. Understanding how chronic peripheral inflammation impacts disease progression, immune cell traffic and the role

of sTNF will not only increase the field's knowledge of the progression of AD but also the translatable nature of treatments such as XPro1595.



Supplementary figure S1. XPro1595 penetrates into the brain parenchyma when dosed peripherally. 5xFAD non-Tg and Tg mice were dosed with 10mg/kg XP1595 (s.c.) or the normal saline vehicle (s.c.) twice weekly for two months. Levels of human TNF (XPro1595, human TNF monomer) were measured via human TNF multiplexed Immunoassay in both the serum and brain. Levels of XPro1595 in plasma (Non-Tg = 22859.100 ± 5844.518 ng/mL, Tg = 39392.430 ± 13182.00 ng/mL) and in brain (Non-Tg = 1.961 ± 1.020 ng/mL, Tg = 3.248 ± 2.820 ng/mL) are consistent with our previous findings (Barnum et al., 2014), and sufficient to neutralize native mouse TNF, which is present in picomolar levels (Steed et al., 2003).

A

	Age (Month)	Non-Tg			Tg		
		2	4	6	2	4	6
CSF	IFN γ (pg/mL)	N.D.	N.D.	N.D.	N.D.	N.D.	N.D.
	IL-10 (pg/mL)	N.D.	N.D.	0.569 \pm 0.250	N.D.	N.D.	N.D.
	IL-12 p70 (pg/mL)	N.D.	N.D.	N.D.	N.D.	N.D.	N.D.
	IL-1 β (pg/mL)	N.D.	N.D.	2.505 \pm 0.095	N.D.	0.837 \pm 0.433	N.D.
	IL-6 (pg/mL)	N.D.	N.D.	N.D.	N.D.	N.D.	N.D.
	TNF (pg/mL)	N.D.	1.019 \pm 0.436	4.391 \pm 1.232	2.832 \pm 2.537	2.300 \pm 1.280	2.100 \pm 0.620
	mKC/CXCL1 (pg/mL)	6.905 \pm 0.745	3.122 \pm 0.671	7.962 \pm 0.438	4.068 \pm 0.912	N.D.	4.303 \pm 1.481 *

B

	Age (Month)	Non-Tg			Tg		
		2	4	6	2	4	6
qPCR	TNF (Midbrain)	0.969 \pm 0.159	1.098 \pm 0.142	1.21 \pm 0.147	1.452 \pm 0.302	1.107 \pm 0.129	3.325 \pm 0.731 *
	CD45 (Midbrain)	1.016 \pm 0.050	1.123 \pm 0.062	1.122 \pm 0.074	1.229 \pm 0.116	1.676 \pm 0.180	3.276 \pm 0.586 ****
	CCL2 (Midbrain)	1.167 \pm 0.250	1.091 \pm 0.153	0.946 \pm 0.186	1.203 \pm 0.347	1.186 \pm 0.175	1.71 \pm 0.339
	TNF (Cortex)	1.104 \pm 0.133	1.199 \pm 0.252	1.433 \pm 0.139	1.372 \pm 0.231	1.026 \pm 0.076	1.922 \pm 0.328
	CD45 (Cortex)	1.026 \pm 0.066	1.214 \pm 0.101	1.188 \pm 0.138	1.005 \pm 0.115	1.307 \pm 0.153	2.901 \pm 0.415 ****
	CCL2 (Cortex)	1.158 \pm 0.211	1.252 \pm 0.168	1.13 \pm 0.155	0.9413 \pm 0.207	1.054 \pm 0.163	1.351 \pm 0.410

Table 2.1. Increased expression of inflammatory cytokines in the brain of Tg mice without evidence of inflammation in the CSF. **A)** CSF cytokine levels from Tg and non-Tg mice at 2, 4 and 6 months of age. N.D. = not detected. * $p < 0.05$ Significant from non-Tg within Age group. Statistical analysis: non-parametric t-test within age across genotype. **B)** Brain inflammatory factor mRNA expression from Tg and non-Tg mice at 2, 4, and 6 months of age. Data is show as fold change in expression from 2-month-old non-Tg. * $p < 0.05$ **** $p < 0.0001$ Significant from non-Tg within the same age group. Statistical analysis: data was normalized to 2-month-old non-Tg and were compared across genotypes and age with two-way analysis of variance (ANOVA).

qPCR	Non-Tg				Tg	
	Target	Saline	XPro1595	Saline	XPro1595	
	CD45	1.025 ± 0.084	0.9319 ± 0.091	5.218 ± 0.766	4.382 ± 0.594	
TNF	1.103 ± 0.182	0.789 ± 0.079	5.390 ± 1.150	3.672 ± 0.626		
CCL2	1.126 ± 0.217	0.741 ± 0.079	6.713 ± 1.170	4.055 ± 0.953 *		
TNFR1	1.018 ± 0.074	0.874 ± 0.079	1.830 ± 0.173	1.885 ± 0.270		
TNFR2	1.004 ± 0.053	0.936 ± 0.067	2.269 ± 0.322	2.101 ± 0.241		
IL-1β	1.011 ± 0.087	0.733 ± 0.069	2.723 ± 0.451	1.941 ± 0.808		
IFNγR	1.030 ± 0.093	0.989 ± 0.071	1.789 ± 0.072	1.473 ± 0.176		
TGFβ	1.015 ± 0.065	1.004 ± 0.069	3.255 ± 0.257	2.547 ± 0.201 **		

Table 2.2. Inhibition of sTNF partially mitigates inflammatory profile in Tg mice.

Hippocampal mRNA expression of inflammatory factors, from Tg and non-Tg mice dose from 5 to 7 months with either XPro1595 or saline. Shown as fold change in expression from non-Tg Saline treated mice, * $p < 0.05$ ** $p < 0.01$ Significant from saline treated group within genotype. Statistical analysis: data was normalized to non-tg saline and analyzed across genotypes and drug treatment conditions with two-way analysis of variance (ANOVA). Sidak's multiple comparisons test was used for *post hoc* comparisons within genotype.

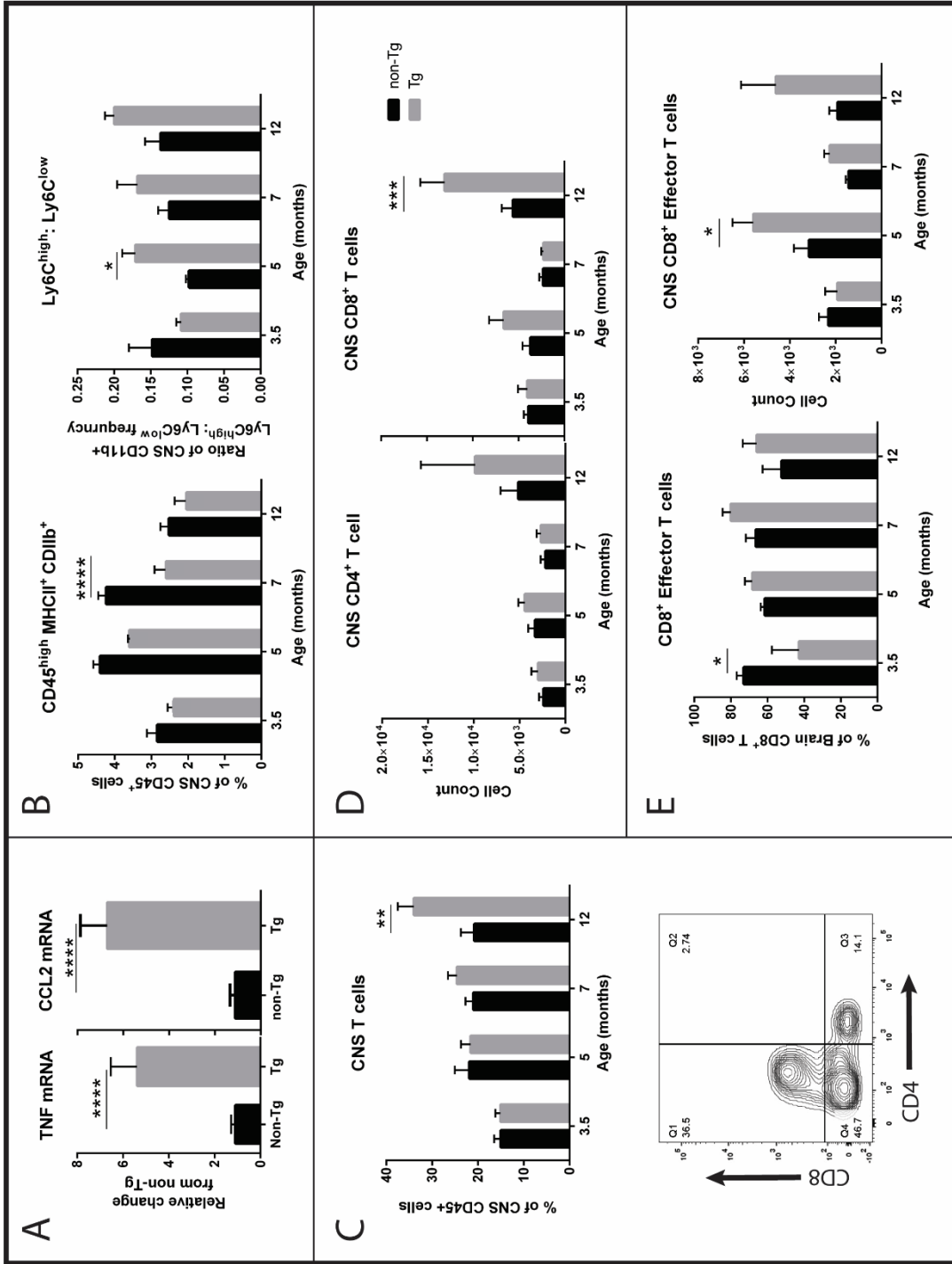


Figure 2.1. Altered peripheral immune cell populations in the pro-inflammatory AD-like brain environment. **A)** Graphical depiction of select results from Table 2. At 7 months of age CCL2 and TNF mRNA expression is significantly increased in the hippocampus of Tg mice as compared to non-Tg mice. By flow cytometry, populations of immune cells within the brain were measured at 3.5, 5, 7, and 12 months of age in non-Tg and Tg mice. **B)** While there are no effects of genotype on frequency or number of CD11b⁺ (microglia and macrophage) or CD11b⁺CD45^{high} (peripheral macrophage and activated microglia) immune cells (data not shown), there is a significant decrease in the frequency of MHCII⁺CD45^{high}CD11b⁺ cells in the brain of Tg mice compared to that in non-Tg mice at 7 months of age, ****p < 0.0001. At 5 months of age the ratio of Ly6C^{high}:Ly6C^{low} is significantly increased as compared to non-Tg mice * p < 0.05. **C)** At 12 months of age the frequency of CD3⁺ T cells is significantly increased in Tg mice as compared to non-Tg mice, ** p < 0.01. Contour plot inset shows CD4 and CD8 gating on the brain CD3⁺ T cell population. Within this population, subsets of CD4⁺ and CD8⁺ T cells were measured. **D)** In both non-Tg and Tg mice, the number of CD4⁺ T cells increases within the CNS with age. No effects were seen within the CD4⁺ T cell population. In Tg mice there was a significant increase in the number of CD8⁺ T cells within the CNS at 12 months of age, ***p < 0.001. **E)** Within the CD8⁺ T cell population, there is a significant decrease in the frequency of CD8⁺ effector T cell (CD62L⁻CD44⁻) population in Tg mice as compared to non-Tg mice at 3.5 months of age. By 5 months of age, the frequency of CD8⁺ effector cells has increased in Tg mice to non-Tg levels. At this same time point, there is a significant increase in the number of CD8⁺ effector T cells within the brain that can account for this return to non-Tg frequency levels, * p < 0.05. 3.5 months: non-Tg n = 8, Tg n = 9; 5 months: non-Tg n = 11, Tg n = 11; 7 months: non-Tg n = 11, Tg n = 13; 12 months: non-Tg n = 10, Tg n = 9. Within these groups, subsets with robust MHCII and Ly6C

staining were used for analysis of these markers in the brain: 3.5 months: non-Tg n= 8 (MHCII)/5 (Ly6C), Tg n = 9/4; 5 months: non-Tg n = 4/7, Tg n = 7/8; 7 months: non-Tg n = 8/6, Tg n = 11/7; 12 months: non-Tg n = 9/10, Tg n = 8/4. From the overall group, a subset of samples had reliable CD44 and CD62L staining and were used for analyses of those markers in brain 3.5 months non-Tg n = 5, Tg n = 3; 5 months: non-Tg n = 4, Tg n = 4; 7 months: non-Tg n = 5, Tg n = 5; 12 months: non-Tg n = 6, Tg n = 4 Data was analyzed across genotypes and age with two-way analysis of variance (ANOVA). Sidak's multiple comparisons test was used for *post hoc* comparisons within each age.

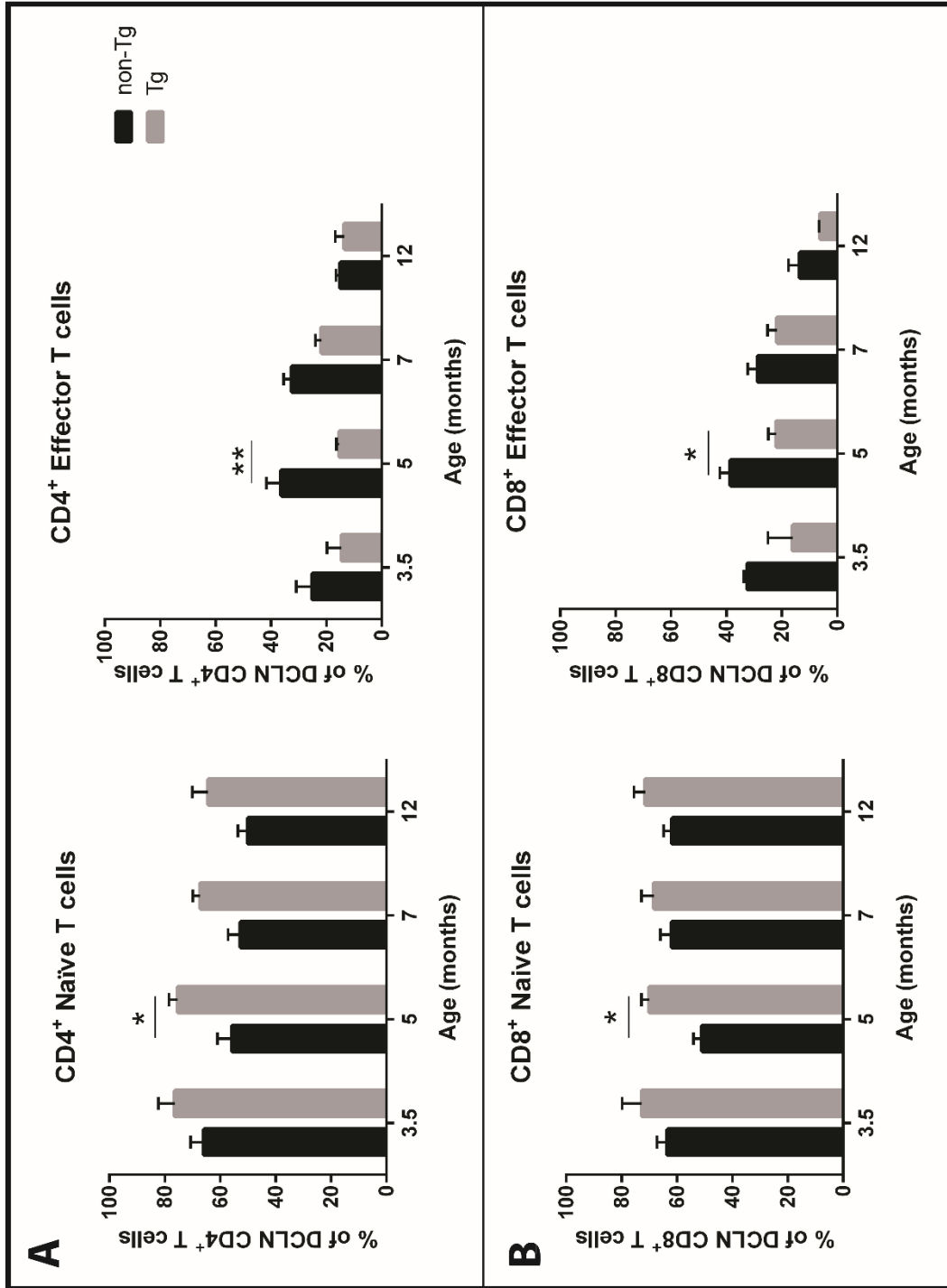


Figure 2.2. Altered naïve and effector T cell populations in deep cervical lymph nodes of 5xFAD mice. While there are no significant differences in DCLN in the number of CD4⁺ or CD8⁺ T cells (data not shown), there are significant changes within the CD4⁺ and CD8⁺ T cell populations. **A)** Tg mice show increased frequency of CD4⁺ naïve T cells, and decreased frequency of CD4⁺ effector T cells, significant difference at 5 months. DCLN CD4⁺ T cell subsets shift, with age, towards memory phenotypes. Frequency of both central and effector memory CD4⁺ T cell subsets are significantly increased at 12 months from 3.5, 5 and 7 months, significant effect of age, no effect of genotype (data not shown). **B)** Tg mice show increased frequency of CD8⁺ naïve T cells, and decreased frequency of CD8⁺ Effector T cells, significant difference at 5 months. DCLN CD8⁺ T cell subsets shift, with age, towards memory phenotypes. Frequency of central memory CD8⁺ T cells are significantly increased at 12 months from 3.5, 5 and 7 months, significant effect of age, no effect of genotype (data not shown). Frequency of effector memory CD8⁺ T cells are significantly increased in non-Tg mice as compared to Tg mice at 12 months of age, significant effect of age and of genotype (data not shown). 3.5 months: non-Tg n = 8, Tg n = 9; 5 months: non-Tg n = 11, Tg n = 11; 7 months: non-Tg n = 11, Tg n = 13; 12 months: non-Tg n = 10, Tg n = 9. Within these groups a subset of samples had reliable CD44 and CD62L staining and were used for analyses of those markers in DCLNs: 3.5 months non-Tg n = 5, Tg n = 3; 5 months: non-Tg n = 4, Tg n = 4; 7 months: non-Tg n = 5, Tg n = 5; 12 months: non-Tg n = 6, Tg n = 4 Data was analyzed across genotypes and age with two-way analysis of variance (ANOVA). Sidak's multiple comparisons test was used for *post hoc* comparisons within each age.

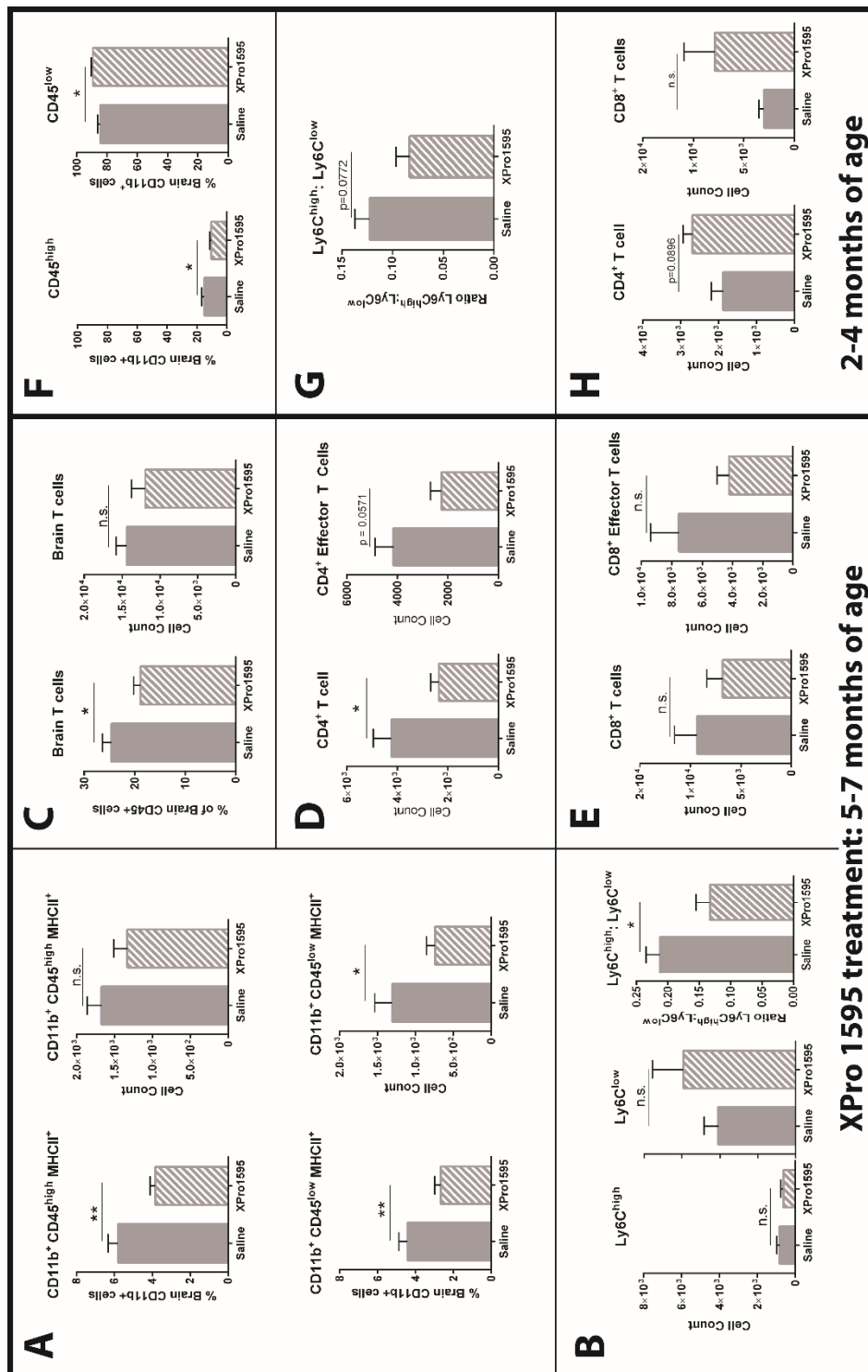


Figure 2.3. Inhibition of soluble TNF with XPro1595 decreases populations of activated CD11b⁺ immune cells and CD4⁺ T cells in the brain of 5xFAD mice. Tg and non-Tg mice were treated with XPro1595 (10mg/kg s.c.) twice weekly for two months either from 5-7 months of age (**A-E**) or 2-4 months of age (**F-H**). **A)** Inhibition of soluble TNF with XPro1595 decreased MHCII⁺ populations within both activated (CD11b⁺ CD45^{high}; frequency but not number) and quiescent (CD11b⁺CD45^{low}; frequency and number) immune cell populations, **p<0.01; * p < 0.05. **B)** Ly6C, a marker of peripheral monocytes, displayed alterations with inhibition of soluble TNF. The ratio of Ly6C^{high}:Ly6C^{low}CD11b⁺ brain immune cells in Tg mice is decreased, * p < 0.05. **C)** Brain T cells are decreased in frequency, but not number, with inhibition of soluble TNF, * p < 0.05. **D)** Within the T cell population, the number of CD4⁺ T cells is decreased with inhibition of soluble TNF with a trend towards decreased CD4⁺ effector T cells, * p < 0.05. **E)** There are no effects of soluble TNF inhibition on the CD8⁺ T cell population. **F)** Inhibition of soluble TNF from 2-4 months of age decreased the activated (CD45^{high}) population and increased the quiescent (CD45^{low}) population, * p < 0.05. **G)** There is a trend towards a decreased ratio of Ly6C^{high}:Ly6C^{low}CD11b⁺ brain immune cells in Tg mice dosed from 2-4 months. **H)** No significant effects are seen in T cell populations at this age. Statistical analysis: significance was determined across treatment using non-parametric T test.

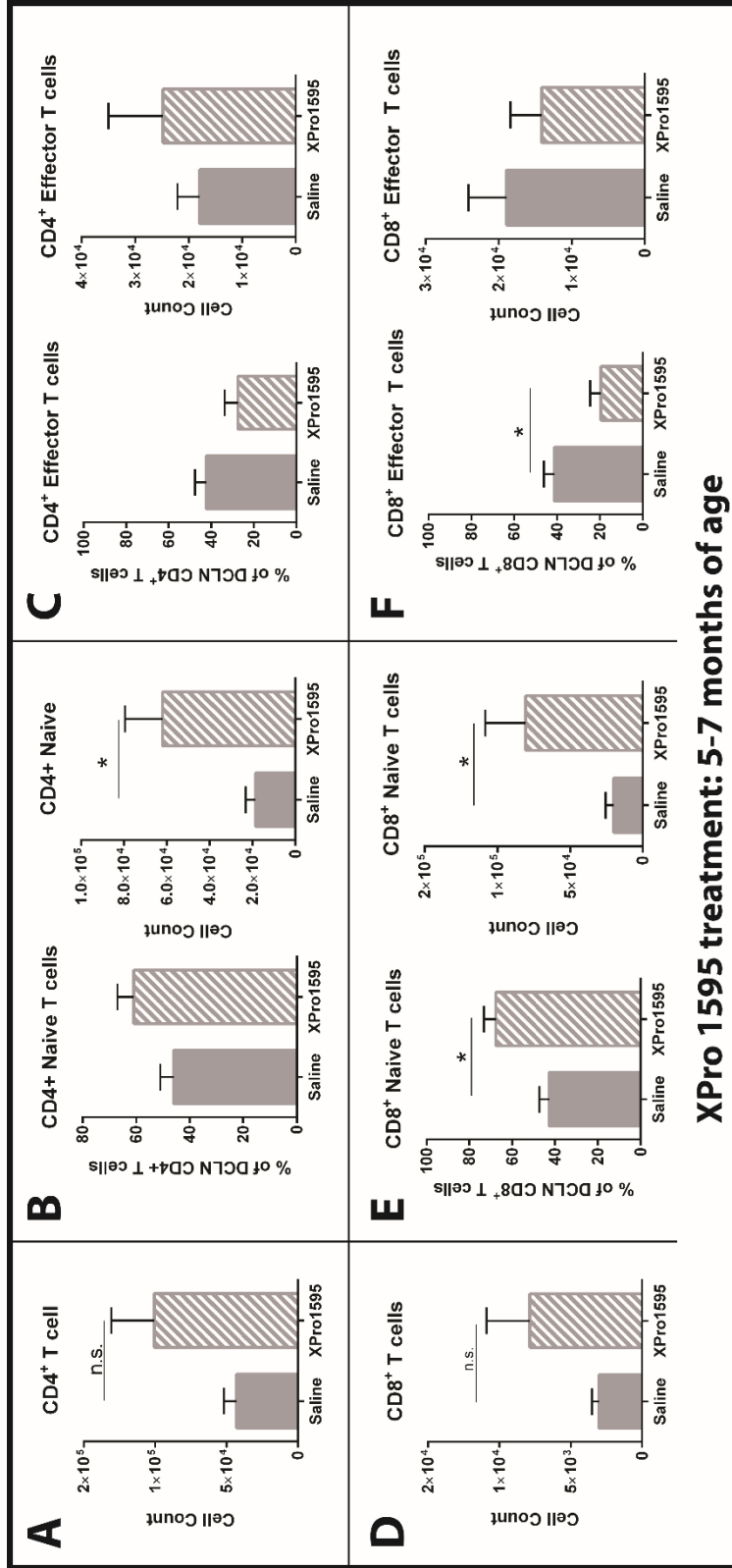


Figure 2.4. Inhibition of soluble TNF with XPro1595 increases the naïve T cell population in the deep cervical lymph nodes (DCLNs) of 5xFAD mice. There is no significant difference in the frequency or number of CD8⁺ (**D**) or CD4⁺ (**A**) T cells within the DCLC following XPro1595 or saline treatment within genotype. **B**) Within the CD4⁺ T cell niche, the number but not frequency of naïve T cells is increased in Tg mice following inhibition of soluble TNF with XPro1595 as compared to saline treated Tg mice, * $p < 0.05$. **C**) The frequency of CD4⁺ effector T cells is unchanged in Tg mice following inhibition of soluble TNF with XPro1595 as compared to saline-treated Tg mice. No effects are seen on population cell counts or within the CD4⁺ central memory or effector memory populations. **E**) Within the CD8⁺ T cell niche, the frequency and count of naïve T cells is increased in Tg mice following inhibition of soluble TNF with XPro1595 as compared to saline treated Tg mice, * $p < 0.05$. **F**) The frequency but not count of effector T cells is decreased in Tg mice following inhibition of soluble TNF with XPro1595 as compared to saline treated Tg mice, * $p < 0.05$. No effects are seen on population cell counts or on the CD8⁺ central memory populations. Statistical analysis: significance was determined across treatment using non-parametric T test.

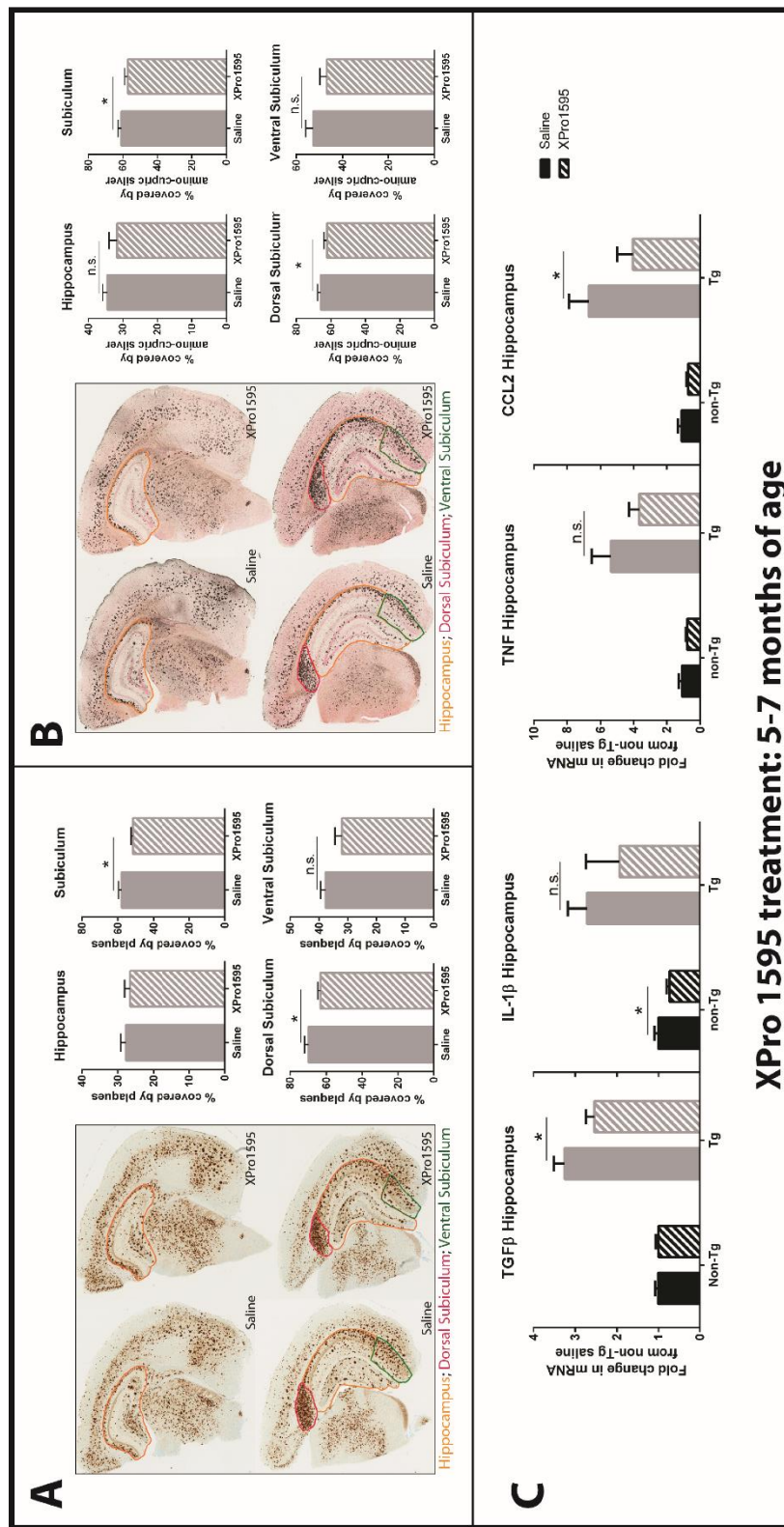


Figure 2.5. Inhibition of soluble TNF with XPro1595 decreases amyloid beta in the subiculum and decreases pro-inflammatory mRNA in the hippocampus of 5xFAD mice. Amyloid- β (6E10) (**A**) and disintegrative degeneration (measured by Amino Cupric Silver staining, NeuroScience Associates) (**B**) density was calculated in the hippocampus (yellow) and subiculum (dorsal: magenta; and ventral: green; posterior (when dorsal and ventral join): not shown) in saline- and XPro1595-treated Tg animals. **A**) No effect of soluble TNF inhibition was detected in the hippocampus; however, within the subiculum there was a significant reduction in amyloid burden specifically within the dorsal subiculum, * $p < 0.5$ **B**) No significant effects for soluble TNF inhibition were detectable in amino-cupric silver staining measuring disintegration of multiple neuronal elements including cell bodies, axons, dendrites, and synaptic terminals in either hippocampus or subiculum. **C**) Inhibition of soluble TNF decreases the expression of pro-inflammatory genes in Tg and non-Tg mice. CCL2 and TFG β are significantly decreased in Tg mice, * $p < 0.05$. Statistical analysis: IHC data significance was determined across treatment using non-parametric T test. qPCR mRNA data was normalized to non-tg saline and analyzed across genotypes and drug treatment conditions with two-way analysis of variance (ANOVA). Sidak's multiple comparisons test was used for *post hoc* comparisons within genotype.

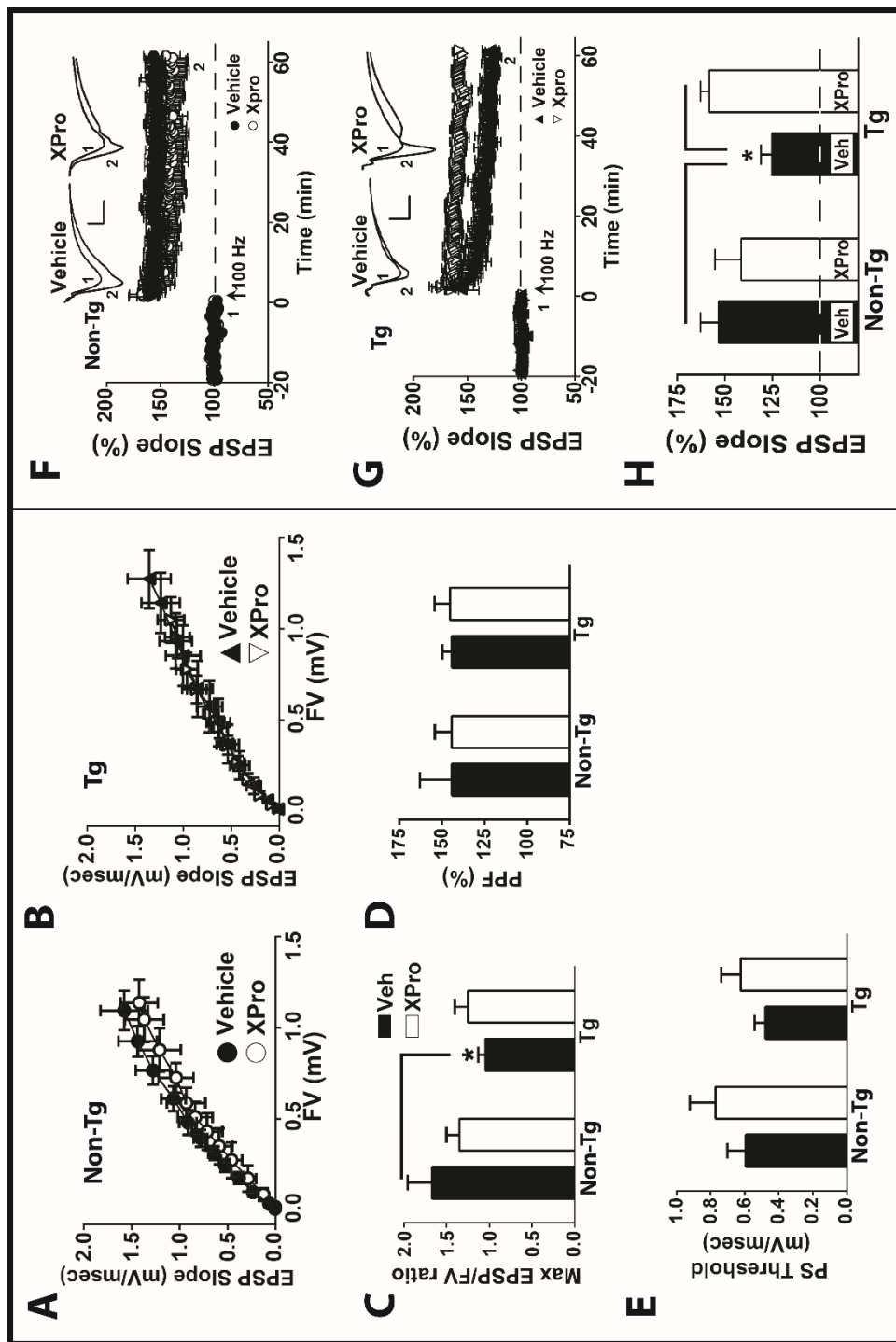
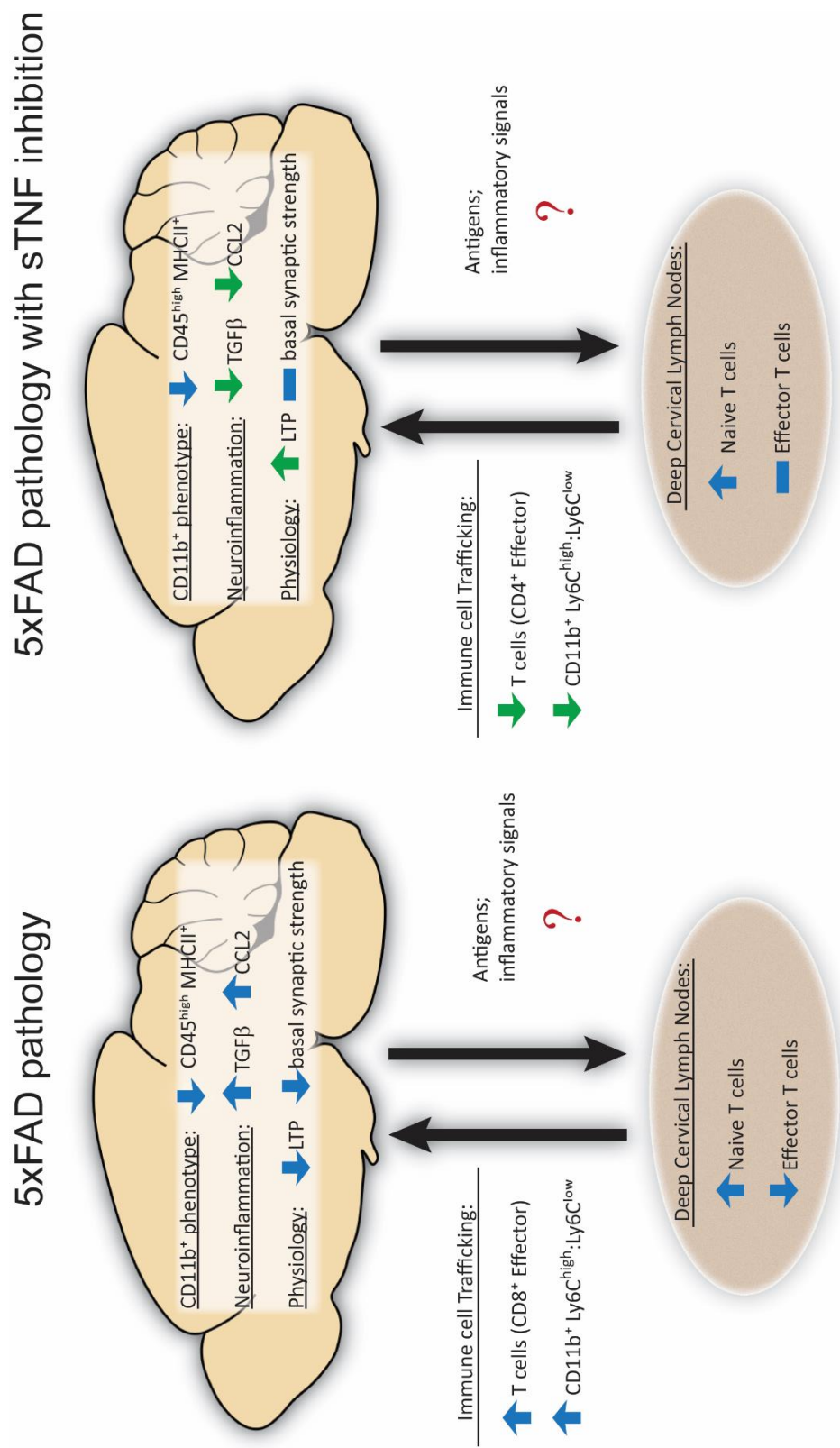


Figure 2.6. Inhibition of soluble TNF with peripheral XPro1595 administration *in vivo* rescued LTP impairment in 5xFAD mice. To determine if peripheral administration of XPro1595 modulates synaptic function in Tg mice, brain slices were harvested for analysis of CA3-CA1 synaptic strength curves (**A** (non-Tg); **B** (Tg)) and LTP levels (**F** (non-Tg); **G** (Tg)). At four months of age, basal synaptic strength deficits were relatively mild in saline-treated Tg mice, characterized by a modest downward shift in the synaptic strength curve and a significant reduction ($p < 0.05$) in the maximal EPSP/FV ratio, relative to non-Tg vehicle-treated mice (**C**). XPro1595 had minimal effect on synaptic strength (**A** (non-Tg); **B** (Tg)), but it did slightly reduce and slightly increase the maximal EPSP/FV ratio in non-Tg and Tg mice, respectively (**C**). No genotype or XPro1595 treatment effects were observed for PPF measures (**D**) or population spike threshold (**E**). XPro1595 had more favorable effects for LTP deficits in Tg mice. LTP was induced in area CA1 using two 100 Hz stimulus trains (one second duration) separated by 10 seconds. Relative to vehicle-treated non-Tg mice, the Tg group showed a significant reduction in LTP levels ($153.3 \pm 9.5\%$ vs $125.3 \pm 5.7\%$, $p < 0.05$) that was prevented by *in vivo* treatment with XPro1595 ($158.2 \pm 5.1\%$, $p < 0.05$ vs 5xFAD vehicle group). In contrast, XPro1595 had minimal effect on LTP in non-Tg mice ($141.4 \pm 15.7\%$, **H**). Together, the results demonstrate that XPro1595 protects against LTP deficits in Tg mice. Synaptic strength parameters and LTP values were compared across genotypes and drug treatment conditions with two-way analysis of variance (ANOVA), Fisher's PLSD was used for *post hoc* comparisons.



5xFAD pathology with sTNF inhibition

Figure 2.7. Specific targeting of sTNF/TNFR1 signaling rescues AD-like synaptic deficits and modulates AD-like associated immune cell population alterations. As Tg mice age, the brain becomes an inflamed environment with altered regulation of immune cell activation and peripheral immune cell trafficking to the CNS. While no evidence of peripheral inflammation is evident in plasma, there is evidence of altered T cell retention in the deep cervical lymph nodes to Tg mice, suggesting that the pro-inflammatory environment or potentially increased antigen presence is modulating peripheral immune cell populations. *In vivo* administration of peripheral XPro1595 to neutralize sTNF rescues LTP deficits and decreases amyloid (6e10) reactivity in the brain. These effects are associated with alterations in the brain inflammatory environment and immune cell traffic to the brain. In addition, XPro1595-treated group show further decrease in populations of activated CD11b⁺ immune cells as well as a decrease in CD4⁺ T cells suggesting these may be adaptive immune responses to the ongoing AD-like pathology.

Chapter 3:

The role of high caloric diet on central and peripheral inflammation and immune cell profiles

3.1 Context, Author's Contribution, and Acknowledgement of Reproduction

The following chapter presents evidence that peripheral inflammation alters not only peripheral blood mononuclear cell (PBMC) population frequency but also the frequency in which they traffic to the brain in response to chronic peripheral inflammation. In conjunction with these altered trafficking patterns, we show evidence to support impaired neuroinflammatory responses following chronic peripheral inflammation. The dissertation author contributed to the chapter by designing and conducting the majority of the experiments, analyzing data, and writing the manuscript under the guidance of Dr. Malú G Tansey.

3.2 Abstract

Studies have linked peripheral inflammation to cognitive decline and increased risk for neurodegenerative diseases, including Alzheimer's disease (AD). Obesity and metabolic syndrome, in particular, are associated with low-grade peripheral inflammation and increased risk for AD. Peripheral inflammation may accelerate neurodegenerative disease by increasing neuroinflammation, altering blood-brain barrier (BBB) integrity, and altering peripheral immune cell trafficking to the CNS. We aim to determine the role of peripheral macrophages and other peripheral immune cell populations in the chronic effects of high-fat high-fructose (HFHF) diet-induced peripheral inflammation on neuroinflammation and neuronal health in a model of AD. C567Bl/6J, male and female, mice were used to assess the effect of 5 weeks of HFHF diet-induced peripheral inflammation on populations of peripheral immune cells that have been shown to traffic to the brain in conditions of neurodegenerative disease. While effects of diet were found within myeloid populations of both male and female mice, male mice showed more changes as compared

to female mice, suggesting female PBMC populations are more resilient to diet induced changes. Peripheral myeloid Ly6C⁺ macrophages were shown to traffic into the brain in response to HFHF diet-induced peripheral inflammation in aged mice, dependent on CCR2 expression, suggesting this population may be a contributor to diet-induced neuroinflammation. Using the 5xFAD mouse crossed to TGF β -Luciferase reporter mice (SBE) we were able to define the kinetics of neuroinflammation associated with HFHF diet-induced peripheral inflammation through bioluminescence imaging (BLI) and confirm female resilience to diet-induced PBMC changes. Our data demonstrated that 8 weeks of HFHF diet suppresses TGF β signaling in the brain, and while there is no compound effect of HFHF diet and AD-like pathology that AD-like pathology alone suppresses the overall TGF β response, which is generally believed to be anti-inflammatory.

3.3 Introduction

Until recently, monocyte-derived peripheral macrophage populations were thought to traffic to the brain and set up residence in the perivascular and subarachnoid spaces as well as the choroid plexus until they became microglia-like populations in the brain (Hickey and Kimura, 1988; Prinz et al., 2011b). Recent evidence has shifted our understanding of the origin and longevity of these macrophage populations under homeostatic conditions. Perivascular and subarachnoid macrophages have recently been shown to derive from early embryonic populations and migrate to the brain where they are long lived, whereas choroid plexus macrophages are short lived and repopulated by peripheral monocyte populations (Goldmann et al., 2016). Populations of perivascular and subarachnoid macrophages that are long lived may also have alternative responses to inflammatory insult, more similar to microglial responses, than short lived peripheral monocyte/macrophage populations. Understanding the origin of these cells is the first step to

understanding how they contribute to the regulation of brain health and regulation of peripheral immune cell traffic. However, it remains unclear when during the course of neuroinflammatory disease peripheral immune cells traffic to the brain and their effect on disease development and progression. Evidence, from both patients and animal models, suggest that at terminal stages of neuroinflammatory diseases, such as Alzheimer's disease (AD), populations of peripheral immune cells are present within the parenchyma (Togo, 2002; Rezai-Zadeh et al., 2009). Our group has recently shown that trafficking patterns of different populations of peripheral immune cells to the CNS have varying time courses that could indicate adaptive as well as maladaptive responses that can contribute to chronic neuroinflammation. Our preliminary work suggests that sTNF signaling plays a role in modulating these trafficking patterns, raising the distinct possibility that sTNF may have a critical role in driving mechanisms of peripheral inflammation that modulate disease progression.

There is mounting evidence that peripheral inflammation is linked to increased risk for developing neurodegenerative disease, such as AD. Increased levels of cytokines, including TNF, have been shown to accelerate cognitive decline and convergence from mild cognitive impairment (MCI) to AD (Holmes et al., 2003; Holmes et al., 2009). Conditions associated with low-grade chronic peripheral inflammation, such as metabolic syndrome, insulin resistance, diabetes, and obesity, commonly associated with poor diet, have all been linked to increased risk for AD (Ojo and Brooke, 2015; Walker and Harrison, 2015). Recently an emphasis has been placed on identifying early life risks and biomarkers likely to contribute to development of AD in order to identify at-risk individual and opportunities for disease prevention. It is estimated that over 34% of Americans over age 20 have metabolic syndrome, defined as abdominal obesity with a combination of high triglycerides, lipoprotein, blood pressure or fasting glucose levels (Yates et

al., 2012). Human studies of both adolescents and adults have linked metabolic syndrome and insulin resistance to decreased executive function and declarative memory, while animal studies have linked obesity and high-fat diet to increased amyloid β levels (Yates et al., 2012; Radler et al., 2015). Insulin receptors, expressed in regions important for learning and memory, have been shown to play a role in hippocampal long-term potentiation and are inhibited by TNF receptor activation and A β (Walker and Harrison, 2015). Consumption of high-fat diet has been shown to induce chronic-low grade systemic inflammation and deficits in cognition, as well as an increase in gram-negative gut bacteria, which is linked to increased proinflammatory cytokine production, disruption of gut epithelium integrity, and systemic inflammation (Proctor et al., 2016). Peripheral dosing of lipopolysaccharide (LPS), from gram-negative bacteria, the proinflammatory cytokine TNF, and high-fat diet have all individually been shown to increase blood-brain barrier (BBB) leakiness and microglia activation (Nadeau and Rivest, 1999; Cunningham et al., 2009; Kanoski et al., 2010). Changes in regulation of peripheral immune cell traffic due to leaky BBB may be a contributor to diet-induced neuroinflammation and acceleration of AD-like pathology. How these low-grade chronic inflammatory conditions contribute to increased AD risk, potentially through alteration in trafficking patterns of peripheral immune cells to the brain, is not well understood. Conditions associated with consumption of poor diet may therefore represent an opportunity for early intervention through modulation of inflammatory mechanisms.

Our group has recently demonstrated that a HFHF diet disrupts inflammatory gene networks in the brain, liver and gut and promotes behavioral deficits in rodents (de Sousa Rodrigues et al., 2016). We hypothesize that soluble TNF (sTNF) is a key cytokine driving these processes; however, cytokine signaling is only one method by which the peripheral immune system impacts the CNS. Here we aim to establish the effects of peripheral inflammation induced

by diet or low-dose LPS on brain neuroinflammation kinetics. We also seek to investigate the relative contributions of trafficking peripheral monocyte immune cell populations in mediating the effects of diet-induced neuroinflammation. We assess these effects using a model of diet-induced low-grade chronic peripheral inflammation to promote neuroinflammation, through changes in peripheral immune cell phenotype, specifically increases Ly6C⁺ and MHCII⁺ peripheral monocyte populations. Our data shows that the peripheral inflammation induced by either low dose LPS or HFHF diet altered PBMC phenotypes differently between male and female mice, as well as altered peripheral immune cell trafficking to the brain. We show that Ly6C⁺ macrophages traffic to the brain in a CCR2-dependent manner following HFHF diet. Chronic low-grade diet-induced peripheral inflammation as well as AD-like pathology was shown to alter the kinetics of the TFGβ inflammatory response within the brain.

3.4 Methods

3.4.1 *Animals*

Male and female CD57BL/6J (B6) mice were ordered from the Jackson Laboratory at 7 weeks of age and left to acclimate for 1 week before starting on either HFHF (n=8 per sex) or CD (n=8 per sex), mice were randomly assigned to treatment group. CCR2-RFP mice were bred in house to generate CCR2 WT/WT (WT), CCR2-RFP/WT (HET), CCR2-RFP/RFP (KO) mice. Mice were randomly assigned to treatment group based on genotype. Male and female mice were aged to 11.5 months of age before starting on either high-fat high-fructose diet (HFHF), or control diet (CD): CD WT 7(2M/5F), HET 11(6M/5F), KO 5(2M/3F); HFHF WT 3(1M/2F), HET 12(5M/7F), KO 8(4M/4F). The 5xFAD (Tg) mouse that displays key pathological hallmarks of

AD including synaptic dysfunction, plaque accumulations, and neuronal degeneration (Oakley et al., 2006), was crossed with the TGF β -Luciferase reporter mouse, also known as the SBE-Luc mouse, (developed by the Wyss-Cory laboratory (Luo and Wyss-Coray, 2009) to study the role of TGF β -dependent signaling pathway), to generate compound male and female 5xFAD; TGF β -Luc reporter (5xSBE) mice for bioluminescence imaging (BLI). 5xFAD Tg; TGF β -Luc reporter (5xSBE Tg) and 5xFAD Non-Tg; TGF β -Luc reporter (5xSBE Non-Tg) were used, all mice expressed the Luc reporter gene confirmed by a real-time PCR genotype assay. This SBE-Luc reporter mouse has been extremely useful to track changes in neuroinflammation in response to systemic lipopolysaccharide (LPS) administration (Luo and Wyss-Coray, 2009). Male and female mice were used to assess the effect of low dose LPS (Female 5xSBE Tg (n= 9) 5xSBE Non-Tg (n= 9) and Male 5xSBE Tg (n= 8) 5xSBE Non-Tg (n= 6)) or diet induced chronic peripheral inflammation (Female 5xSBE Tg (HFHF n= 9, CD n= 8) 5xSBE Non-Tg (HFHF n= 8, CD n= 7) and Male 5xSBE Tg (HFHF n= 4, CD n= 4), 5xSBE Non-Tg (HFHF n= 3, CD n= 3)) on the kinetics of neuroinflammation, mice were randomly assigned to treatment group based on genotype. All mice were co-housed in a vivarium at Emory University with *ad libitum* access to food and water on a 12hr light/dark cycle. Mice were only handled during the light cycle between the hours of 7 a.m. and 7 p.m. All experimental procedures were approved by the Institutional Animal Care and Use Committee of Emory University and comply with the National Institutes of Health guide for the care and use of Laboratory animals.

3.4.2 High-fat high-fructose diet (HFHF)

To assess the effect of diet-induced peripheral inflammation on neuroinflammation 5xSBE male and female mice received either HFHF diet or CD for 8 weeks and CCR2-RFP and B6 mice

received either HFHF diet or CD for 5 weeks (Ingredient composition **table 3.1**; Calculated nutrient composition **table 3.2**). CCR2 is downregulated as monocytes differentiate into macrophages (Phillips et al., 2005), which occurs upon monocyte brain infiltration (Goldmann et al., 2016), thus a shorter duration of diet was selected for the CCR2-RFP and B6 studies to assess early infiltrating populations in response to HFHF diet. While on special diet measurements of diet intake, bi-weekly, and weekly weight measurements were made and samples of PBMCs and plasma were collected once every two weeks.

3.4.3 *Low-dose (LD) LPS administration*

To assess the effect of LD-LPS-induced peripheral inflammation on neuroinflammation 5xSBE male and female mice received LD LPS (7.5×10^5 endotoxin units (EU)/ kg) twice a week for 4 weeks. Plasma and PBMCs were collected prior to the first dose and at end point. BLI measurements were taken 6 hours following each LD LPS dose.

3.4.4 *Brain Dissociation for Immune Cell Isolation*

CCR2-RFP mice were anesthetized with isoflurane. Brain was removed from skull and whole brain tissue was finely minced in 1xHBSS (without Calcium, Magnesium, and phenol red, Invitrogen, 14175) and transferred to an enzymatic DDP solution (DMEM/F12 media containing 1mg/ml papain from papaya latex (P4762 Sigma Aldrich, St. Louis, MO), 1.2U/mL dispase II (4942078001 Roche diagnostics, Risch-Rotkreuz, Switzerland), and 220U/mL DNase I (18047-019 Invitrogen, Carlsbad, CA)). The minced tissue in DDP mixture were incubated at 37°C for 20 minutes before being neutralized with 10% heat-inactivated fetal bovine serum (FBS) (Atlanta

Biologicals, S11150). The tissue pellet was homogenized in ice-cold 1xHBSS using a fine-tip fire-polished glass pipette. The homogenate was filtered through a 70 μ M cell strainer. The pellet was resuspended in 37% Percoll (Percoll pH8.5-9.5; Sigma Aldrich Co, P1644) and 70% Percoll layered below, and 30% Percoll layered above, with 1xHBSS layered on the top. The Percoll gradient was centrifuged and immune cells were collected from the cell cloud between the 70% and 37% Percoll layer, and washed with 4x volume of 1xHBSS.

3.4.5 Plasma and Peripheral blood mononuclear cell (PBMC) isolation

Whole blood was collected from cheek bleeds, approximately 200ul per mouse per sampling. 5xSBE and B6 blood samples were collected at baseline and once every two weeks following onset of diet manipulation. Whole blood was collected in EDTA coated tubes (Covidien 8881311248) and 100ul was treated with 1x RBC lysis buffer (BioLegend 420301) as per manufacturer's instructions to isolate PBMCs before staining for flow cytometry. From the remaining whole blood sample, plasma was collected by centrifugation and frozen promptly on dry ice then subsequent storage at -80 degrees until processing.

3.4.6 Multi-color Flow Cytometry

All cells were stained with Live/Dead Fixable Aqua (1:2000, L34957 Invitrogen) and incubated with anti-mouse CD16/CD32 (1:100, 14-0161085 eBioscience). PBMCs isolated from 5xBSE and B6 mice were stained with the following antibody panel: Fc Block (1:00, 14-0161-85, eBioscience), CD45 PerCP (1:100, 130-102-785, Miltenyi Biotec), CD11b PE_Vio770 (1:200, 130-109-365, Miltenyi Biotec), MHCII APC (1:50, 130-102-898, Miltenyi Biotec), Ly6C PE

(1:200, 128007, BioLegend), CD4 Alexa Fluor 488 (1:200, 53-0041 eBioscience), CD8b APC-eFluor780 (1:100, 47-0083 eBioscience), CD3 e450 (1:50, 48-0031-82, eBioscience) in FACS buffer. Samples were run on a MACSQuant (Miltenyi Biotec) and analyzed with FlowJo_V10. Immune cells isolated from CCR2-RFP brains were stained with the following antibody panel: CD11b FITC (1:50, 11-0112 eBioscience), CD19 PE (1:500, 561736 BD Bioscience), CD45 PerCP-Cy5.5 (1:100, 45-0451 eBioscience), MHCII Pe-Cy7 (1:100, 25-5321 eBioscience), CD3 APC (1:100 17-0031-81, eBioscience), Ly6C APC-Cy7 (1:100, 128026 BioLegend), Ly6G PacBlue (1:50, 127611 BioLegend), CD11c Alexa Fluor 700 (1:50, 117320 BioLegend), CD4 BV711 (1:200, 100447, BioLegend), CD8 BV785 (1:100, 100750, BioLegend) in FACS buffer. Samples were run on a LSRII multi-color flow cytometer (BD Biosciences) and analyzed with FlowJo_V10.

Single cell lymphocytes were gated based on Forward Scatter Height (FSH) (size) and Side Scatter Height (SSH) (granularity) and then by FSH by Forward Scatter Area (FSA). Live cells were then selected as the Fixable Aqua-negative population. From the PBMC live cell populations, CD45⁺ cells were gated for CD3⁺ T cells and CD11b⁺ myeloid cells. All CD3⁺ T cells were then gated for CD4⁺ and CD8⁺, while all CD11b⁺ myeloid cells were gated for MHCII⁺ and MHCII⁻ and Ly6C^{high} and Ly6C^{low} from the histogram distribution (**Supplemental figure 3.1**).

To determine overall changes in immune cell trafficking from CCR2-RFP mouse brain live cell populations, CD45⁺ cells were gated for CD3⁺ T cells and CD19⁺ B cells. All CD3⁺ T cells were then gated for CD4⁺ and CD8⁺. The CD3⁻CD19⁻ cell population was gated for CD11c (Dendritic cells) and Ly6G (Neutrophils) and the CD11c⁻Ly6G⁻ (microglia/macrophages) population was gated for Ly6C^{high} and Ly6C^{low} and CD45^{high} and CD45^{low} from the histogram distribution. CD45^{high} (peripheral macrophages and activated microglia) and CD45^{low}

(homeostatic/resting microglia) were gated for MHCII⁺ and MHCII⁻ from the histogram distribution (**Supplemental figure 3.2**). To determine trafficking patterns of CCR2-RFP positive cells CCR2-RFP mouse brain live cell populations CD45⁺ cells were gated for CCR2-RFP from the histogram distribution; the gate was determined from CCR2-RFP/+ spleen histogram distribution. The RFP⁺ population was then gated for CD3⁺ T cells and CD19⁺ B cells. All CD3⁺ T cells were then gated for CD4⁺ and CD8⁺. The CD3⁻CD19⁻ population was gated for CD11c (Dendritic cells) and Ly6G (Neutrophils) and the CD11c⁻Ly6G⁻ (microglia/macrophages) was gated for Ly6C^{high} and Ly6C^{low} and CD45^{high} and CD45^{low} from the histogram distribution. CD45^{high} (peripheral macrophages and activated microglia) and CD45^{low} (homeostatic/resting microglia) were gated for MHCII⁺ and MHCII⁻ from the histogram distribution (**Supplemental figure 3.2**). From every sample, counting beads (AccuCheck Counting Beads, Invitrogen PCB100, 10µl were added to each sample before running on the LSRII multi-color flow cytometer) were selected on size from the FSH vs FHA plot and then again from FSH vs FSA plot. Sample counts of all target populations were calculated in FlowJo and from these counts total tissue counts were obtained: (population count/bead count) x (bead concentration in sample run) x run volume x (whole sample volume/volume processed for 1x10⁶ cells).

3.4.7 Bioluminescence imaging (BLI) Measurements

To inform the selection of specific time points for molecular, electrophysiological and histological analyses we first aimed to define the kinetics of diet-induced brain inflammation. Hair was removed using a depilatory (Nair with soothing Aloe & Lanolin) on all 5xSBE mice while under isoflurane anesthesia 24hrs prior to the imaging sessions. Bioluminescence imaging was performed on an In-Vivo Imaging System (IVIS) Spectrum (Caliper Life Sciences). Mice were

anesthetized using an XG1-8 Gas Anesthesia System (Caliper Life Sciences) with isoflurane (2.5% in O₂), and given either subcutaneous injections of luciferin (450mg/kg) (LPS studies), or IP injections of luciferin (150mg/kg) (Diet studies) before being transferred from the isoflurane induction unit to the IVIS' imaging chamber. Luciferin was reconstituted in saline at 40mg/ml. Three images (5 minute exposures) were taken 10min (LPS studies) or 7 min (Diet studies) after injection with Luciferin. Anesthetization was maintained during imaging by isoflurane (2.5% in O₂) pumped into nosecones within the imaging chamber itself. Bi-weekly PBMC collection occurred 2hr after final BLI image. Only mice that had a baseline level of 100 counts (counts are packets of photons of an arbitrary size programmed into and measured by the hardware and software associated with the IVIS; those are then calculated out into the "real" measurements used for analysis) were used for BLI measurement, mice with baseline level lower than 100 counts were injected with saline and exposed to the same duration of isoflurane but not imaged. These mice were used in assessment of PBMC and neuroinflammatory measurements. Although all mice were confirmed to express the Luc transgene, only approximately 59% of all 5xFAD x SBE mice expressed luciferase protein and were used for imaging studies.

3.4.8 Statistical Analysis

Immune cell population values, from PBMCs and brain, and BLI data was compared across genotypes and treatment conditions with two-way analysis of variance (ANOVA) using GraphPad Prism 6 software (La Jolla, CA). Sidak's multiple comparisons was used for *post hoc* comparisons. Percent of baseline data (from PBMC analysis) was normalized to group baseline for analysis as percentage (%) of baseline at each time point assessed. Data was compared across genotypes and

treatment conditions with two-way analysis of variance (ANOVA) using GraphPad Prism 6 software. Sidak's multiple comparisons was used for *post hoc* comparisons. BLI % of baseline average radiance data, from diet and LD-LPS studies, was normalized within animal to the animal's own baseline to reduce within group variability. Data at each time point represents the % change from the animal's own baseline within each treatment group. Data was compared across genotypes and treatment conditions with two-way analysis of variance (ANOVA) using GraphPad Prism 6 software. Sidak's multiple comparisons was used for *post hoc* comparisons.

3.5 Results

3.5.1 PBMC populations in male mice are altered by LD LPS-induced peripheral inflammation

To assess how chronic peripheral inflammation alters PBMC populations shown to traffic to the brain in neurodegenerative disease (Togo et al., 2002; Martin et al., 2016), 5xSBE mice with (5xTG_SBE) and without (5xNon-Tg_SBE) the 5xFAD transgenes were treated with LD LPS for 4 weeks to induce chronic peripheral inflammation. Analysis of PBMCs, collected at baseline and following 4 weeks of LD LPS were assessed via multicolor flow cytometry, **figure 3.1I**, revealed significant effects of genotype within PBMC populations from male, but not female, mice. While no significant effects were seen in CD3⁺ T cell population change from baseline, (CD3⁺ T cell population change from baseline: Male 5xNon-Tg_SBE: 68.363 ± 8.351 , 5xTg_SBE: 84.987 ± 5.654 $p = n.s.$; Female 5xNon-Tg_SBE: 85.539 ± 7.707 , 5xTg_SBE: 78.520 ± 4.037 $p = n.s.$, from 2-Way ANOVA Sidak's post hoc, **figure 3.1A**) or CD4⁺ T cell change population from baseline within CD3⁺ T cells (CD4⁺ T cell population change from baseline: Male 5xNon-Tg_SBE: 84.190 ± 6.219 , 5xTg_SBE: 92.828 ± 5.889 $p = n.s.$; Female 5xNon-Tg_SBE: 89.425 ± 4.885 , 5xTg_SBE: 103.779 ± 4.037 $p = n.s.$, from 2-Way ANOVA Sidak's post hoc, **figure 3.1B**), 5xTg_SBE male,

but not female, mice show significant decrease in the change of CD8⁺ T cell population from baseline as compared to 5xNon-Tg_SBE male mice (CD8⁺ T cell population change from baseline: Male 5xNon-Tg_SBE: 143.655 ± 4.894 , 5xTg_SBE: 129.346 ± 4.092 $t = 2.555$ $df = 29$ $p < 0.05$; Female 5xNon-Tg_SBE: 109.308 ± 3.652 , 5xTg_SBE: 118.863 ± 2.363 $p = n.s.$, from 2-Way ANOVA Sidak's post hoc, **figure 3.1C**). 5xTg_SBE male, but not female, mice also show a significant decrease in the change of CD11b⁺ PBMCs from baseline as compared to 5xNon-Tg_SBE male mice (CD11b⁺ PBMCs change from baseline: Male 5xNon-Tg_SBE: 275.185 ± 17.550 , 5xTg_SBE: 186.004 ± 11.076 $t = 5.964$ $df = 29$ $p < 0.0001$; Female 5xNon-Tg_SBE: 171.251 ± 7.035 , 5xTg_SBE: 143.069 ± 5.329 $p = n.s.$, from 2-Way ANOVA Sidak's post hoc, **figure 3.1D**). Within the CD11b⁺ myeloid PBMC population significant effects of genotype on activation status (Ly6C and MHCII expression) were found in male, but not female mice. While there were no effects within the change of Ly6C^{high}CD11b⁺ PBMC population from baseline (Ly6C^{high}CD11b⁺ PBMCs change from baseline: Male 5xNon-Tg_SBE: 45.285 ± 5.051 , 5xTg_SBE: 53.678 ± 6.719 $p = n.s.$; Female 5xNon-Tg_SBE: 54.497 ± 3.492 , 5xTg_SBE: 51.072 ± 9.187 $p = n.s.$, from 2-Way ANOVA Sidak's post hoc, **figure 3.1E**), 5xTg_SBE male, but not female, mice showed significant decreased in the change of Ly6C^{low}CD11b⁺ PBMCs from baseline as compared to 5xNon-Tg_SBE male mice (Ly6C^{low}CD11b⁺ PBMCs change from baseline: Male 5xNon-Tg_SBE: 127.260 ± 0.627 , 5xTg_SBE: 119.448 ± 2.326 $t = 3.605$ $df = 29$ $p < 0.01$; Female 5xNon-Tg_SBE: 119.271 ± 0.662 , 5xTg_SBE: 115.170 ± 5.329 $p = n.s.$, from 2-Way ANOVA Sidak's post hoc, **figure 3.1F**). The change of MHCII⁺CD11b⁺ PBMCs from baseline was significantly increased in 5xTg_SBE male, but not female, mice as compared to 5xNon-Tg_SBE mice (MHCII⁺CD11b⁺ PBMCs change from baseline: Male 5xNon-Tg_SBE: 42.065 ± 4.718 , 5xTg_SBE: 68.174 ± 5.624 $t = 2.716$ $df = 29$ $p < 0.05$; Female 5xNon-Tg_SBE: 59.284 ± 5.303 ,

5xTg_SBE: 69.891 ± 7.244 $p = \text{n.s.}$, from 2-Way ANOVA Sidak's post hoc, **figure 3.1G**). These complements the significant decreased in the change of MHCII⁺CD11b⁺ PBMCs from baseline in 5xTg_SBE male, but not female, mice as compared to 5xNon-Tg_SBE mice (MHCII⁺CD11b⁺ PBMCs change from baseline: Male 5xNon-Tg_SBE: 102.520 ± 0.196 , 5xTg_SBE: 100.965 ± 0.167 $t = 5.129$ $df = 29$ $p < 0.0001$; Female 5xNon-Tg_SBE: 101.404 ± 0.190 , 5xTg_SBE: 100.864 ± 0.206 $p = \text{n.s.}$, from 2-Way ANOVA Sidak's post hoc, **figure 3.1H**).

3.5.2 HFHF diet-induced dynamic changes within CD11b⁺ myeloid PBMC populations in both male and female C57Bl/6J mice

To elucidate how diet-induced peripheral inflammation impacts populations of immune cells shown to traffic to the brain in neurodegenerative disease, T cell and myeloid PBMC populations were assessed in male and female C56Bl/6J mice fed either a HFHF diet or control diet (CD) at baseline, 2 weeks, and 5 weeks on diet, **figure 3.2G**. No significant effects of diet were seen at baseline within many of the measured populations (data not shown), except for significant effects of sex, by 2-way ANOVA, in both the frequency of CD4⁺ T cells ($p = 0.0421$) and CD8⁺ T cells ($p = 0.0486$) CD3⁺ T cells, data not shown.

Within the myeloid PBMC populations the overall CD11b⁺ PBMC population change from baseline was significantly increased in male mice on CD diet at week 5 as compared to male mice on CD diet at week 2 (CD11b⁺ PBMCs % from baseline: Male CD week 2: 87.782 ± 5.215 , week 5: 188.669 ± 16.817 $t = 7.580$ $df = 56$ $p < 0.0001$ by 2-way ANOVA Sidak's post hoc, **figure 3.2A**) as well as from male mice on HFHF diet at week 5 (CD11b⁺ PBMCs % from baseline: Male CD week 5: 188.669 ± 16.817 , Male HFHF week 5: 140.338 ± 7.060 $t = 3.631$ $df = 56$ $p < 0.05$

by 2-way ANOVA Sidak's post hoc, **figure 3.2A**). At week 5 there was a significant decrease in frequency of CD11b⁺ PBMCs in HFHF male mice as compared to CD males, but no effect of diet within female mice (CD11b⁺ PBMCs: Male Control diet: 34.550 ± 3.080 , HFHF diet: 25.962 ± 1.306 $t = 2.840$ $df = 28$ $p < 0.05$; Female control diet: 23.163 ± 1.852 , HFHF diet: 21.313 ± 1.916 $p = n.s.$ by 2-way ANOVA, **figure 3.2E**). Within the CD11b⁺ myeloid population frequency of the MHCII⁺CD11b⁺ myeloid population from baseline was significantly decreased in CD males, but not HFHF males, at week 5 as compared to week 2 (MHCII⁺CD11b⁺ PBMCs % from baseline: male CD week 2: 155.220 ± 20.563 , week 5: 71.164 ± 10.541 $t = 3.832$ $df = 56$ $p < 0.01$, by 2 Way ANOVA Sidak's post hoc analysis, **figure 3.2B**), while no significant differences in change from baseline of the MHCII⁺CD11b⁺ myeloid population were found in female mice, **figure 3.2B**. At 5 weeks the frequency of MHCII⁺CD11b⁺ myeloid cells was significantly increased in male, but not female mice (MHCII⁺ CD11b⁺ PBMCs frequency: Male CD: 2.974 ± 0.440 , Male HFHF: 4.745 ± 0.316 $p < 0.01$; Female CD: 3.931 ± 0.161 , Female HFHF: 4.224 ± 0.391 , by 2 Way ANOVA Sidak's post hoc analysis, **figure 3.2F**). Changes in Ly6C expression were found within the CD11b⁺ myeloid population in both male and female mice. HFHF female mice showed a significant increase as compared to CD female at week 2 and week 5 from baseline in the ratio of Ly6C^{high}:Ly6C^{low} CD11b⁺ myeloid population (Ly6C^{high}:Ly6C^{low} CD11b⁺ PBMCs % of baseline: Female CD week 2: 111.560 ± 9.600 , HFHF week 2: 153.528 ± 8.805 $t = 3.306$ $df = 56$ $p < 0.01$; Female CD week 5: 79.329 ± 6.202 , HFHF week 5: 122.087 ± 11.300 $t = 3.368$ $df = 56$ $p < 0.01$, by 2 Way ANOVA Sidak's post hoc analysis, **figure 3.2C**). At week 2 and week 5 HFHF female mice had significantly increased change from baseline as compared to HFHF male mice (Ly6C^{high}:Ly6C^{low} CD11b⁺ PBMCs % of baseline: week 2 HFHF male 91.141 ± 3.318 , week 2 HFHF female 153.528 ± 8.805 $t = 4.914$ $df = 56$ $p < 0.0001$; week 5 HFHF male 77.023 ± 6.632 ,

week 5 HFHF female 122.087 ± 11.300 $t = 3.550$ $df = 56$ $p < 0.01$, **figure 3.2C**). In contrast to these results HFHF male mice showed a significant decrease at week 2 from CD male mice in the Ly6C^{high}:Ly6C^{low} CD11b⁺ myeloid change from baseline (Ly6C^{high}:Ly6C^{low} CD11b⁺ PBMCs % of baseline: Week 2 male CD: 147.543 ± 10.001 , male HFHF 91.141 ± 3.318 $t = 4.443$ $df = 56$ $p < 0.001$, by 2-way ANOVA Sidak's post hoc, **figure 3.2C**). At 5 weeks, the ratio of Ly6C^{high}:Ly6C^{low} CD11b⁺ myeloid population was significantly increased in male, but not female mice, (Ly6C^{high}:Ly6C^{low} CD11b⁺ myeloid frequency: Male CD: 0.072 ± 0.014 , HFHF: 0.120 ± 0.010 $t = 3.189$ $df = 28$ $p < 0.05$; Female CD: 0.096 ± 0.007 , HFHF: 0.101 ± 0.009 , $p = n.s.$, **figure 3.2F**).

3.5.3 *T cell populations show resistance to changes induced by HFHF-dependent peripheral inflammation*

Assessing the dynamics of the T cell PBMC populations from C56Bl/6J mice over the course of 5 weeks of either HFHF or CD (**figure 3.3G**) we found that the change from baseline in the CD3⁺ T cell population in male mice was significantly decreased at week 5 from week 2 in both CD and HFHF diet groups, (CD3⁺ T Cells % of baseline: male CD week 2: 114.453 ± 4.245 , week 5: 60.568 ± 4.970 $t = 5.384$ $df = 56$ $p < 0.0001$; male HFHF week 2: 96.392 ± 3.762 , week 5: 55.493 ± 5.514 $t = 4.086$ $df = 56$ $p < 0.01$ by 2-way ANOVA Sidak's post hoc analysis, **figure 3.3A**). While no effects of diet were found in female mice (CD3⁺ T Cells % of baseline: female CD week 2: 105.695 ± 6.784 , week 5: 85.546 ± 12.097 $p = n.s.$; female HFHF week 2: 99.587 ± 3.211 , week 5: 93.198 ± 10.466 $p = n.s.$, by 2-way ANOVA Sidak's post hoc analysis, **figure 3.3A**) the % change from baseline in male HFHF mice was significantly lower than female HFHF mice at 5 weeks (CD3⁺ T Cells % of baseline: week 5 male HFHF: 55.493 ± 5.514 , female HFHF

93.198 ± 10.466 t = 3.767 df = 56 p < 0.01 **figure 3.3A**). At 5 weeks, the frequency of CD3⁺ T cells was significantly higher in female HFHF diet mice as compared to male HFHF diet mice (T cells % of CD45⁺ PBMCs: Control diet male: 18.125 ± 1.487, female: 27.225 ± 3.850; HFHF diet male: 17.112 ± 1.700, female: 31.000 ± 3.481 t = 3.469 df = 28 p < 0.05 by 2-way ANOVA Sidak's post hoc analysis, **figure 3.3D**). Within the T cell population no significant changes from baseline were found within the CD4⁺ T cell population across diet or sex (CD4⁺ T Cells % of baseline: Female CD week 2: 74.262 ± 3.397, week 5: 94.999 ± 6.144 p = n.s.; Female HFHF week 2: 71.170 ± 3.115, week 5: 87.629 ± 6.751 p = n.s.; Male CD week 2: 76.417 ± 2.023, week 5: 103.516 ± 11.695 p = n.s.; Male HFHF week 2: 77.010 ± 2.907, week 5: 102.741 ± 7.695 by 2-way ANOVA Sidak's post hoc analysis, **figure 3.3B**) nor at the 5 week end point (CD4⁺ T cells % of CD3⁺ T cells: CD male: 42.688 ± 4.823, female: 42.263 ± 2.733 p = n.s.; HFHF diet male: 42.175 ± 3.159, female: 42.325 ± 3.261 p = n.s. by 2-way ANOVA, **figure 3.3E**). Within the CD8⁺ T cell population significant changes from baseline were found in male and female mice on CD diet as well as male mice on HFHF diet (CD8⁺ T Cells % of baseline: Female HFHF week 2: 89.314 ± 4.070, week 5: 105.556 ± 4.185 p = n.s.; Female CD week 2: 82.681 ± 3.380, week 5: 102.494 ± 1.644 t = 5.176 df = 56 p < 0.05; Male HFHF week 2: 71.942 ± 4.224, week 5: 97.795 ± 4.208 t = 6.754 df = 56 p < 0.001; Male CD week 2: 78.780 ± 3.171, week 5: 100.194 ± 4.839 t = 5.594 df = 56 p < 0.01 by 2-way ANOVA Sidak's post hoc analysis, **figure 3.3C**), however after 5 weeks of diet no significant effect were found in the frequency of CD8⁺ T cells (CD8⁺ T cells % of CD3⁺ T cells: CD male: 32.225 ± 1.556, female: 36.987 ± 0.593 p = n.s.; HFHF diet male: 34.375 ± 1.479, female: 37.287 ± 1.478 p = n.s. by 2-way ANOVA, **figure 3.3F**).

3.5.4 PBMC populations in female 5xSBE mice are resilient to changes induced by diet-dependent chronic peripheral inflammation

To assess how diet-induced peripheral inflammation alters PBMC population dynamics in a model of Alzheimer's disease 5xSBE_Non-Tg and 5xSBE_Tg female mice were fed either HFHF diet or CD for 8 weeks. PBMCs were collected at baseline and every two weeks while mice were on diet and T cell and myeloid populations were assessed via multicolor flow cytometry, **figure 3.4I**. A significant effect of week on diet was found the dynamics of the CD3⁺ T cell population from baseline by 2-way ANOVA ($F(4, 124) = 2.753$ $p = 0.0310$, **figure 3.4A**), however no effects were found within weeks by post hoc analysis, **figure 3.4A**, or at 8 weeks in the frequency of CD3⁺ T cells, **figure 3.4E**. Within the CD3⁺ T cell population changes were found within the dynamic response of the CD4⁺ T cell population a significant effect of week by 2-way ANOVA ($F(4, 124) = 6.441$ $p < 0.0001$, **figure 3.4B**) post hoc analysis revealed a significant increase in CD4⁺ T cells from baseline in 5xTg_SBE HFHF mice as compared to 5xNon-Tg_SBE CD mice at 6 weeks of diet (CD4⁺ T cell % of baseline: 6 weeks 5xNon-Tg_SBE CD: 72.344 ± 5.359 , 5xTg_SBE HFHF: 112.191 ± 20.203 $t = 3.758$ $df = 124$ $p < 0.05$ by Sidak's post hoc, **figure 3.4B**), however no effects of diet were seen in the frequency of CD4⁺ T cells at the 8 week PBMC snapshot, **figure 3.4F**. A significant effect of week on diet was found the dynamics of the CD11b⁺ PBMC population from baseline by 2-way ANOVA ($F(4, 133) = 2.819$ $p = 0.0277$, **figure 3.4C**), however no effects were found within weeks by post hoc analysis, **figure 3.4C**, or at 8 weeks in the frequency of CD11b⁺ PBMCs, **figure 3.4G**. Within the CD11b⁺ PBMC population significant effects of both week and genotype were found in the Ly6C^{high}CD11b⁺ PBMC change from baseline (significant effect of week: $F(4, 133) = 4.906$ $p = 0.0010$; genotype: $F(3, 133) = 3.332$ $p = 0.0215$

by 2-way ANOVA, **figure 3.4D**), however no effects were seen within weeks by post hoc analysis, **figure 3.4D**, or at 8 weeks in the frequency of Ly6C^{high}CD11b⁺ PBMCs, **figure 3.4H**.

3.5.6 HFHF diet reduces frequency of CD3⁺ T cell populations trafficking to the brain in CCR2-RFP/+ mice

Using aged, male and female, CCR2-RFP mice we assessed the populations of peripheral immune cells that traffic to the brain in response to 5 weeks of either CD or HFHF diet, **figure 3.5H, 3.6K**. While no changes in frequency of B cells or frequency of MHCII⁺ B cells capable of antigen presentation trafficking to the brain were detected across diet or genotype, **figure 3.5A-B**, a significant decrease in the brain CD3⁺ T cells population was found in RFP/+ mice following HFHF diet (CD3⁺ T cell frequency: +/+ CD: 49.371 ± 4.751, HFHF: 44.333 ± 1.475 p = n.s.; RFP/+ CD: 48.855 ± 4.156, HFHF: 38.900 ± 0.969 t = 2.626 df = 40 p < 0.05; RFP/RFP CD: 43.780 ± 3.310, HFHF: 42.050 ± 1.294 p = n.s., **figure 3.5C**). Within the CD3⁺ T cell population there were no detectable changes in the CD4⁺ T cell population, however within the CD8⁺ T cell population significant effects of both diet (F (2, 40) = 3.357 p = 0.0399) and genotype (F (1, 40) = 4.512 p = 0.0449) by 2-way ANOVA were found although post hoc analysis did not reveal any significant effects of diet within genotypes, **figure 3.5E**. No significant changes were found in number of cells within the T cell populations, data not show. Analysis of the CCR2⁺ RFP populations within the brain of RFP/+ and RFP/RFP mice did not reveal significant changes in the CCR2⁺CD3⁺ T cell populations across genotype of diet, **figure 3.5F**, nor within CCR2⁺CD8⁺ T cell populations, **figure 3.5G**.

3.5.7 HFHF diet alters CD11b⁺ microglia/macrophage population within and trafficking to the brain

Using the CCR2-RFP model as a tool to modulate CCR2-dependent trafficking in RFP/RFP homozygous mice we were able to assess the role monocyte/macrophage trafficking has on diet-induced neuroinflammation. Within the CD11b⁺ myeloid population the CD11b⁺Ly6G⁻CD11c⁻ microglia/macrophage population a significant effect of diet was found by 2 Way ANOVA ($F(1,40) = 8.095$ $p = 0.0070$) and post hoc analysis revealed a significant increase in the frequency but not number of microglia/macrophage population following HFHF diet in RFP/+ mice (frequency of CD11b⁺ microglia/macrophage: +/+ CD: 26.943 ± 3.729 HFHF: 34.367 ± 2.809 $p = \text{n.s.}$; RFP/+ CD: 26.582 ± 2.570 HFHF: 34.217 ± 1.547 $t = 2.602$ $df = 40$ $p < 0.05$; RFP/RFP CD: 28.340 ± 2.632 HFHF: 33.037 ± 1.717 $p = \text{n.s.}$, **figure 3.6A**). Within the CD11b⁺ microglia there was a significant effect of genotype in the frequency of CD45^{high}CD11b⁺ microglia/macrophages by 2 way ANOVA ($F(2, 40) = 8.039$ $p = 0.0012$) and Sidak's post hoc analysis revealed significant decreases in the frequency of CD45^{high}CD11b⁺ microglia/macrophages in RFP/RFP mice as compared to RFP/+ mice within CD and HFHF diet (frequency of CD45^{high}CD11b⁺ microglia/macrophages: CD RFP/+: 18.682 ± 2.5626 , RFP/RFP: 10.790 ± 2.092 $t = 2.368$ $df = 40$ $p < 0.05$; HFHF RFP/+: 18.361 ± 1.832 , RFP/RFP: 9.906 ± 1.272 $t = 2.631$ $df = 40$ $p < 0.05$, by 2 way ANOVA Sidak's post hoc, **figure 3.6B**). Within this population of activated microglia and peripheral macrophage (CD45^{high}CD11b⁺ microglia/macrophages) the frequency but not count of MHCII⁺CD45^{high} microglia/macrophages population showed significant effects of both diet ($F(1, 40) = 4.565$ $p = 0.0388$) and genotype ($F(2, 40) = 6.521$ $p = 0.0035$) by 2-Way ANOVA, however post hoc analysis did not reveal any significant effects of diet within genotype (frequency of MHCII⁺CD45^{high}CD11b⁺ microglia/macrophages: +/+ CD: 9.199 ± 1.610 HFHF: 5.827 ± 0.419 p

= n.s.; RFP/+ CD: 9.983 ± 1.634 HFHF: 6.846 ± 0.831 $p = \text{n.s.}$; RFP/RFP CD: 4.406 ± 0.841 HFHF: 3.287 ± 0.490 $p = \text{n.s.}$; by 2-way ANOV Sidak's post hoc, **figure 3.6C**). Significant effect of genotype was found in the frequency, but not count, of homeostatic/resting microglia (CD45^{low}CD11b⁺ microglia) by 2-way ANOVA ($F(2, 40) = 8.183$ $p = 0.0010$), post hoc analysis revealed a significant increase in HFHF RFP/RFP mice as compared to both HFHF RFP/+ and HFHF +/+ mice (frequency of CD45^{low}CD11b⁺ microglia/macrophage: HFHF +/+: 78.400 ± 4.504 , RFP/RFP: 90.300 ± 1.307 $t = 2.678$ $df = 40$ $p < 0.05$; HFHF RFP/+: 81.775 ± 1.814 , RFP/RFP: 90.300 ± 1.307 $t = 2.845$ $df = 40$ $p < 0.05$, by 2-Way ANOVA Sidak's post hoc **figure 3.6D**). Within this population of homeostatic/resting microglia (CD45^{low}CD11b⁺ microglia) no significant changes were found in the frequency or count of MHCII⁺CD45^{low}CD11b⁺ microglia/macrophage, **figure 3.6E**. Using Ly6C expression to assess peripheral macrophages that have trafficked into the brain we found the frequency, but not count, of Ly6C⁺CD11b⁺ macrophages was increased in RFP/+ mice following HFHF diet as compared to CD RFP/+ mice (frequency of Ly6C⁺CD11b⁺ macrophages: +/+ CD: 10.811 ± 3.007 , HFHF: 9.230 ± 2.513 $p = \text{n.s.}$; RFP/+ CD: 5.675 ± 0.537 , HFHF: 12.543 ± 2.884 $t = 2.622$ $df = 40$ $p < 0.05$; RFP/RFP CD: 3.568 ± 0.580 , HFHF: 3.871 ± 0.612 $p = \text{n.s.}$, by 2-way ANOVA Sidak's post hoc, **figure 3.6F**). Within the Ly6C⁺ macrophage population the majority of cells are CD45^{high}, no effects of diet or genotype by 2-way ANOVA, **figure 3.6G**. Of this Ly6C⁺CD45^{high} populations no effects of diet or genotype were found in frequency, or count (data not shown), of MHCII⁺Ly6C⁺CD45^{high} macrophages, **figure 3.6H**. Analysis of the CCR2⁺ RFP populations within the brain of RFP/+ and RFP/RFP mice did not reveal significant changes in the very small population of CCR2⁺CD11b⁺ macrophage frequency, or count (data not shown), **figure 3.6I**. Within this population a significant effect of diet was found by 2-way ANOVA in the frequency, but not count (data not shown), of

CCR2⁺Ly6C⁺CD11b⁺ macrophages ($F(1, 32) = 8.922$ $p = 0.0054$) and post hoc analysis revealed a significant increase in HFHF RFP/+ mice as compared to CD RFP/+ mice (frequency of CCR2⁺Ly6C⁺CD11b⁺ macrophages: RFP/+ CD: 23.327 ± 2.873 , HFHF: 33.042 ± 3.483 $t = 2.359$ $df = 32$ $p < 0.05$; RFP/RFP CD: 26.280 ± 3.087 , HFHF: 37.388 ± 2.724 $p = n.s.$, by 2-way ANOVA Sidak's post hoc, **figure 3.6J**).

3.5.8 Peripheral inflammation from both LD LPS and HFHF diet alters the neuroinflammatory response in 5xTg_SBE mice

To assess how chronic peripheral inflammation, induced by LD LPS and HFHF diet, impacts the neuroinflammatory response 5xSBE mice were dosed with either LD LPS for 4 weeks, **figure 3.7E**, or fed HFHF or control diet for 8 weeks, **figure 3.7H**. BLI measurements were collected at baseline and during intervention to assess levels of TGF β , a cytokine known to play in a role in the regulation of inflammation as an anti-inflammatory cytokine (Sanjabi et al., 2009). When dosed with 4 weeks of LD LPS a trend for an effect of day was found in percent of baseline BLI in 5xNon-Tg_SBE mice ($F(4, 50) = 2.306$ $p = 0.0685$, by 2-way ANOVA) no significant effects of sex within days were found in percent change in BLI from baseline by post hoc analysis, **figure 3.7A**. Within LD LPS treated 5xTg_SBE mice there was a significant effect of sex in percent of baseline BLI ($F(1, 65) = 4.528$ $p = 0.0372$, by 2-way ANOVA), however post-hoc analysis revealed no significant effects of sex within days in percent change in BLI from baseline, **figure 3.7B**. Within male, but not female (**figure 3.7D**), 5xSBE mice there is significant effect of genotype on percent of baseline BLI ($F(1, 54) = 7.746$ $p = 0.0074$, by 2-way ANOVA), post hoc analysis revealed a significant decrease in percent of baseline BLI at day 7 in 5xTg_SBE male mice as compared to 5xNon-Tg_SBE male mice (percent of baseline BLI day 7: 5xNon-Tg_SBE

male: 171.682 ± 30.709 , 5xTg_SBE male: 82.173 ± 23.518 $t = 3.063$ $df = 54$ $p < 0.05$, **figure 3.7C**). Following 8 weeks of either HFHF or control diet a significant effect of genotype was found in percent of baseline BLI in female 5xSBE mice ($F(3, 28) = 4.349$ $p = 0.0123$, **figure 3.7F**), post hoc analysis revealed a significant decrease in percent of baseline BLI of 5xTg_SBE HFHF mice as compared to 5xNon-Tg_SBE HFHF mice at 8 weeks (percent of baseline BLI week 8: 5xNon-Tg_SBE HFHF: 133.190 ± 64.070 , 5xTg_SBE HFHF: 43.033 ± 12.396 $t = 3.991$ $df = 28$ $p < 0.05$, by 2-way ANOVA Sidak's post hoc, **figure 3.7F**). At 8 weeks, a significant decrease in average radiance was found in 5xNon-Tg_SBE HFHF mice as compared to 5xNon-Tg_SBE CD mice, no effect of diet were found within 5xTg_SBE mice (average radiance: 5xNon-Tg_SBE CD: 27750 ± 9150.000 , 5xNon-Tg_SBE HFHF: 3214.667 ± 1985.422 $t = df = p < 0.05$; 5xTg_SBE CD: 17600.000 ± 3200.00 , 5xTg_SBE HFHF: 7871.750 ± 5232.799 $p = \text{n.s.}$, by 2-way ANOVA Sidak's post hoc, **figure 3.7G**).

3.6 Discussion

In a commonly used and well described method to induce chronic peripheral inflammation, LD LPS administration in the 5xSBE mice revealed that PBMC populations in female 5xTg_SBE mice are more resilient to inflammation induced PBMC changes than male 5xTg_SBE mice. We found that while male 5xTg_SBE mice had significant changes in the dynamics of CD8⁺ T cells, CD11b⁺ PBMC and activation of CD11b⁺ PBMCs, MHCII⁺ and Ly6C expression, female mice did not, **figure 3.1C-F**. 5xSBE female mice also show a smaller change from baseline in CD11b⁺ than 5xSBE male mice, **figure 3.1D**. These suggest that PBMC populations in female mice are more resilient to change within the myeloid compartment of the innate immune system and overall more resilient even when LD LPS is compounded with 5x transgene expression. While we do see

changes in regulation of neuroinflammation through BLI measurements with this model of chronic peripheral inflammation, **figure 3.7A-D**, using HFHF diet to induce peripheral inflammation creates a more clinically relevant model of increased AD risk (Yates et al., 2012) in which to study how peripheral immune cells traffic to and impact the brain during the course of AD-like pathology.

Assessing how diet-induced peripheral inflammation impacts PBMC populations shown to traffic to the brain in neurodegenerative disease we found sex specific changes in the dynamics of these populations. Changes in PBMC populations from baseline reveal dynamic changes in PBMC populations that are not revealed by endpoint ‘snapshot’ measurements. From assessing the changes in PBMC populations from baseline over the course of 5 weeks of novel diet in C57Bl/6J mice we saw dynamic changes suggesting dietary change, especially to a HFHF diet, does induce changes in the frequency of subpopulations of PBMCs in both male and female mice, however these changes found were sex dependent. Within the myeloid compartment, CD male mice show a significant increase in change from baseline of CD11b⁺ PBMCs at week 5 from week 2, as well as from HFHF male mice at week 5, **figure 3.2A**, while there are no effects in female mice. In the 5 week, endpoint snapshot HFHF male mice show a significant decrease in the frequency of CD11b⁺ PBMCs as compared to CD males, **figure 3.2D**. These results support our previous findings that PBMC populations in female mice are more resilient to changes induced by chronic inflammation. However, within the CD11b⁺ PBMC population we do find specific effects of sex and diet in the activation status of myeloid PBMCs. While MHCII⁺CD11b⁺ PBMCs from female mice do not exhibit the diet specific changes seen between male HFHF and CD groups, **figure 3.2B and 3.2E**, the female mice do show a HFHF diet specific increase in the change from baseline in the ratio of Ly6C^{high} to Ly6C^{low} CD11b⁺ PBMCs as compared to CD at week 2 and week 5,

figure 3.2C. This result contrasts with the significant decrease in the change from baseline in the ratio of Ly6C^{high} to Ly6C^{low} CD11b⁺ PBMCs found in HFHF male mice as compared to CD male mice, **figure 3.2C.** Thus, the few changes in myeloid PBMCs seen in female mice in response to HFHF diet are opposite in direction as compared to male mice, however whether this is an adaptive response is not yet determined. Overall across the CD3⁺ T cell populations C56Bl/6J male, but not female, mice showed significant decrease in CD3⁺ population change from baseline from week 2 to week 5 on both HFHF and control diet, **figure 3.3A.** At the 5 week endpoint, male HFHF also had decreased frequency of CD3⁺ T cells as compared to the female HFHF group, **figure 3.3D.** Within the CD3⁺ T cell population male mice showed an increase at week 5 from week 2 in CD8⁺ T cell change from baseline in both HFHF and CD group. These results showing population changes independent of diet group suggest that change in diet in male mice is sufficient to induce changes in the T cell population. This diet is purified with lower fiber levels than regular mouse chow and fiber has been linked to anti-inflammatory changes in the gut (Kuo, 2013), which may account for changes in T cells across both diets. However, the results seen with in the myeloid compartment suggest that HFHF-induced chronic inflammation does induce specific effects in PBMC populations. The changes seen in Ly6C^{high} to Ly6C^{low} suggest that HFHF diet increases the frequency of activated CD11b⁺ populations capable of trafficking into inflamed tissues, such as the brain during neurodegenerative disease. While 5 weeks of HFHF diet was sufficient to induce several changes in PBMC populations in male mice, we found that even up to 8 weeks on HFHF diet female 5xSBE mice did not show robust changes in PBMCs populations similar to male C56Bl/6 mice, **figure 3.4A-H.** Several studies suggests that peripheral inflammatory responses to diet are different in male and female mice (Amengual-Cladera et al., 2012), however high fat diet effects on cognition have been shown independent of sex (Underwood and Thompson,

2016). Less understood are the sex differences in neuroinflammatory kinetics and overall response to peripheral inflammation in the brain. Epidemiological data shows women are more likely to develop AD, thus we sought to investigate the sex effects of diet-induced peripheral inflammation on peripheral immune cell trafficking patterns and the kinetics of the neuroinflammatory response.

To assess if the trafficking patterns of these populations of peripheral PBMCs are altered by HFHF diet we assessed the immune cell populations in the brain of CCR2-RFP mice following 5 weeks of either HFHF or control diet, **figure 3.5H**. While no effects were found within the B cell population, **figure 3.5A-B**, a significant decrease in the frequency of CD3⁺ T cells was found within the T cell population, in RFP/+ mice, **figure 3.5C**. Lack of significant effects in T cell counts suggest the changes in T cell frequency in RFP/+ mice following HFHF diet are due to an increase in another population of immune cells. Increased variability in cell counts could be masking any effects due to HFHF diet while another explanation may be a non-significant increase across many populations. This genotype specific effect suggests that T cell trafficking to the brain may be partially dependent upon CCR2 signaling. Subpopulations of CD4⁺ T cells are known to express CCR2 (Mack et al., 2001), however significant changes within the trafficking CD4⁺ T cell were not found. Further investigation of the specific subpopulations of CD3⁺ T cells trafficking to the brain following HFHF diet may reveal changes in trafficking patterns of CD4⁺ subtypes that are not seen by looking at all CD4⁺ T cells together. However, the changes in the frequency CD3⁺ T cells may be an indirect response to changes in expression of other recruitment signals from the brain dependent on CCR2-expressing immune populations. While no diet effects are seen within genotype of CD8⁺ T cell populations, the overall effect of diet across genotype, **figure 3.5E**, suggests that trafficking populations of cytotoxic CD8⁺ T cells

are increased by HFHF diet. As this subset of T cells is more pro-inflammatory, this population may be contributing to the overall change in brain inflammatory status with HFHF diet.

Within the CD11b⁺ brain myeloid population of microglia and macrophages, the overall effect of diet and significant increase in the frequency of microglia/macrophages in RFP/+ HFHF mice suggest that this increase in the microglia/macrophage population may primarily indicate proliferation of brain-resident microglial populations rather than increased trafficking, **figure 3.6A**. Trafficking of peripheral macrophage populations has been shown to be dependent on CCR2 expression (Saederup et al., 2010). Microglial proliferation is known to occur in response to peripheral inflammation (Hoogland et al., 2015), and likely increased cytokine signaling from the peripheral immune system in response to HFHF diet is a possible mechanism for this increased microglial proliferation. However, the significant effect of genotype in the frequency of CD45^{high} and CD45^{low} microglia/macrophages independent of diet, **figure 3.6B and 3.6D**, suggests that within the RFP/RFP mice the overall population of microglia is less activated than within +/+ and RFP/+ mice, even in response to HFHF diet. Within the MHCII⁺CD45^{high} microglia/macrophage population there was a significant effect of both diet and genotype by 2-Way ANOVA, while post hoc analysis did not reveal any significant effects of diet within genotype, **figure 3.6C**, these results suggest that HFHF reduces the frequency of MHCII⁺CD45^{high} microglia/macrophages across genotypes. Trends across this data suggest that, overall, the frequency of MHCII⁺CD45^{high} microglia/macrophages is a decrease in RFP/RFP mice. These results may suggest that a small population of peripheral macrophages expressing MHCII do traffic into the brain in a CCR2-dependent manner, and that trafficking of this population is altered with HFHF diet.

Supporting the conclusion that there is a population of peripheral macrophages that traffics to the brain in response to HFHF diet is the result showing the frequency but not count of

Ly6C⁺CD11b⁺ macrophages was increased in RFP/+ mice following HFHF diet, **figure 3.6F**. No effects of diet were seen in +/+ or RFP/RFP mice, and a significant effect of genotype by 2-way ANOVA suggests that, overall, there is a genotype effect on the frequency of Ly6C⁺ macrophages. This is consistent with published results showing that macrophage trafficking is dependent on CCR2 signaling. The lack of a diet effect in the +/+ mice may be due to a CCR2 dose dependent effect that reduces the baseline frequency of Ly6C⁺ macrophage in CD mice such that following HFHF diet there is a significant increase in RFP/+ mice but not RFP/RFP mice since they lack CCR2 signaling and thus the ability to recruit peripheral macrophage to the brain. What may account for the low, yet not absent level of Ly6C⁺ macrophages in the RFP/RFP mice may be due to Ly6C expression on perivascular macrophage that traffic to the brain vasculature early in development and are long lived. Within the Ly6C⁺ macrophage population the majority of cells are CD45^{high}, further suggesting these are peripherally derived macrophages, **figure 3.6G**. While there are no significant changes in the frequency of MHCII⁺CD45^{high}Ly6C⁺ macrophages, **figure 3.6H**, further investigation of this population may reveal altered cytokine secretion or evidence of increased phagocytosis.

Studies have indicated that CCR2 competent cells, such as Ly6C⁺ macrophages, protect against AD-like pathology in a mouse model (Naert and Rivest, 2012). Our data shows a significant increase in frequency of CCR2⁺Ly6C⁺ macrophages in HFHF RFP/+ mice as compared to CD RFP/+ mice, **figure 3.6J**. The detectable levels of CCR2⁺Ly6C⁺ macrophages in both HFHF and CD RFP/RFP mice may be evidence of perivascular macrophages, however since this is a small population we are also not able to rule out background signaling. Follow up analysis of tissue sections stained for markers of peripheral macrophages may further support the hypothesis that these are perivascular macrophages. In further support of the hypothesis that trafficking

populations of peripheral immune cells are protective against neuroinflammatory disease we found in female 5xSBE mice genotype dependent changes in the kinetics of neuroinflammation in response to HFHF diet, **figure 3.7F**. 5xTg_SBE mice on HFHF diet overall showed a decrease in change from baseline average radiance with a significant decrease from 5xNon-Tg_SBE HFHF mice, suggesting that brain's response to HFHF diet is blunted when HFHF diet is compounded with AD-like pathology. Analysis of average radiance (a surrogate for TGF β levels) at 8 weeks of diet showed a significant decrease in 5xNon-Tg_SBE HFHF mice as compared to 5xNon-Tg_SBE CD mice and overall lower levels in 5xTg-SBE mice independent of diet, **figure 3.7G**. These results suggest that both diet and AD-like pathology suppress the TGF β response in the brain. TGF β is known to have anti-inflammatory roles, thus decrease in TGF β response could indicate decreased regulation of neuroinflammation. Further assessment of changes in brain cytokine profile may support this hypothesis. Overall our data has shown that HFHF diet does alter both populations of PBMCs as well as populations of immune cells in the brain and that traffic to the brain. In addition, HFHF diet-induced chronic peripheral inflammation was shown to compound with AD-like pathology to alter the kinetics of neuroinflammatory response in the brain. These studies support the use of this model of diet-induce chronic peripheral inflammation to study the role of peripheral inflammation, trafficking peripheral immune cell populations, and cytokine signaling, such as TNF, in the progression of AD-like pathology.

3.7 Summary

Our findings demonstrate that chronic low-grade peripheral inflammation that is associated with conditions such as metabolic syndrome and obesity, alters peripheral immune cell populations and trafficking of these populations to the brain. Male, as compared to female, mice showed greater

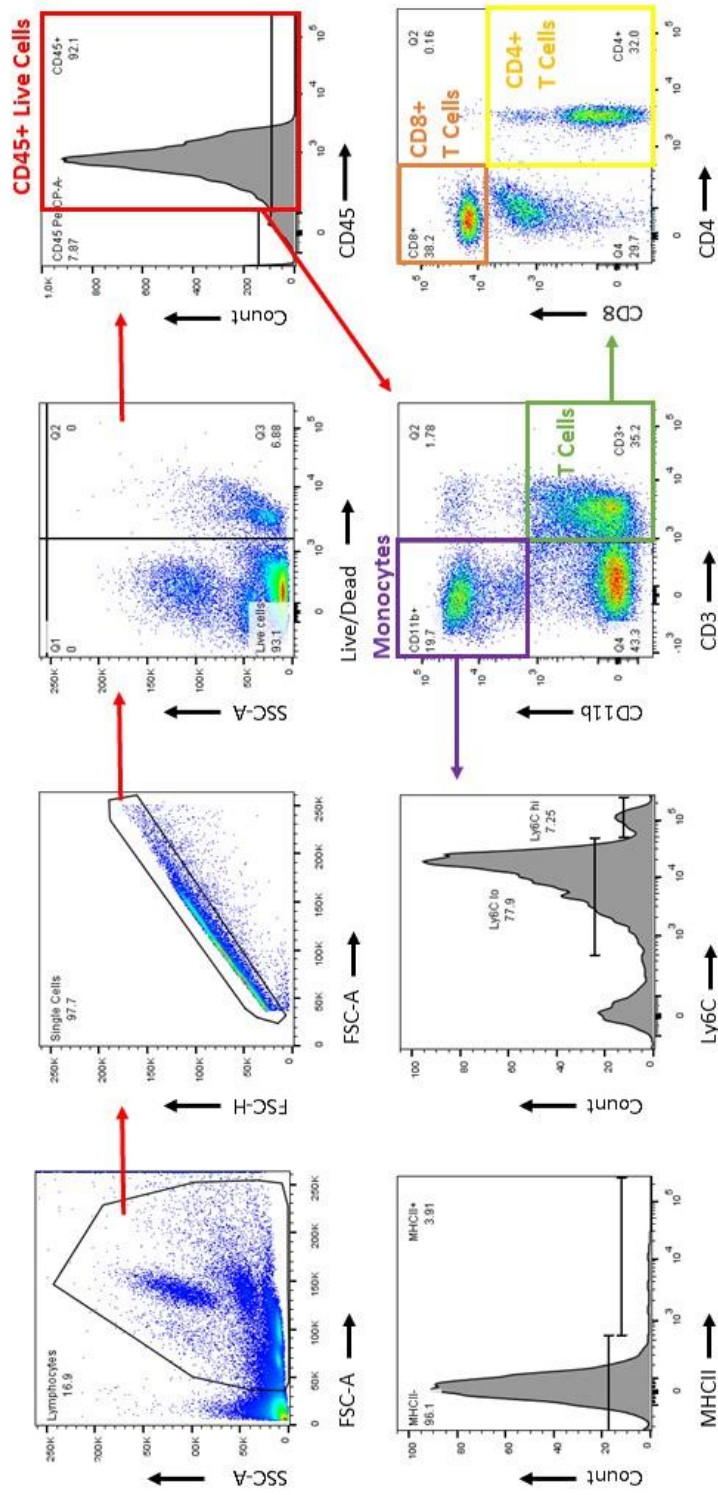
change in PBMC populations from baseline with HFHF diet; however, despite few changes in PBMC populations, female mice showed suppressed TGF β neuroinflammatory responses following HFHF diet. In addition, the kinetics of the neuroinflammatory response was altered in male mice with on-going AD-like pathology (5xTg_SBE) as compared to male mice without AD-like pathology (5xNon-Tg_SBE). Together the data from this study suggest that chronic low-grade peripheral inflammation, a condition that increases risk for developing AD in human populations, modulates not only peripheral immune cell populations but the trafficking of those populations to the brain, and represents a new model in which to study the impact of dietary changes on the progression of AD-like pathology.

Ingredients (g/kg)	TD.150111 SFA Rich Diet with Fructose	TD.150112 Control Diet
Casein	180.0	180.0
L-Cystine	3.0	3.0
Corn Starch	31.0	404.492
Maltodextrin	95.5	155.0
Sucrose	100.0	100.0
Fructose	290.0	-
Milkfat	185.0	10.0
Beef Tallow	18.0	-
Soybean Oil	-	50.0
Cellulose	50.0	50.0
Mineral Mix	35.0	35.0
Vitamin Mix	10.0	10.0
Choline Bitartrate	2.5	2.5
TBHQ, antioxidant	0.04	0.008
Total	1000.000	1000.000

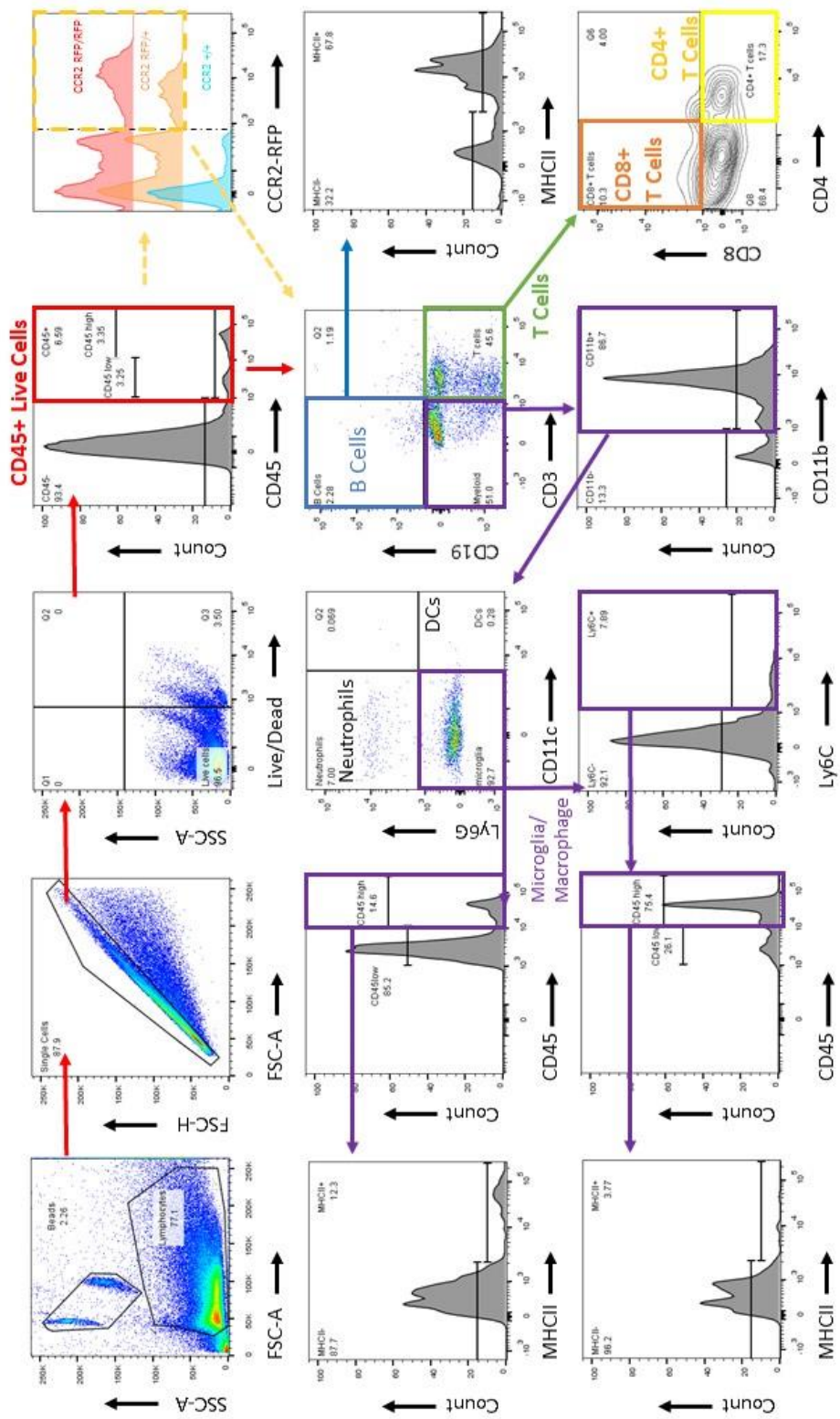
Table 3.1 – Special diet ingredient composition. To assess the effect of diet-induced peripheral inflammation on neuroinflammation, 5xSBE male and female mice received either HFHF diet or CD for 8 weeks and CCR2-RFP and B6 mice received either HFHF diet or CD for 5 weeks.

Nutrients	TD.150111 SFA Rich and Fructose Diet	TD.150112 Control Diet
Protein, g/Kg	159.6	159.6
CHO, g/Kg	520.5	623.2
Fat, g/Kg	204.8	61.8
Fiber (NDF), g/Kg	50	50
ME, kCal/g	4.56	4.56
Cholesterol, mg/Kg	529.3	61.6
SFA, g/Kg	130.101	14.01
MUFA, g/Kg	65.645	14.83
PUFA, g/Kg	7.051	30.95
n-3, g/Kg	1.033	4.05
n-6, g/Kg	6.018	26.9
4:0, g/Kg	7.03	0.38
6:0, g/Kg	4.255	0.23
8:0, g/Kg	2.035	0.11
10:0, g/Kg	3.7	0.2
12:0, g/Kg	5.735	0.31
14:0, g/Kg	22.239	1.17
14:1, g/Kg	1.48	0.08
15:0, g/Kg	3.194	0.16
16:0, g/Kg	53.15	8.12
16:1, g/Kg	4.127	0.19
17:0, g/Kg	1.565	0.07
18:0, g/Kg	27.013	3.25
18:1, g/Kg	59.136	14.52
18:2, g/Kg	5.761	26.89
18:3, g/Kg	1.033	4.05

Table 3.2. Calculated nutrient composition and fatty acid profile. To assess the effect of diet-induced peripheral inflammation on neuroinflammation, 5xSBE male and female mice received either HFHF diet or CD for 8 weeks and CCR2-RFP and B6 mice received either HFHF diet or CD for 5 weeks.



Supplemental figure 3.1 – Gating strategy for PBMC immune cell populations isolated from C56Bl-6J and 5xSBE mice. Single-cell lymphocytes were gated based on Forward Scatter Height (FSH) (size) and Side Scatter Height (SSH) (granularity) and then by FSH by FSA (Forward Scatter Area). Live cells were then selected as the Fixable Aqua-negative population. From the PBMC live-cell populations, CD45⁺ cells were gated for CD3⁺ T cells and CD11b⁺ myeloid cells. All CD3⁺ T cells were then gated for CD4⁺ and CD8⁺, while all CD11b⁺ myeloid cells were gated for MHCII⁺ and MHCII⁻ and Ly6C^{high} and Ly6C^{low} from the histogram distribution.



Supplemental figure 3.2 – Gating strategy for brain immune cell populations isolated from CCR2-RFP mice. CCR2-RFP mouse brain live-cell populations, CD45⁺ cells were gated for CD3⁺ T cells and CD19⁺ B cells. All CD3⁺ T cells were then gated for CD4⁺ and CD8⁺. The CD3⁻CD19⁻ cell population was gated for CD11c (dendritic cells) and Ly6G (neutrophils) and the CD11c⁻Ly6G⁻ (microglia/macrophage) population was gated for Ly6C^{high} and Ly6c^{low} and CD45^{high} and CD45^{low} from the histogram distribution. CD45^{high} (peripheral macrophage and activated microglia) and CD45^{low} (homeostatic microglia) were gated for MHCII⁺ and MHCII⁻ from the histogram distribution. To determine the immunophenotype of CCR2⁺ cells, total CD45⁺ cells were also gated for CCR2⁺ before applying the same gating strategy beginning with gating for CD3⁺ T cells and CD19⁺ B cells.

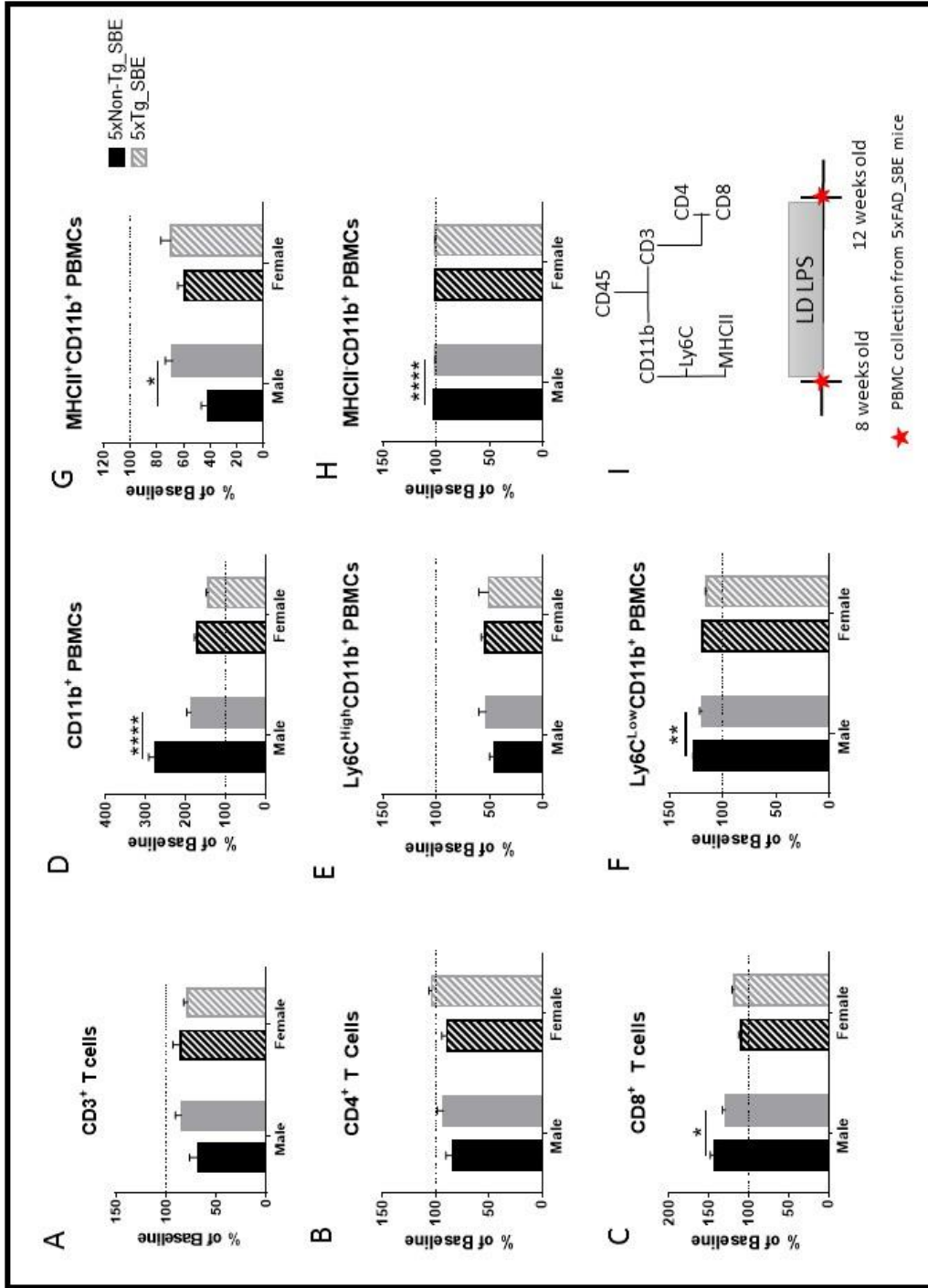


Figure 3.1 PBMC populations in male mice are altered by low-dose LPS-induced peripheral inflammation PBMCs were collected at baseline and following 4 weeks LD LPS from 5xTG_SBE and 5xNon-Tg_SBE mice (**I**). While no significant effects were seen in CD3⁺ T cell change from baseline (**A**), or CD4⁺ T cells change from baseline within CD3⁺ T cell (**B**), 5xTg_SBE male, but not female, mice showed significant decrease in the change of CD8⁺ T cells from baseline as compared to 5xNon-Tg_SBE male mice * $p < 0.05$ (**C**). 5xTg_SBE male, but not female, mice also show a significant decrease in the change of CD11b⁺ PBMCs from baseline as compared to 5xNon-Tg_SBE male mice **** $p < 0.0001$ (**D**). While there were no effects within the change of Ly6C^{high}CD11b⁺ PBMC population from baseline (**E**), 5xTg_SBE male, but not female, mice showed significant decreased in the change of Ly6C^{low}CD11b⁺ PBMCs from baseline as compared to 5xNon-Tg_SBE male mice ** $p < 0.01$ (**F**). The change of MHCII⁺CD11b⁺ PBMCs from baseline was significantly increased in 5xTg_SBE male, but not female, mice as compared to 5xNon-Tg_SBE mice * $p < 0.05$ (**G**). This complements the significant decreased in the change of MHCII⁻CD11b⁺ PBMCs from baseline in 5xTg_SBE male, but not female, mice as compared to 5xNon-Tg_SBE mice **** $p < 0.0001$ (**H**).

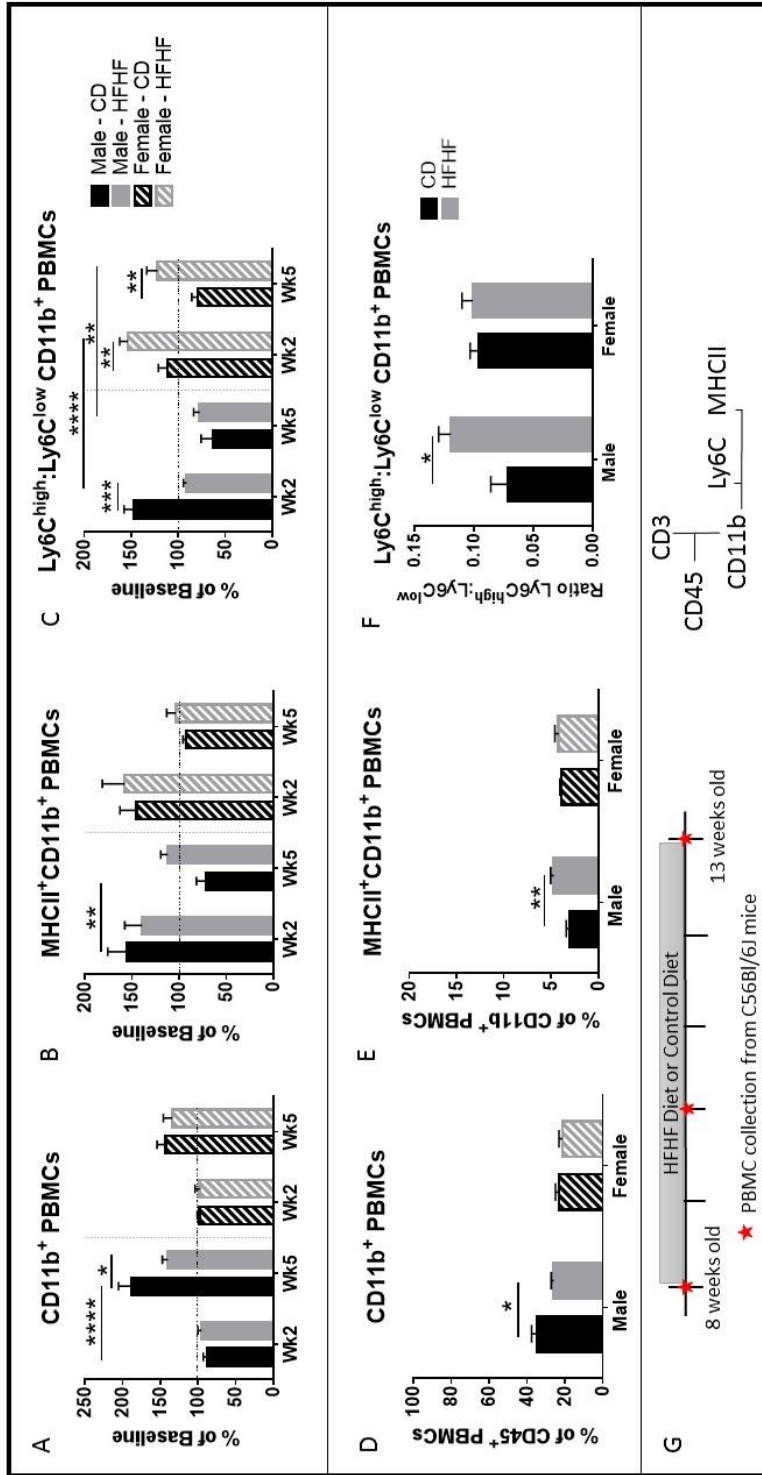


Figure 3.2 HFHF diet induced dynamic changes within CD11b⁺ myeloid PBMC populations in both male C57Bl/6J mice. T cell and myeloid PBMC populations were assessed in male and female C56Bl/6J mice fed either a high-fat high fructose diet or control diet at baseline, 2 weeks, and 5 weeks on diet (**G**). Within the myeloid PBMC populations the overall CD11b⁺ PBMC population change from baseline was significantly increased in male mice on CD diet at week 5 as compared to male mice on CD diet at week 2 **** $p < 0.0001$ (**A**) as well as from male mice on HFHF diet at week 5 * $p < 0.05$ (**A**). At week 5 there was a significant decrease in frequency of CD11b⁺ PBMCs in HFHF male mice as compared to CD males, but no effect of diet within female mice ** $p < 0.01$ (**D**). Within the CD11b⁺ myeloid population frequency of the MHCII⁺ CD11b⁺ myeloid population from baseline was significantly decreased in CD males, but not HFHF males, at week 5 as compared to week 2 ** $p < 0.01$ (**B**). At 5 weeks, the frequency of MHCII⁺CD11b⁺ myeloid cells was significantly increased in male, but not female mice ** $p < 0.01$ (**E**). HFHF female mice showed a significant increase as compared to CD female at week 2 and week 5 from baseline in the ratio of Ly6C^{high}:Ly6C^{low} CD11b⁺ myeloid population ** $p < 0.01$ (**C**). At week 2 and week 5 HFHF female mice had significantly increased change from baseline as compared to HFHF male mice **** $p < 0.0001$, *** $p < 0.01$ (**C**). In contrast to these results HFHF male mice showed a significant decrease at week 2 from CD male mice in the Ly6C^{high}:Ly6C^{low} CD11b⁺ myeloid change from baseline *** $p < 0.001$ (**C**). At 5 weeks, the ratio of Ly6C^{high}:Ly6C^{low} CD11b⁺ myeloid population was significantly increased in male, but not female mice * $p < 0.05$ (**F**).

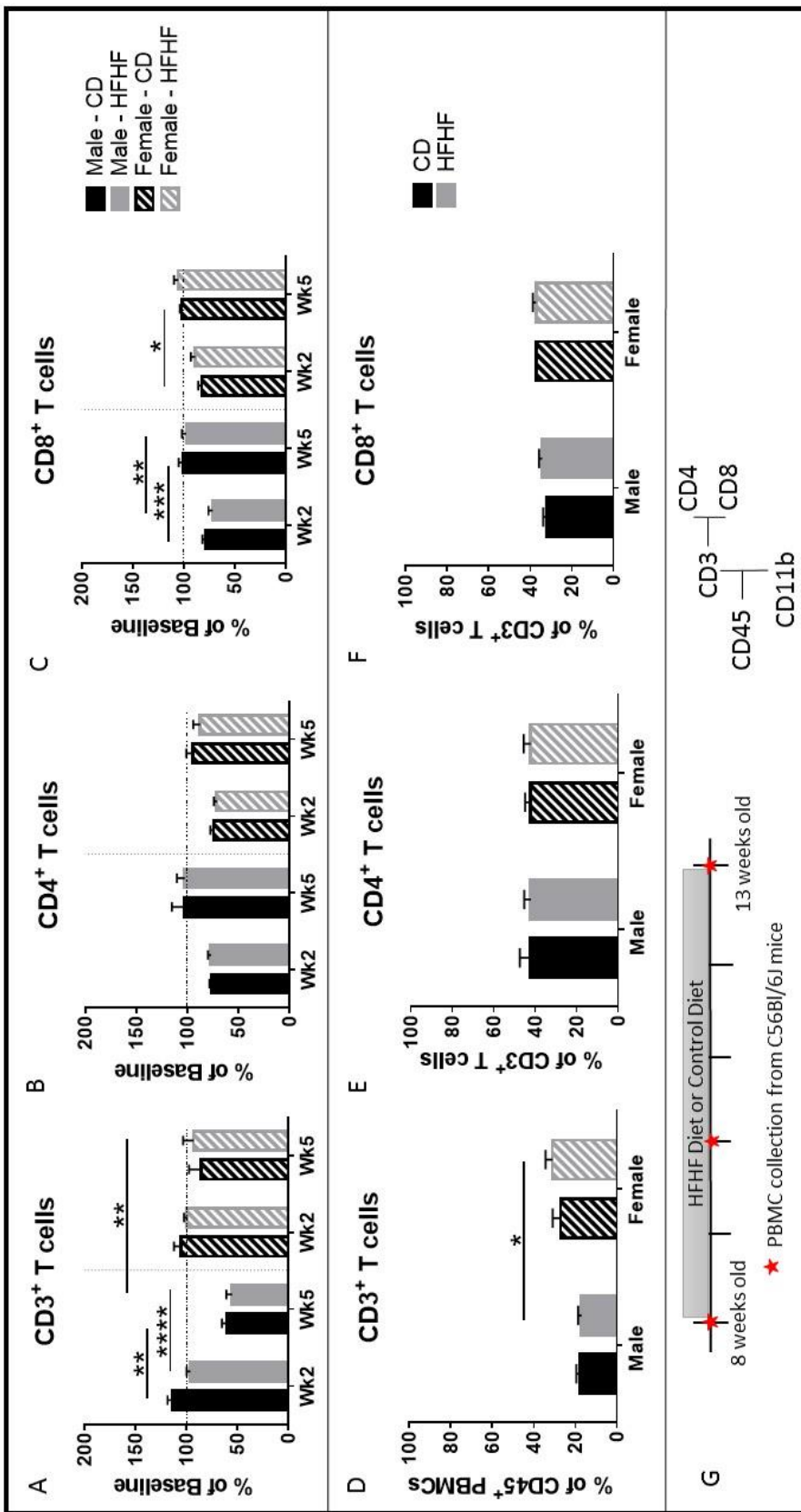


Figure 3.3 T cell populations show resistance to changes induced by HFHF-dependent peripheral inflammation. CD3⁺ T cell PBMC populations from C56Bl/6J mice fed 5 weeks of either HFHF or Control diet (**G**) was significantly decreased at week 5 from week 2 in both CD and HFHF diet groups, **** $p < 0.0001$, ** $p < 0.01$ (**A**). While no effects of diet were found in female mice the % change from baseline in male HFHF mice was significantly lower than female HFHF mice at 5 weeks ** $p < 0.01$ (**A**). At 5 weeks, the frequency of CD3⁺ T cells was significantly higher in female HFHF diet mice as compared to male HFHF diet mice * $p < 0.05$ (**D**). Within the T cell population, no significant changes from baseline were found within the CD4⁺ T cell population across diet or sex (**B**) nor at the 5 week end point (**E**). Within the CD8⁺ T cell population significant changes from baseline were found in male and female mice on CD diet as well as male mice on HFHF diet * $p < 0.05$, ** $p < 0.01$, *** $p < 0.001$ (**C**), however after 5 weeks of diet no significant effect were found in the frequency of CD8⁺ T cells (**F**).

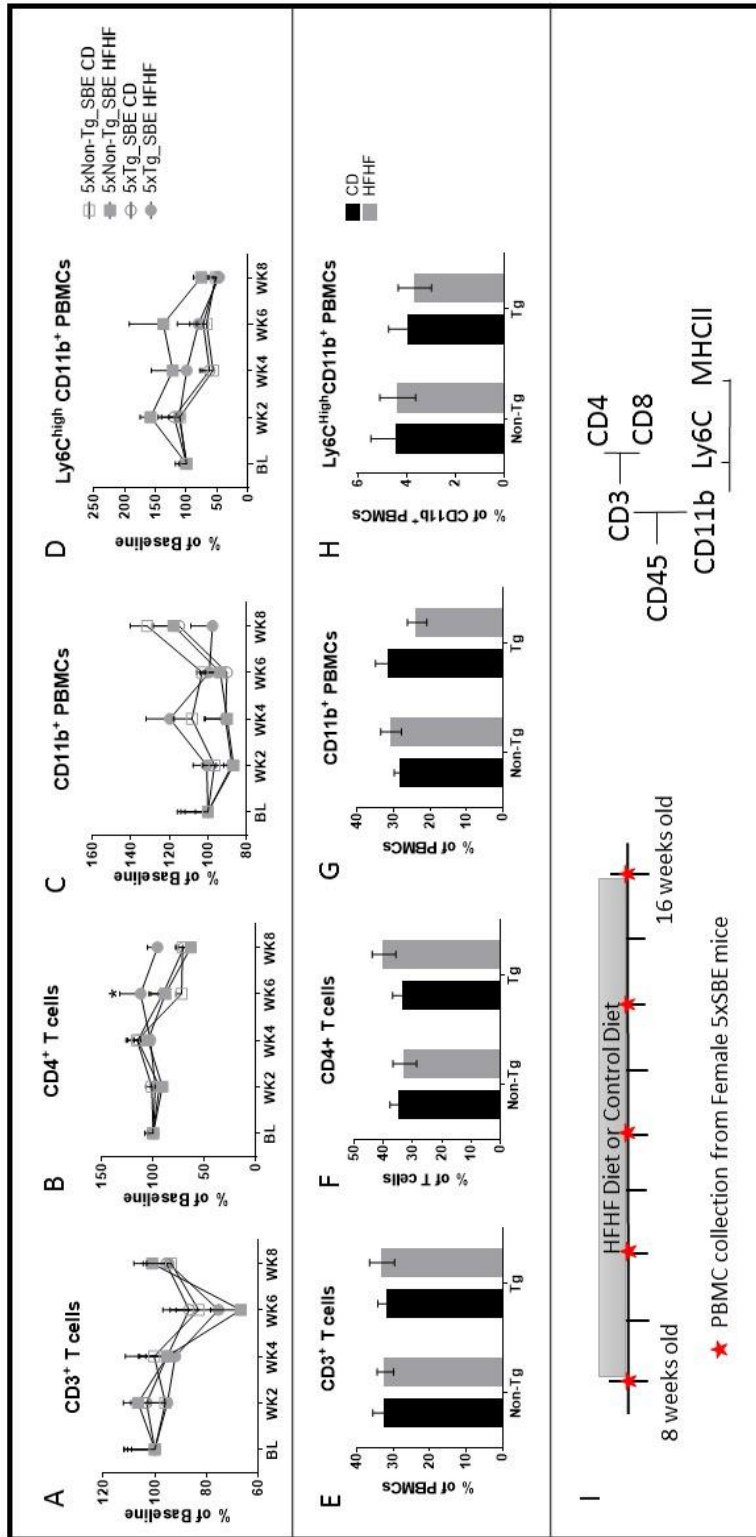


Figure 3.4 PBMC populations in female 5xSBE mice are resilient to changes induced by diet-dependent chronic peripheral inflammation. PBMCs were collected at baseline and every two weeks from 5xSBE_Non-Tg and 5xSBE_Tg female mice fed either HFHF diet or CD for 8 weeks (**I**). A significant effect of week on diet was found the dynamics of the CD3⁺ T cell population, however (**A**), or at 8 weeks in the frequency of CD3⁺ T cells, (**E**). Within the CD3⁺ T cell population changes were found in the dynamic response of the CD4⁺ T cell population a significant effect of week by 2-way ANOVA **** $p < 0.0001$ (**B**) post hoc analysis revealed a significant increase in CD4⁺ T cells from baseline in 5xTg_SBE HFHF mice as compared to 5xNon-Tg_SBE CD mice at 6 weeks of diet * $p < 0.05$ (**B**), however no effects of diet were seen in the frequency of CD4⁺ T cells at the 8 week PBMC snapshot (**F**). A significant effect of week on diet was found the dynamics of the CD11b⁺ PBMC population from baseline by 2-way ANOVA * $p < 0.05$, (**C**), however no effects were found within weeks by post hoc analysis (**C**), or at 8 weeks in the frequency of CD11b⁺ PBMCs (**G**). Within the CD11b⁺ PBMC population significant effects of both week and genotype were found in the Ly6C^{high}CD11b⁺ PBMC change from baseline (significant effect of week: $p < 0.001$; genotype: $p < 0.05$) (**D**), however no effects were seen within weeks by post hoc analysis (**D**), or at 8 weeks in the frequency of Ly6C^{high}CD11b⁺ PBMCs (**H**).

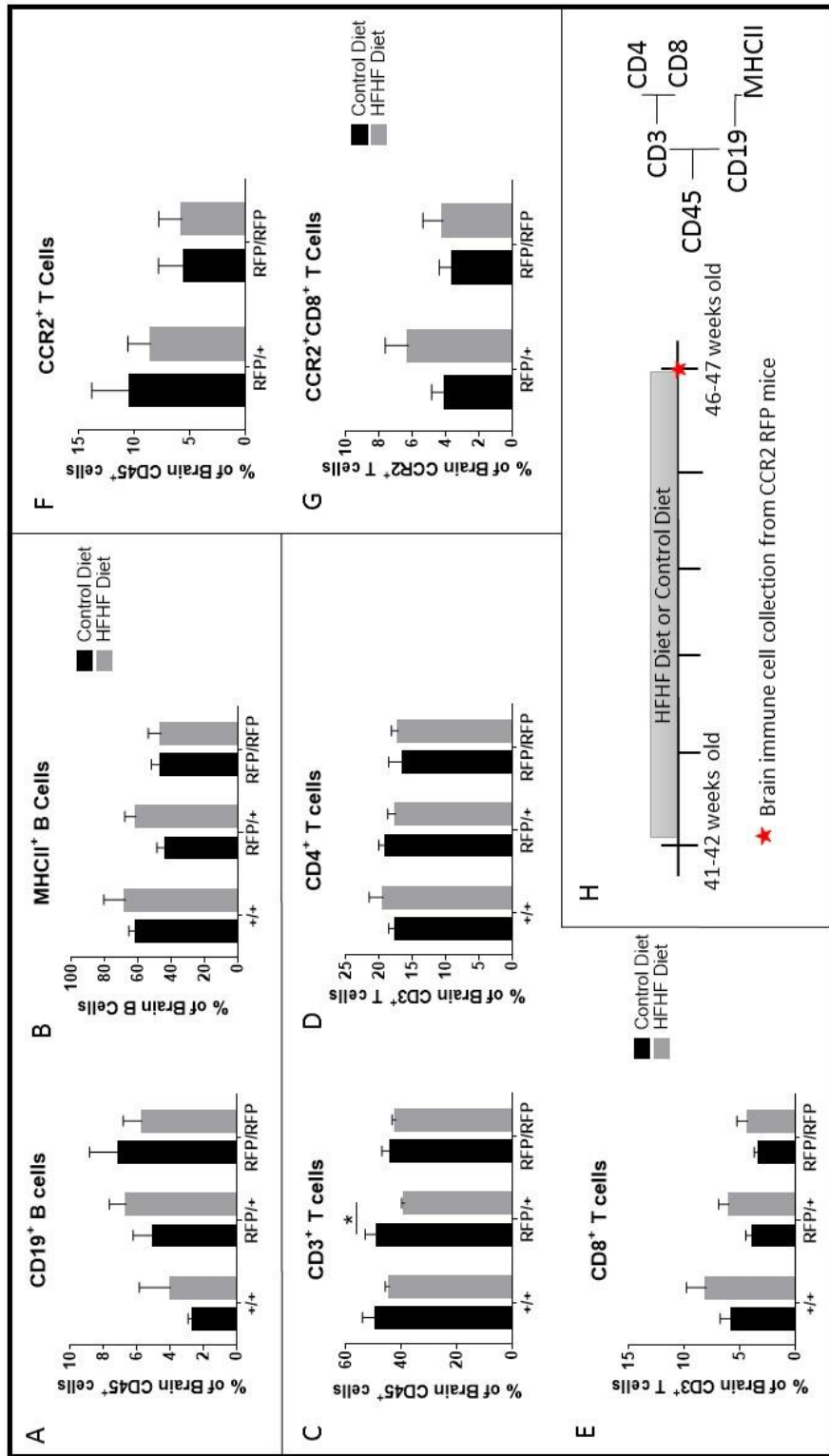


Figure 3.5 HFHF diet reduces frequency of CD3⁺ T cell populations trafficking to the brain in CCR2 RFP/+ mice. Following 5 weeks of either CD or HFHF diet in aged, male and female, CCR2 RFP mice (**H**) no changes in frequency of B cells (**A**) or frequency of MHCII⁺ B cells capable of antigen presentation (**B**) trafficking to the brain were detected across diet or genotype. A significant decrease in the brain CD3⁺ T cells population was found in RFP/+ mice following HFHF diet * $p < 0.05$ (**C**). Within the CD3⁺ T cell population there were no detectable changes in the CD4⁺ T cell population (**D**), however within the CD8⁺ T cell population significant effects of both diet ($p = 0.0399$) and genotype ($p = 0.0449$) by 2-way ANOVA were found although post hoc analysis did not reveal any significant effects of diet within genotypes (**E**). No significant changes were found in number cells within the T cell populations, data not shown. Analysis of the CCR2⁺ RFP populations within the brain of RFP/+ and RFP/RFP mice did not reveal significant changes in the CCR2⁺ CD3⁺ T cell populations across genotype of diet (**F**), nor within CCR2⁺ CD8⁺ T cell populations (**G**).

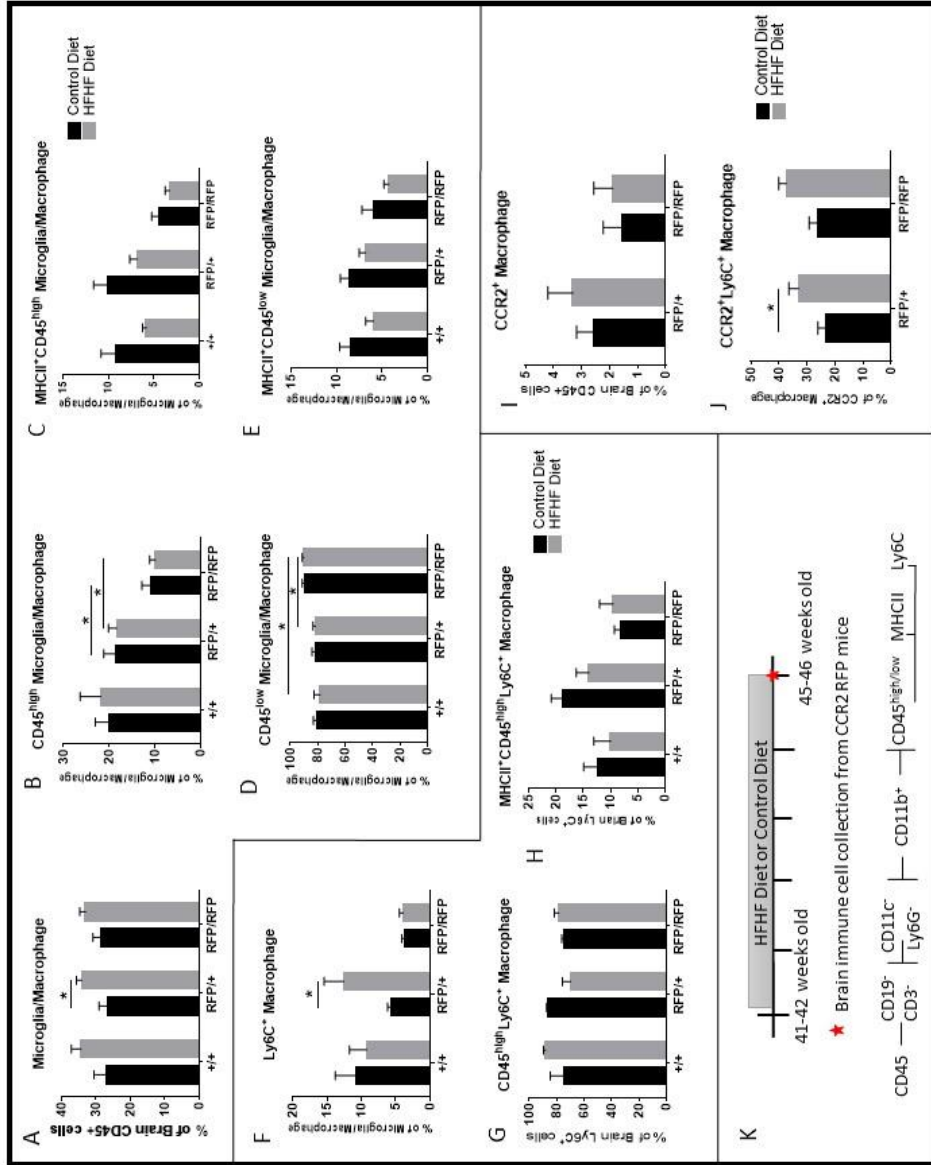


Figure 3.6 HFHF diet alters CD11b⁺ microglia/macrophage population within and trafficking to the brain. Following 5 weeks of either CD or HFHF diet in aged, male and female, CCR2 RFP mice (**K**) a significant effect of diet ($p = 0.0070$) was found by 2 Way ANOVA within the CD11b⁺ myeloid population the CD11b⁺Ly6G⁻CD11c⁻ microglia/macrophage population and post hoc analysis revealed a significant increase in the frequency but not number of microglia/macrophage population following HFHF diet in RFP/+ mice * $p < 0.05$ (**A**). Within the CD11b⁺ microglia there was a significant effect of genotype in the frequency of CD45^{high}CD11b⁺ microglia/macrophage by 2-way ANOVA ($p = 0.0012$), post hoc analysis revealed significant decreases in the frequency of CD45^{high}CD11b⁺ microglia/macrophages in RFP/RFP mice as compared to RFP/+ mice within CD and HFHF diet * $p < 0.05$ (**B**). Within this population of activated microglia and peripheral macrophages (CD45^{high}CD11b⁺ microglia/macrophages) the frequency, but not count, of MHCII⁺CD45^{high} microglia/macrophages population showed significant effects of both diet ($p = 0.0388$) and genotype ($p = 0.0035$) by 2-Way ANOVA, however post hoc analysis did not reveal any significant effects of diet within genotype (**C**). Significant effect of genotype was found in the frequency, but not count, of homeostatic/resting microglia (CD45^{low}CD11b⁺ microglia) by 2-way ANOVA ($p = 0.0010$), post hoc analysis revealed a significant increase in HFHF RFP/RFP mice as compared to both HFHF RFP/+ and HFHF +/+ mice * $p < 0.05$ (**D**). Within this population of homeostatic/resting microglia (CD45^{low}CD11b⁺ microglia) no significant changes were found in the frequency or count of MHCII⁺CD45^{low}CD11b⁺ microglia (**E**). Frequency, but not count, of Ly6C⁺CD11b⁺ macrophage was increased in RFP/+ mice following HFHF diet as compared to CD RFP/+ mice (**F**). Within the Ly6C⁺ macrophage population the majority of cells are CD45^{high}, no effects of diet or genotype by 2-way ANOVA (**G**). No effects of diet or genotype were found in frequency, or count (data not shown), of

MHCII⁺Ly6C⁺CD45^{high} macrophages (**H**). Analysis of the CCR2⁺ RFP populations within the brain of RFP/+ and RFP/RFP mice did not reveal significant changes (**I**). Within this population, a significant effect of diet ($p = 0.0054$) was found by 2-way ANOVA of CCR2⁺Ly6C⁺CD11b⁺ macrophages and post hoc analysis revealed a significant increase in HFHF RFP/+ mice as compared to CD RFP/+ mice * $p < 0.05$ (**J**).

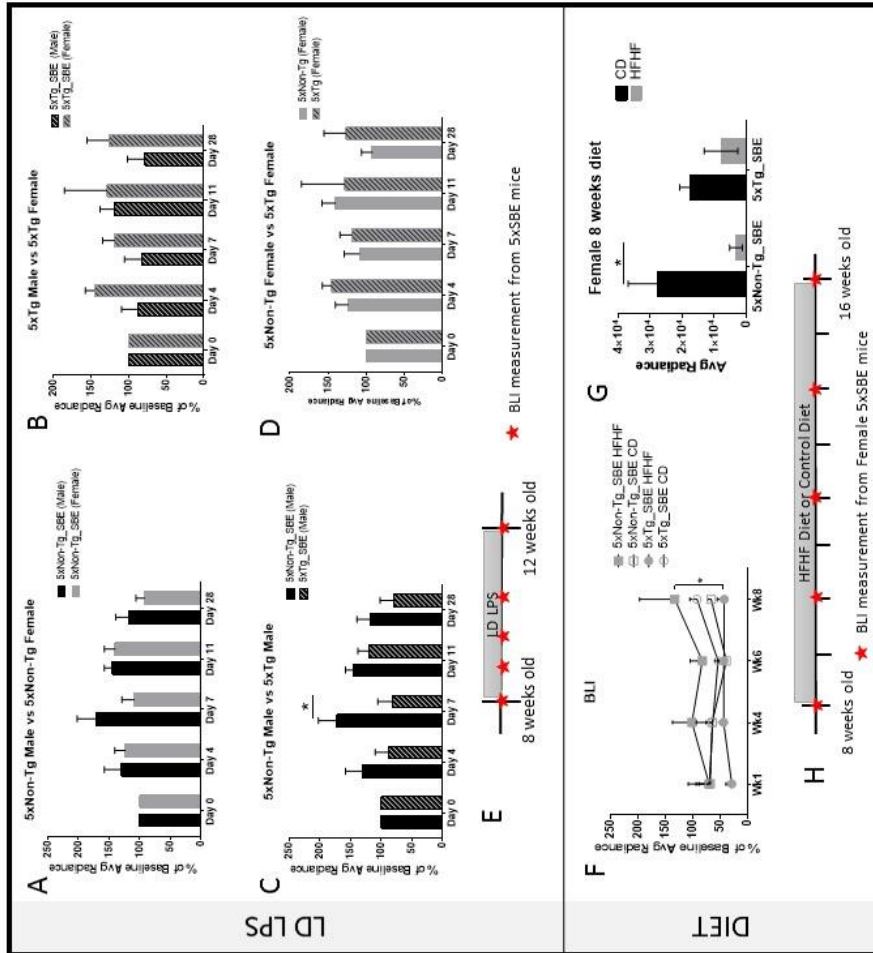


Figure 3.7 Peripheral inflammation from both LD LPS and HFHF diet alters the neuroinflammatory response in 5xTg_SBE mice. BLI measurements were collected at baseline and during intervention to assess levels of TGF β in 5xSBE mice were dosed with either LD LPS for 4 weeks (**E**) and 5xSBE_Non-Tg and 5xSBE_Tg female mice fed either HFHF diet or CD for 8 weeks (**H**). A trend for effect of day was found following LD LPS in percent change in BLI from baseline in 5xNon-Tg_SBE mice ($p = 0.0685$, by 2-way ANOVA) no significant effects of sex within days were found in percent change in BLI from baseline by post hoc analysis (**A**). Within LD LPS treated 5xTg_SBE mice there was a significant effect of sex ($p = 0.0372$, by 2-way ANOVA) in percent change in BLI from baseline, however post-hoc analysis revealed no significant effects (**B**). Within male, but not female (**D**), 5xSBE mice there is significant effect of genotype ($p = 0.0074$, by 2-way ANOVA) on percent change in BLI from baseline, post hoc analysis revealed a significant decrease in percent change in BLI from baseline at day 7 in 5xTg_SBE male mice as compared to 5xNon-Tg_SBE male mice * $p < 0.05$ (**C**). Following 8 weeks of either HFHF or control diet a significant effect of genotype ($p = 0.0123$, by 2-way ANOVA) was found in percent of baseline BLI in female 5xSBE mice (**F**), post hoc analysis revealed a significant decrease in percent of baseline BLI of 5xTg_SBE HFHF mice as compared to 5xNon-Tg_SBE HFHF mice at 8 weeks * $p < 0.05$ (**F**). At 8 weeks, a significant decrease in average radiance was found in 5xNon-Tg_SBE HFHF mice as compared to 5xNon-Tg_SBE CD mice * $p < 0.05$ (**G**).

Chapter 4:

Conclusions

4.1 Summary of Results

4.1.1 *Peripheral immune cell trafficking patterns in a mouse model of AD-like pathology*

Supported by previous findings that peripheral immune cells are found in the brain and play a role in AD pathology (Togo et al., 2002; Rosenkranz et al., 2007; Jay et al., 2015; Meyer-Luehmann and Prinz, 2015), we first investigated the extent to which peripheral innate and adaptive immune cells traffic to the brain in a mouse model of AD-like pathology. We found both T cells and myeloid cells with cellular markers suggestive of a peripheral (non-brain) origin in the brains of 5xFAD mice. Importantly, our work shows the trafficking patterns of these immune cell subsets change with increasing AD-like pathology. We found that while a significant increase in the overall frequency of CD3⁺ CD8⁺ T cells does not occur until late (12 months), a shift in the dynamics of the CD8⁺ T cell trafficking does occur between 3.5 and 5 months of age in Tg 5xFAD mice relative to non-Tg mice. This time period coincides with reports of early stages of synaptic loss. Following this disruption in CD8⁺ T cell trafficking regulation, we show at 5 and 7 months of age a shift in the activation of myeloid cells within the brain, specifically a decrease in the frequency of CD45^{high}MHCII⁺CD11b⁺ cells and a shift in the ratio of Ly6C^{high}:Ly6C^{low} in favor of Ly6C^{low} myeloid cells. Together these data suggest that populations of myeloid cells that are trafficking to the brain have an alternative activation status in Tg as compared to non-Tg mice, including their ability to present antigen to CD4⁺ T cells. Together these shifts in trafficking populations may underlie mechanisms of AD-like pathophysiology. In support of this, CD8⁺ T cells are cytotoxic (Harty et al., 2000) and trafficking of peripheral macrophages has been shown to suppress AD-like pathology in CCR2-RFP mice crossed

to Tg 2576 mouse model of AD (El Khoury et al., 2007), thus decreased activation of this population may signal impairments in their normal regulatory function.

Within the deep cervical lymph nodes (DCLNs) we found evidence of altered patterns of immune cell activation and trafficking. Specifically, Tg mice showed significantly increased populations of naïve T cells and significantly decreased populations of effector T cells. These results suggest that either altered differentiation or retention of T cells occurs in the draining lymph nodes of the brain with AD-like pathology as early as 5 months of age. No evidence of peripheral inflammation was found in the plasma or within the CSF of Tg mice at this time point, suggesting that these changes are in response to neuroinflammatory responses within the brain. These altered trafficking patterns associated with progression of AD-like pathology suggest that modulation of immune cell trafficking patterns early in the course of AD progression may represent an opportunity for therapeutic intervention.

4.1.2 Regulation of peripheral immune cell trafficking patterns via soluble TNF (sTNF)-dependent signaling

We have shown that inhibition of sTNF signaling with the use of the dominant-negative sTNF inhibitor XPro1595 results in alterations in peripheral immune cell trafficking patterns in the brain of Tg mice. Our data show that with inhibition of sTNF in Tg mice, the ratio of Ly6C^{high}:Ly6C^{low} is significantly decreased. This shift is opposite in direction as compared to the shift between Tg and non-Tg mice, suggesting that this shift may be restoring the activation status in myeloid populations trafficking into the brain. Our

data support the idea that sTNF signaling is responsible for the decrease in the frequency of CD45^{high}MHCII⁺CD11b⁺ cells in Tg mice as compared to non-Tg mice, suggesting loss of this specific population may be an adaptive response to AD-like pathology. The frequency of CD3⁺ T cells, specifically CD4⁺ effector T cells, was decreased with inhibition of sTNF signaling. Further investigation into specific CD4⁺ T helper subsets may reveal the specific effect of reduction in this population given that CD4⁺ effector T cells have a variety of functions (Luckheeram et al., 2012).

Inhibition of sTNF was also associated with amelioration of AD-like pathology. Albeit small in magnitude, a significant decrease in A β -plaque pathology was found in mice treated with XPro1595. Specifically, inhibition of sTNF signaling reversed the impaired LTP found in Tg mice as compared to vehicle-treated-Tg mice. While we are not able to conclude that changes in peripheral immune cell trafficking directly mediated this rescue of impaired LTP, a recent trial of a TNF inhibitor (Enbrel) that does not penetrate the brain showed non-significant but promising results in stabilizing cognitive decline in patients with AD (Butchart et al., 2015), suggesting that TNF signaling inhibition in the periphery (and potentially changes in immune cell traffic to the CNS and/or their activation status) may have indirectly contributed to improved functional outcome in the 5xFAD model of AD-like pathology.

4.1.3 Effects of chronic inflammation on peripheral immune cell trafficking and brain neuroinflammatory response

In a mouse model of AD-like pathology, we found that peripheral immune cell populations that traffic to the brain during development of A β -plaque pathology can be modulated with chronic peripheral inflammation. In a model devoid of A β pathology, we observed a larger frequency of Ly6C⁺ macrophages in the brain in CCR2 RFP/+ mice fed a high-caloric diet and this increase was associated with an increase in the frequency of the CD45^{high} myeloid population. These results suggest that in response to high-caloric diet there is activation of microglia populations along with an influx of peripheral macrophages. Independent of diet, we found a decrease in the frequency of CD45^{high} myeloid cells in CCR2 RFP/RFP mice (functionally devoid of surface CCR2) and a corresponding increase in the frequency of CD45^{low} myeloid cells. These results suggest CCR2-dependent mechanisms are required to elicit activation of brain-resident myeloid (microglia) cells potentially via latent trafficking of peripheral myeloid populations into the brain; however, trafficking of peripheral macrophages into the brain under homeostatic conditions has been shown to be limited (Goldmann et al., 2016). Our data have shown that overall trafficking of CD3⁺ T cells is reduced following high-caloric diet in RFP/+ mice and within the CD8⁺ T cell population we found a significant effect of diet across genotypes. Together, these data suggest that changes in T cell populations following high-caloric diet may have contributed to the neuroinflammatory changes we observed in the brain following high-caloric diet. While PBMC populations in male vs female mice show more changes in response to LD LPS and high-caloric diet, both male and female mice showed altered dynamic responses in the ratio of Ly6C^{high}:Ly6C^{low} myeloid cells; however, the responses

were opposite in direction. This suggests that while this population is sensitive to the effects of diet that sex-specific conditions lead to alternate responses. While few changes in responses to diet were found in PBMC populations in female mice, changes were seen within the dynamics of TGF β signaling in response to high-caloric diet and in a genotype-dependent manner. Together this set of data provides the ground work to further investigate the mechanism by which high-caloric diet-induced low-grade chronic peripheral inflammation contributes to acceleration of AD-like pathology and sheds a considerable amount of light on our understanding of the link between chronic peripheral inflammation and increased risk for AD.

4.2 Implications and Future Directions

4.2.1 Modulation of peripheral immune cell activation and/or their trafficking may be a potential therapeutic target

Here we have shown AD-like pathology, inhibition of sTNF, as well as chronic peripheral inflammation modulates peripheral immune cell trafficking to the brain. Our data suggests that modulation of trafficking patterns via inhibition of sTNF is protective while modulation via chronic peripheral inflammation may lead to dysregulation of the neuroinflammatory response. Our data indicate these changes in trafficking patterns occur in conjunction with A β accumulation but prior to reported significant neurodegeneration (Oakley et al., 2006) and our group has not found significant cognitive deficits at these early time points (unpublished observations). Thus, modulation of peripheral immune cell trafficking to the CNS is supported as an early intervention prior to detectable cognitive

deficits. However, further investigation into the direct effects of more specific subsets of trafficking populations is warranted. A recently published study found that the use of fingolimod, a drug that targets the sphingosine-1 receptor and acts by sequestering CCR7⁺ T cells populations within lymph nodes (Blaho et al., 2015), significantly reduced markers of AD-like pathology in the 5xFAD mouse model (Aytan et al., 2016). While fingolimod has also been shown to have direct effects on microglia (Blaho and Hla, 2014), this report also supports a role for modulation of T cell trafficking to the brain to treat AD pathology. Further support for this idea comes from the modulation of the timing of Treg trafficking in that temporary inhibition of Tregs improved AD-like pathology upon removal of Treg inhibition (Baruch et al., 2015). While sequestering subsets of immune cells may lead to potential negative side effects of overall immune function, modulation of trafficking patterns at the BBB either through inhibition of TNF signaling with etanercept (trade name Enbrel) or XPro1595, or modulation of adhesion molecules that regulate BBB permeability directly may lead to specific regulation of immune cell trafficking into the brain. Future studies on the effect of XPro1595 as compared to etanercept in the 5xFAD mouse will help to elucidate the direct versus indirect effects of sTNF signaling in modulating BBB permeability and immune cell traffic into the CNS. Further work investigating the BBB as a whole or region-specific changes, such as at the choroid plexus where the BBB is highly permeable, will enable investigators to determine the extent to which specific more BBB-targeted approaches can help mitigate the effects of chronic peripheral inflammation on AD-like pathology and/or may reveal whether modulation of trafficking patterns of specific immune cell subsets (i.e. increase entry of protective populations while minimizing entry

of cells that exacerbate inflammation and tissue damage) is also a plausible path forward to ameliorate disease progression.

4.2.2 Second-hit model of progression of AD-like pathology

While investigation of immune cell regulation in a mouse model of AD-like pathology that replicates the neuroinflammatory environment is crucial to understanding AD pathology in humans; understanding how various chronic inflammatory diseases increase risk for AD in human populations is also an unmet need. For this reason, we felt that identifying environmental conditions that modulate the traffic of immune cell populations into the brain could provide a more relevant model to study the dynamic changes in the peripheral circulation and brain-immune system network that occur during the course of AD-like pathology. This second-hit model, chronic peripheral inflammation in a mouse model of AD-like pathology, is a starting point to help us elucidate the mechanisms by which changes in the peripheral inflammation may disrupt peripheral immune cell populations to increase risk for AD. Using this model, we were able to further test our integrated hypotheses on the role of sTNF signaling in regulating the effects of peripheral inflammation on AD-like pathology as well as other mechanisms that may synergize with high-caloric diet to increase risk for AD in the human population. With this second-hit model, one can assess the contribution of genetic (5xFAD transgenes or other AD risk factor genes) as well as environmental (diet-induced peripheral inflammation) factors and their interaction to begin formulating hypotheses about how peripheral immune cell trafficking changes in at-risk human populations to contribute to the development of AD. In addition, the apolipoprotein E (ApoE) (important in lipid transport and metabolism)

ε4 allele has been linked to increased risk for AD (Tanzi, 2012). Investigation into how lipid handling is altered in a high-caloric diet models in conjunction with AD-associated transgenes to modulate AD-like pathology may reveal additional therapeutic targets beyond peripheral immune cell trafficking that may be more relevant to certain sub-populations of AD patients and could help us stratify subjects for clinical trials by enriching cohorts for those with the highest levels of central and peripheral inflammation and dysregulated immune cell phenotypes. Work in this area is the subject of ongoing studies in our laboratory.

4.2.3 Assessing changes in peripheral immune cell populations in at-risk human populations

The number of risk factors for sporadic AD suggests there may be several pathogenic routes to a single diagnosis, and identification of sub-populations of AD patients with greater immune dysfunction may reveal some such routes. While modulation of peripheral immune cell trafficking by chronic peripheral inflammatory conditions may work in an animal model, this has yet to be investigated in human populations. Reports suggest that peripheral macrophage function is impaired in AD patients (Fiala et al., 2005) however deep immunophenotyping by flow cytometry in human populations at risk for MCI or AD or even in patients with a clinical diagnosis of either MCI or AD the way the studies herein have been done in mice needs to be explored. While epidemiological data suggest that chronic NSAID use is protective against AD, clinical trials were unable to provide support for their use as an AD therapy (McGeer and McGeer, 2007). While this may be due to the timing of the intervention or the fact that they were dosed too late in the

course of AD, the negative results may have also been due in part to inclusion of a heterogeneous group of AD patients, some of which may have had less immune dysregulation or no underlying inflammatory diseases that we posit contribute to AD pathophysiology. To move forward with clinical trials of immune therapies that can modulate peripheral immune trafficking to the brain and neuroinflammation, we must first establish that populations of those individuals at risk for AD as well as those with a positive diagnosis of AD show dysregulation in peripheral T cell and monocyte populations that are potentially trafficking to the brain. To this end, our research group is in the early stages of investigating how sub-populations of myeloid cells and T cells are altered within the blood and within the CSF in populations at risk for AD because of mid-life hypertension (renin-angiotensin system dysfunction), metabolic syndrome or obesity, and parental history of AD. Furthermore, assessing how peripheral immune cell populations change within the blood and CSF of populations with decreased risk for AD, either genetic (ApoE ϵ 2 status) (Tanzi, 2012) or through drug interventions with chronic NSAIDs earlier in life (McGeer and McGeer, 2007) or with anti-hypertension medications (Forette et al., 2002), will further increase our understanding of the central and peripheral mechanisms that influence peripheral immune cell phenotype and trafficking patterns to the brain to promote chronic neuroinflammation and affect the course of AD.

4.2.4 *Revitalization of an aging immune system*

Age is the number one risk factor for AD and as we age, our immune system no longer functions with the same vitality, leading to a sort of age-related immunodeficient state also characterized with autoimmune responses as specialized immune cells begin

failing to recognize ‘self’ antigens as well as in our younger years (Goronzy et al., 2013). While the studies herein have not directly addressed the impact of an aging immune system, immune senescence may also be a contributing factor in aging human populations and play an important role in how trafficking of peripheral immune cell populations impact the brain and cognition. In AD patients, it has been shown that peripheral macrophages have decreased phagocytic functioning as compared to healthy aged matched controls (Fiala et al., 2005), suggesting that there is disease-related impairment in addition to immunosenescence. In our model, we saw evidence of an aging immune system at around 12 months of age (in spleen and DCLNs T cell memory populations were increased); and there were no effects of genotype within these populations, suggesting that immune system phenotype does display changes with age alone in our mice. Investigating peripheral immune cell trafficking patterns with age in a mouse model with slower progression of AD-like pathology such as the APP/PS1 mouse, may provide the opportunity to elucidate how age x diet x AD-like pathology interact to modulate onset or progression of AD-like pathology. Due to immune senescence and altered immune cell function the trafficking patterns found within these studies may be more pronounced. The effects of diet may also be more pronounced in an aging population. Our current work in the CCR2-RFP mouse model shows diet-induced changes in immune cell trafficking patterns at around 11 months of age and additional ongoing studies aimed at investigating this process in younger populations will begin to address the questions on the effects of immune senescence and peripheral immune cell traffic to the brain.

4.3 Conclusions

The novel findings contained herein involve the changes in peripheral innate and adaptive immune cell trafficking to the brain during the course of AD-like pathology and strongly suggest these patterns as well as synaptic function can be modulated via sTNF inhibitors and perhaps via other immunomodulatory interventions. Further work on elucidating the specific mechanisms that regulate these changes is warranted such as looking more closely at BBB and choroid plexus regulation and sub-populations of T cells retained within the DCLNs in response to AD-like pathology. Further investigation of the effects of high-caloric diet on brain neuroinflammation and trafficking PBMCs will enable us to use this model in a more sophisticated manner to selectively modulate potential targets such as insulin signaling as well as cytokine and chemokine production to alter disease progression. Finally, our findings provide compelling rationale to initiate studies in humans with chronic inflammatory diseases (e.g. metabolic syndrome, obesity) and investigate the extent to which their central and peripheral immune cell populations become dysregulated. Such changes could be used to identify patients at higher risk for development of MCI and progression to AD and support development of therapies that may target sub-populations of AD patients.

**Appendix: Complete list of publications to which the author has contributed during
her graduate training**

- MacPherson, K.P.**, Sompol, P., Kannarkat, G.T., Chang, J., Sniffen, L., Wildner, M.E., Norris, C.M., Tansey, M.G. Inhibition of soluble TNF modifies brain immune cell profiles, rescues impaired long-term potentiation, and decreases beta-amyloid plaque load in the subiculum of 5xFAD mice. (2017) *Neurobiology of disease* PMID: 28237313
- MacPherson, K.P.**, de Sousa Rodrigues, M., Cintron, A.F., and Tansey, M.G. The molecular and Cellular Basis of Neurodegenerative Diseases: Underlying mechanisms chapter on Neurodegenerative Disease and Neuroinflammation *Submitted to Elsevier*
- MacPherson, K.P.**, Amran, A.Y., Goodson, M., Oliver, D., Eissen, G., and Tansey MG. The role of high caloric diet on central and peripheral inflammation and immune cell profiles *In preparation*
- MacPherson, K.P.**, Eidson, L.N., Herrick, M.K., de Sousa Rodrigues, M., and Tansey MG. The role of sTNF in diet-induced AD-like pathology and CNS immune cell trafficking. *In preparation*
- Cintron, A.F., **MacPherson, K.P.**, Kannarkat, G.T., Cook, D.A., Hess, C., Galvez, N., Singer, C., Isaacson, S., Zesiewicz, T., Boss, J.M., and Tansey, M.G. Immunophenotyping of LRRK2 G2019S mutation carriers reveals immune dysregulation in peripheral immune cells and a pro-inflammatory environment that may influence risk for development of Parkinson's disease symptoms. In preparation for *Journal of Clinical Investigation*.
- Cintron, A.F., **MacPherson, K.P.**, Eidson, L.N, Goldstein, F. C., Wharton, W., and Tansey, M.G. Peripheral and central immune dysregulation in a middle-aged hypertensive population at risk for Alzheimer's disease. In preparation for submission to *Brain, Behavior and Immunity*.
- Cintron, A.F., **MacPherson, K.P.**, Kannarkat, G.T., Carr, C., Erdei, T., Factor, S., Caudle, W.M., and Tansey, M.G., Pyrethroid exposure *in vivo* and *in vitro* dysregulates antigen presentation and T-cell differentiation and contributes to degeneration of nigral dopaminergic neurons. In preparation for submission to *Journal of Neuroimmune Pharmacology*.
- Rotterman, T.M., **MacPherson, K.P.**, Fisher, S., Chopra, T., Tansey, M.G., Alvarez, F.J. Infiltration of CCR2-dependent myeloid cells into the spinal cord increases in nerve injury with worse regenerative outcomes in the periphery and increase the level of adaptive spinal motor circuit plasticity centrally. In preparation for submission to *Nature Neuroscience*.

REFERENCES

- Ajami B, Bennett JL, Krieger C, Tetzlaff W, Rossi FM (2007) Local self-renewal can sustain CNS microglia maintenance and function throughout adult life. *Nat Neurosci* 10:1538-1543.
- Akiyama H et al. (2000) Inflammation and Alzheimer's disease. *Neurobiology of aging* 21:383-421.
- Allen NJ (2014) Astrocyte regulation of synaptic behavior. *Annu Rev Cell Dev Biol* 30:439-463.
- Aloisi F, Borsellino G, Care A, Testa U, Gallo P, Russo G, Peschle C, Levi G (1995) Cytokine regulation of astrocyte function: in-vitro studies using cells from the human brain. *Int J Dev Neurosci* 13:265-274.
- Amengual-Cladera E, Llado I, Gianotti M, Proenza AM (2012) Sex differences in the effect of high-fat diet feeding on rat white adipose tissue mitochondrial function and insulin sensitivity. *Metabolism* 61:1108-1117.
- Aspelund A, Antila S, Proulx ST, Karlsen TV, Karaman S, Detmar M, Wiig H, Alitalo K (2015) A dural lymphatic vascular system that drains brain interstitial fluid and macromolecules. *J Exp Med* 212:991-999.
- Axtell RC, Steinman L (2009) Gaining entry to an uninflamed brain. *Nat Immunol* 10:453-455.
- Aytan N, Choi JK, Carreras I, Brinkmann V, Kowall NW, Jenkins BG, Dedeoglu A (2016) Fingolimod modulates multiple neuroinflammatory markers in a mouse model of Alzheimer's disease. *Sci Rep* 6:24939.
- Bachstetter AD, Norris CM, Sompol P, Wilcock DM, Goulding D, Neltner JH, St Clair D, Watterson DM, Van Eldik LJ (2012) Early stage drug treatment that normalizes proinflammatory cytokine production attenuates synaptic dysfunction in a mouse model that exhibits age-dependent progression of Alzheimer's disease-related pathology. *J Neurosci* 32:10201-10210.
- Barkauskas DS, Evans TA, Myers J, Petrosiute A, Silver J, Huang AY (2013) Extravascular CX3CR1+ cells extend intravascular dendritic processes into intact central nervous system vessel lumen. *Microsc Microanal* 19:778-790.
- Barna BP, Estes ML, Jacobs BS, Hudson S, Ransohoff RM (1990) Human astrocytes proliferate in response to tumor necrosis factor alpha. *J Neuroimmunol* 30:239-243.
- Barnum CJ, Chen X, Chung J, Chang J, Williams M, Grigoryan N, Tesi RJ, Tansey MG (2014) Peripheral administration of the selective inhibitor of soluble tumor necrosis factor (TNF) XPro(R)1595 attenuates nigral cell loss and glial activation in 6-OHDA hemiparkinsonian rats. *J Parkinsons Dis* 4:349-360.
- Baruch K, Schwartz M (2013) CNS-specific T cells shape brain function via the choroid plexus. *Brain, behavior, and immunity* 34:11-16.
- Baruch K, Rosenzweig N, Kertser A, Deczkowska A, Sharif AM, Spinrad A, Tsitsou-Kampeli A, Sarel A, Cahalon L, Schwartz M (2015) Breaking immune tolerance by targeting Foxp3(+) regulatory T cells mitigates Alzheimer's disease pathology. *Nature communications* 6:7967.
- Bayraktar OA, Fuentealba LC, Alvarez-Buylla A, Rowitch DH (2015) Astrocyte development and heterogeneity. *Cold Spring Harb Perspect Biol* 7:a020362.
- Biber K, Neumann H, Inoue K, Boddeke HW (2007) Neuronal 'On' and 'Off' signals control microglia. *Trends Neurosci* 30:596-602.
- Biessels G, Staekenborg S, Brunner E, Brayne C, Scheltens P (2006) Risk of dementia in diabetes mellitus: a systematic review. *Lancet neurology* 5:64-74.
- Blaho VA, Hla T (2014) An update on the biology of sphingosine 1-phosphate receptors. *J Lipid Res* 55:1596-1608.

- Blaho VA, Galvani S, Engelbrecht E, Liu C, Swendeman SL, Kono M, Proia RL, Steinman L, Han MH, Hla T (2015) HDL-bound sphingosine-1-phosphate restrains lymphopoiesis and neuroinflammation. *Nature* 523:342-346.
- Bolos M, Antequera D, Aldudo J, Kristen H, Bullido MJ, Carro E (2014) Choroid plexus implants rescue Alzheimer's disease-like pathologies by modulating amyloid-beta degradation. *Cellular and molecular life sciences : CMLS* 71:2947-2955.
- Brambilla R, Ashbaugh J, Magliozzi R, Dellarole A, Karmally S, Szymkowski D, Bethea J (2011) Inhibition of soluble tumour necrosis factor is therapeutic in experimental autoimmune encephalomyelitis and promotes axon preservation and remyelination. *Brain : a journal of neurology* 134:2736-2754.
- Brosseron F, Krauthausen M, Kummer M, Heneka MT (2014) Body fluid cytokine levels in mild cognitive impairment and Alzheimer's disease: a comparative overview. *Molecular neurobiology* 50:534-544.
- Bryson KJ, Lynch MA (2015) Linking T cells to Alzheimer's disease: from neurodegeneration to neurorepair. *Curr Opin Pharmacol* 26:67-73.
- Butchart J, Brook L, Hopkins V, Teeling J, Puntener U, Culliford D, Sharples R, Sharif S, McFarlane B, Raybould R, Thomas R, Passmore P, Perry VH, Holmes C (2015) Etanercept in Alzheimer disease: A randomized, placebo-controlled, double-blind, phase 2 trial. *Neurology* 84:2161-2168.
- Carare RO, Bernardes-Silva M, Newman TA, Page AM, Nicoll JA, Perry VH, Weller RO (2008) Solutes, but not cells, drain from the brain parenchyma along basement membranes of capillaries and arteries: significance for cerebral amyloid angiopathy and neuroimmunology. *Neuropathology and applied neurobiology* 34:131-144.
- Carson MJ, Doose JM, Melchior B, Schmid CD, Ploix CC (2006) CNS immune privilege: hiding in plain sight. *Immunol Rev* 213:48-65.
- Cebrian C, Loike JD, Sulzer D (2014a) Neuronal MHC-I expression and its implications in synaptic function, axonal regeneration and Parkinson's and other brain diseases. *Front Neuroanat* 8:114.
- Cebrian C, Zucca FA, Mauri P, Steinbeck JA, Studer L, Scherzer CR, Kanter E, Budhu S, Mandelbaum J, Vonsattel JP, Zecca L, Loike JD, Sulzer D (2014b) MHC-I expression renders catecholaminergic neurons susceptible to T-cell-mediated degeneration. *Nature communications* 5:3633.
- Cho S-H, Sun B, Zhou Y, Kauppinen T, Halabisky B, Wes P, Ransohoff R, Gan L (2011) CX3CR1 protein signaling modulates microglial activation and protects against plaque-independent cognitive deficits in a mouse model of Alzheimer disease. *The Journal of biological chemistry* 286:32713-32722.
- Crocker PR (2005) Siglecs in innate immunity. *Curr Opin Pharmacol* 5:431-437.
- Cunningham AJ, Murray CA, O'Neill LA, Lynch MA, O'Connor JJ (1996) Interleukin-1 beta (IL-1 beta) and tumour necrosis factor (TNF) inhibit long-term potentiation in the rat dentate gyrus in vitro. *Neurosci Lett* 203:17-20.
- Cunningham C, Campion S, Lunnon K, Murray C, Woods J, Deacon R, Rawlins J, Perry V (2009) Systemic inflammation induces acute behavioral and cognitive changes and accelerates neurodegenerative disease. *Biological psychiatry* 65:304-312.
- Dando SJ, Naranjo Golborne C, Chinnery HR, Ruitenber MJ, McMennamin PG (2016) A case of mistaken identity: CD11c-eYFP(+) cells in the normal mouse brain parenchyma and neural retina display the phenotype of microglia, not dendritic cells. *Glia* 64:1331-1349.

- Davalos D, Grutzendler J, Yang G, Kim JV, Zuo Y, Jung S, Littman DR, Dustin ML, Gan WB (2005) ATP mediates rapid microglial response to local brain injury in vivo. *Nat Neurosci* 8:752-758.
- de Sousa Rodrigues ME, Bekhbat M, Houser MC, Chang J, Walker DI, Jones DP, Oller do Nascimento CM, Barnum CJ, Tansey MG (2016) Chronic psychological stress and high-fat high-fructose diet disrupt metabolic and inflammatory gene networks in the brain, liver, and gut and promote behavioral deficits in mice. *Brain, behavior, and immunity*.
- Dixon-Salazar TJ, Fourgeaud L, Tyler CM, Poole JR, Park JJ, Boulanger LM (2014) MHC class I limits hippocampal synapse density by inhibiting neuronal insulin receptor signaling. *J Neurosci* 34:11844-11856.
- Efremova L, Chovancova P, Adam M, Gutbier S, Schildknecht S, Leist M (2016) Switching from astrocytic neuroprotection to neurodegeneration by cytokine stimulation. *Arch Toxicol*.
- El Khoury J, Toft M, Hickman SE, Means TK, Terada K, Geula C, Luster AD (2007) Ccr2 deficiency impairs microglial accumulation and accelerates progression of Alzheimer-like disease. *Nat Med* 13:432-438.
- Engelhardt B (2008) Immune cell entry into the central nervous system: involvement of adhesion molecules and chemokines. *Journal of the neurological sciences* 274:23-26.
- Engelhardt B, Ransohoff RM (2005) The ins and outs of T-lymphocyte trafficking to the CNS: anatomical sites and molecular mechanisms. *Trends in immunology* 26:485-495.
- Engelhardt B, Ransohoff R (2012a) Capture, crawl, cross: the T cell code to breach the blood-brain barriers. *Trends in immunology* 33:579-589.
- Engelhardt B, Ransohoff RM (2012b) Capture, crawl, cross: the T cell code to breach the blood-brain barriers. *Trends in immunology* 33:579-589.
- Engelhart M, Geerlings M, Meijer J, Kiliaan A, Ruitenbergh A, van Swieten J, Stijnen T, Hofman A, Witteman J, Breteler M (2004) Inflammatory proteins in plasma and the risk of dementia: the rotterdam study. *Archives of neurology* 61:668-672.
- Erickson MA, Banks WA (2011) Cytokine and chemokine responses in serum and brain after single and repeated injections of lipopolysaccharide: multiplex quantification with path analysis. *Brain, behavior, and immunity* 25:1637-1648.
- Erickson MA, Banks WA (2013) Blood-brain barrier dysfunction as a cause and consequence of Alzheimer's disease. *Journal of cerebral blood flow and metabolism : official journal of the International Society of Cerebral Blood Flow and Metabolism* 33:1500-1513.
- Evangelidou M, Tseveleki V, Vamvakas SS, Probert L (2010) TNFRI is a positive T-cell costimulatory molecule important for the timing of cytokine responses. *Immunol Cell Biol* 88:586-595.
- Farber K, Cheung G, Mitchell D, Wallis R, Weihe E, Schwaebler W, Kettenmann H (2009) C1q, the recognition subcomponent of the classical pathway of complement, drives microglial activation. *J Neurosci Res* 87:644-652.
- Ferretti MT, Merlini M, Spani C, Gericke C, Schweizer N, Enzmann G, Engelhardt B, Kulic L, Suter T, Nitsch RM (2016) T-cell brain infiltration and immature antigen-presenting cells in transgenic models of Alzheimer's disease-like cerebral amyloidosis. *Brain, behavior, and immunity* 54:211-225.
- Fiala M, Lin J, Ringman J, Kermani-Arab V, Tsao G, Patel A, Lossinsky AS, Graves MC, Gustavson A, Sayre J, Sofroni E, Suarez T, Chiappelli F, Bernard G (2005) Ineffective phagocytosis of amyloid-beta by macrophages of Alzheimer's disease patients. *J Alzheimers Dis* 7:221-232; discussion 255-262.
- Fontana A, Fierz W, Wekerle H (1984) Astrocytes present myelin basic protein to encephalitogenic T-cell lines. *Nature* 307:273-276.

- Forette F, Seux ML, Staessen JA, Thijs L, Babarskiene MR, Babeanu S, Bossini A, Fagard R, Gil-Extremera B, Laks T, Kobalava Z, Sarti C, Tuomilehto J, Vanhanen H, Webster J, Yodfat Y, Birkenhager WH, Systolic Hypertension in Europe I (2002) The prevention of dementia with antihypertensive treatment: new evidence from the Systolic Hypertension in Europe (Syst-Eur) study. *Arch Intern Med* 162:2046-2052.
- Fu H, Liu B, Frost J, Hong S, Jin M, Ostaszewski B, Shankar G, Costantino I, Carroll M, Mayadas T, Lemere C (2012) Complement component C3 and complement receptor type 3 contribute to the phagocytosis and clearance of fibrillar A β by microglia. *Glia* 60:993-1003.
- Furman JL, Sama DM, Gant JC, Beckett TL, Murphy MP, Bachstetter AD, Van Eldik LJ, Norris CM (2012) Targeting astrocytes ameliorates neurologic changes in a mouse model of Alzheimer's disease. *J Neurosci* 32:16129-16140.
- Ginhoux F, Lim S, Hoeffel G, Low D, Huber T (2013) Origin and differentiation of microglia. *Frontiers in cellular neuroscience* 7:45.
- Ginhoux F, Greter M, Leboeuf M, Nandi S, See P, Gokhan S, Mehler MF, Conway SJ, Ng LG, Stanley ER, Samokhvalov IM, Merad M (2010) Fate mapping analysis reveals that adult microglia derive from primitive macrophages. *Science* 330:841-845.
- Goldmann J, Kwidzinski E, Brandt C, Mahlo J, Richter D, Bechmann I (2006) T cells traffic from brain to cervical lymph nodes via the cribroid plate and the nasal mucosa. *J Leukoc Biol* 80:797-801.
- Goldmann T et al. (2016) Origin, fate and dynamics of macrophages at central nervous system interfaces. *Nat Immunol* 17:797-805.
- Goldstein GW (1988) Endothelial cell-astrocyte interactions. A cellular model of the blood-brain barrier. *Ann N Y Acad Sci* 529:31-39.
- Goronzy JJ, Li G, Yang Z, Weyand CM (2013) The janus head of T cell aging - autoimmunity and immunodeficiency. *Front Immunol* 4:131.
- Greter M, Lelios I, Croxford AL (2015) Microglia Versus Myeloid Cell Nomenclature during Brain Inflammation. *Front Immunol* 6:249.
- Greter M, Lelios I, Pelczar P, Hoeffel G, Price J, Leboeuf M, Kundig TM, Frei K, Ginhoux F, Merad M, Becher B (2012) Stroma-derived interleukin-34 controls the development and maintenance of langerhans cells and the maintenance of microglia. *Immunity* 37:1050-1060.
- Griciuc A, Serrano-Pozo A, Parrado AR, Lesinski AN, Asselin CN, Mullin K, Hooli B, Choi SH, Hyman BT, Tanzi RE (2013) Alzheimer's disease risk gene CD33 inhibits microglial uptake of amyloid beta. *Neuron* 78:631-643.
- Guerreiro R et al. (2013) TREM2 variants in Alzheimer's disease. *N Engl J Med* 368:117-127.
- Gyoneva S, Davalos D, Biswas D, Swanger SA, Garnier-Amblard E, Loth F, Akassoglou K, Traynelis SF (2014) Systemic inflammation regulates microglial responses to tissue damage in vivo. *Glia* 62:1345-1360.
- Haan N, Zhu B, Wang J, Wei X, Song B (2015) Crosstalk between macrophages and astrocytes affects proliferation, reactive phenotype and inflammatory response, suggesting a role during reactive gliosis following spinal cord injury. *J Neuroinflammation* 12:109.
- Harty JT, Tvinnereim AR, White DW (2000) CD8+ T cell effector mechanisms in resistance to infection. *Annu Rev Immunol* 18:275-308.
- Hatterer E, Davoust N, Didier-Bazes M, Vuillaud C, Malcus C, Belin MF, Nataf S (2006) How to drain without lymphatics? Dendritic cells migrate from the cerebrospinal fluid to the B-cell follicles of cervical lymph nodes. *Blood* 107:806-812.
- Heneka MT et al. (2015) Neuroinflammation in Alzheimer's disease. *Lancet Neurol* 14:388-405.

- Hennessy E, Gormley S, Lopez-Rodriguez AB, Murray C, Murray C, Cunningham C (2016) Systemic TNF-alpha produces acute cognitive dysfunction and exaggerated sickness behavior when superimposed upon progressive neurodegeneration. *Brain, behavior, and immunity*.
- Hickey WF, Kimura H (1988) Perivascular microglial cells of the CNS are bone marrow-derived and present antigen in vivo. *Science* 239:290-292.
- Hickman SE, El Khoury J (2010) Mechanisms of mononuclear phagocyte recruitment in Alzheimer's disease. *CNS Neurol Disord Drug Targets* 9:168-173.
- Holmes C, El-Okli M, Williams... A (2003) Systemic infection, interleukin 1 β , and cognitive decline in Alzheimer's disease. *Journal of Neurology*.
- Holmes C, Cunningham C, Zotova E, Woolford J, Dean C, Kerr S, Culliford D, Perry V (2009) Systemic inflammation and disease progression in Alzheimer disease. *Neurology* 73:768-774.
- Hong S, Beja-Glasser VF, Nfonoyim BM, Frouin A, Li S, Ramakrishnan S, Merry KM, Shi Q, Rosenthal A, Barres BA, Lemere CA, Selkoe DJ, Stevens B (2016) Complement and microglia mediate early synapse loss in Alzheimer mouse models. *Science* 352:712-716.
- Hoogland IC, Houbolt C, van Westerlo DJ, van Gool WA, van de Beek D (2015) Systemic inflammation and microglial activation: systematic review of animal experiments. *J Neuroinflammation* 12:114.
- Jay TR, Miller CM, Cheng PJ, Graham LC, Bemiller S, Broihier ML, Xu G, Margevicius D, Karlo JC, Sousa GL, Cotleur AC, Butovsky O, Bekris L, Staugaitis SM, Leverenz JB, Pimplikar SW, Landreth GE, Howell GR, Ransohoff RM, Lamb BT (2015) TREM2 deficiency eliminates TREM2+ inflammatory macrophages and ameliorates pathology in Alzheimer's disease mouse models. *J Exp Med* 212:287-295.
- Kamer A, Dasanayake A, Craig R, Glodzik-Sobanska L, Bry M, de Leon M (2008) Alzheimer's disease and peripheral infections: the possible contribution from periodontal infections, model and hypothesis. *Journal of Alzheimer's disease : JAD* 13:437-449.
- Kamphuis W, Kooijman L, Schettters S, Orre M, Hol EM (2016) Transcriptional profiling of CD11c-positive microglia accumulating around amyloid plaques in a mouse model for Alzheimer's disease. *Biochim Biophys Acta* 1862:1847-1860.
- Kannarkat GT, Lee JK, Ramsey CP, Chung J, Chang J, Porter I, Oliver D, Shepherd K, Tansey MG (2015) Age-related changes in regulator of G-protein signaling (RGS)-10 expression in peripheral and central immune cells may influence the risk for age-related degeneration. *Neurobiol Aging* 36:1982-1993.
- Kanoski SE, Zhang Y, Zheng W, Davidson TL (2010) The effects of a high-energy diet on hippocampal function and blood-brain barrier integrity in the rat. *J Alzheimers Dis* 21:207-219.
- Kierdorf K, Katzmarski N, Haas CA, Prinz M (2013) Bone marrow cell recruitment to the brain in the absence of irradiation or parabiosis bias. *PLoS One* 8:e58544.
- Kipnis J (2016) Multifaceted interactions between adaptive immunity and the central nervous system. *Science* 353:766-771.
- Kiyota T, Yamamoto M, Xiong H, Lambert MP, Klein WL, Gendelman HE, Ransohoff RM, Ikezu T (2009) CCL2 accelerates microglia-mediated A β oligomer formation and progression of neurocognitive dysfunction. *PLoS One* 4:e6197.
- Kuo SM (2013) The interplay between fiber and the intestinal microbiome in the inflammatory response. *Adv Nutr* 4:16-28.
- Laman JD, Weller RO (2013) Drainage of cells and soluble antigen from the CNS to regional lymph nodes. *J Neuroimmune Pharmacol* 8:840-856.
- Lambert JC et al. (2013) Meta-analysis of 74,046 individuals identifies 11 new susceptibility loci for Alzheimer's disease. *Nat Genet* 45:1452-1458.

- Limatola C, Ransohoff RM (2014) Modulating neurotoxicity through CX3CL1/CX3CR1 signaling. *Frontiers in cellular neuroscience* 8:229.
- Louveau A, Smirnov I, Keyes TJ, Eccles JD, Rouhani SJ, Peske JD, Derecki NC, Castle D, Mandell JW, Lee KS, Harris TH, Kipnis J (2015) Structural and functional features of central nervous system lymphatic vessels. *Nature* 523:337-341.
- Luckheeram RV, Zhou R, Verma AD, Xia B (2012) CD4(+)T cells: differentiation and functions. *Clin Dev Immunol* 2012:925135.
- Luo J, Wyss-Coray T (2009) Bioluminescence analysis of Smad-dependent TGF-beta signaling in live mice. *Methods Mol Biol* 574:193-202.
- MacEwan D (2002) TNF receptor subtype signalling: differences and cellular consequences. *Cellular signalling*.
- Mack M, Cihak J, Simonis C, Luckow B, Proudfoot AE, Plachy J, Bruhl H, Frink M, Anders HJ, Vielhauer V, Pfirstinger J, Stangassinger M, Schlondorff D (2001) Expression and characterization of the chemokine receptors CCR2 and CCR5 in mice. *J Immunol* 166:4697-4704.
- Mackay F, Loetscher H, Stueber D, Gehr G, Lesslauer W (1993) Tumor necrosis factor alpha (TNF-alpha)-induced cell adhesion to human endothelial cells is under dominant control of one TNF receptor type, TNF-R55. *J Exp Med* 177:1277-1286.
- Mandrekar-Colucci S, Landreth GE (2010) Microglia and inflammation in Alzheimer's disease. *CNS Neurol Disord Drug Targets* 9:156-167.
- Marsh SE, Abud EM, Lakatos A, Karimzadeh A, Yeung ST, Davtyan H, Fote GM, Lau L, Weinger JG, Lane TE, Inlay MA, Poon WW, Blurton-Jones M (2016) The adaptive immune system restrains Alzheimer's disease pathogenesis by modulating microglial function. *Proc Natl Acad Sci U S A* 113:E1316-1325.
- Martin-Blondel G, Pignolet B, Tietz S, Yshii L, Gebauer C, Perinat T, Van Weddingen I, Blatti C, Engelhardt B, Liblau R (2015) Migration of encephalitogenic CD8 T cells into the central nervous system is dependent on the alpha4beta1-integrin. *Eur J Immunol* 45:3302-3312.
- Martin E, Boucher C, Fontaine B, Delarasse C (2016) Distinct inflammatory phenotypes of microglia and monocyte-derived macrophages in Alzheimer's disease models: effects of aging and amyloid pathology. *Aging Cell*.
- Mathis DM, Furman JL, Norris CM (2011) Preparation of acute hippocampal slices from rats and transgenic mice for the study of synaptic alterations during aging and amyloid pathology. *J Vis Exp*.
- McAlpine F, Lee J-K, Harms A, Ruhn K, Blurton-Jones M, Hong J, Das P, Golde T, LaFerla F, Oddo S, Blesch A, Tansey M (2009) Inhibition of soluble TNF signaling in a mouse model of Alzheimer's disease prevents pre-plaque amyloid-associated neuropathology. *Neurobiology of disease* 34:163-177.
- McCoy M, Tansey M (2008) TNF signaling inhibition in the CNS: implications for normal brain function and neurodegenerative disease. *Journal of neuroinflammation* 5:45.
- McCoy M, Martinez T, Ruhn K, Szymkowski D, Smith C, Botterman B, Tansey K, Tansey M (2006) Blocking soluble tumor necrosis factor signaling with dominant-negative tumor necrosis factor inhibitor attenuates loss of dopaminergic neurons in models of Parkinson's disease. *The Journal of neuroscience : the official journal of the Society for Neuroscience* 26:9365-9375.
- McGeer P, McGeer E (2007) NSAIDs and Alzheimer disease: epidemiological, animal model and clinical studies. *Neurobiology of aging* 28:639-647.
- Meyer-Luehmann M, Prinz M (2015) Myeloid cells in Alzheimer's disease: culprits, victims or innocent bystanders? *Trends Neurosci* 38:659-668.

- Misiak B, Leszek J, Kiejna A (2012) Metabolic syndrome, mild cognitive impairment and Alzheimer's disease--the emerging role of systemic low-grade inflammation and adiposity. *Brain research bulletin* 89:144-149.
- Montagne A, Barnes SR, Sweeney MD, Halliday MR, Sagare AP, Zhao Z, Toga AW, Jacobs RE, Liu CY, Amezcua L, Harrington MG, Chui HC, Law M, Zlokovic BV (2015) Blood-brain barrier breakdown in the aging human hippocampus. *Neuron* 85:296-302.
- Montgomery SL, Narrow WC, Mastrangelo MA, Olschowka JA, O'Banion MK, Bowers WJ (2013) Chronic neuron- and age-selective down-regulation of TNF receptor expression in triple-transgenic Alzheimer disease mice leads to significant modulation of amyloid- and Tau-related pathologies. *The American journal of pathology* 182:2285-2297.
- Montgomery SL, Mastrangelo MA, Habib D, Narrow WC, Knowlden SA, Wright TW, Bowers WJ (2011) Ablation of TNF-RI/RII expression in Alzheimer's disease mice leads to an unexpected enhancement of pathology: implications for chronic pan-TNF-alpha suppressive therapeutic strategies in the brain. *The American journal of pathology* 179:2053-2070.
- Murray C, Sanderson D, Barkus C, Deacon R, Rawlins J, Bannerman D, Cunningham C (2012) Systemic inflammation induces acute working memory deficits in the primed brain: relevance for delirium. *Neurobiology of aging* 33:603-616000.
- Nadeau S, Rivest S (1999) Effects of circulating tumor necrosis factor on the neuronal activity and expression of the genes encoding the tumor necrosis factor receptors (p55 and p75) in the rat brain: a view from the blood-brain barrier. *Neuroscience* 93:1449-1464.
- Naert G, Rivest S (2012) Hematopoietic CC-chemokine receptor 2 (CCR2) competent cells are protective for the cognitive impairments and amyloid pathology in a transgenic mouse model of Alzheimer's disease. *Molecular medicine (Cambridge, Mass)* 18:297-313.
- Naude PJ, Nyakas C, Eiden LE, Ait-Ali D, van der Heide R, Engelborghs S, Luiten PG, De Deyn PP, den Boer JA, Eisel UL (2012) Lipocalin 2: novel component of proinflammatory signaling in Alzheimer's disease. *FASEB J* 26:2811-2823.
- Neefjes J, Jongsma ML, Paul P, Bakke O (2011) Towards a systems understanding of MHC class I and MHC class II antigen presentation. *Nature reviews Immunology* 11:823-836.
- Oakley H, Cole S, Logan S, Maus E, Shao P, Craft J, Guillozet-Bongaarts A, Ohno M, Disterhoft J, Van Eldik L, Berry R, Vassar R (2006) Intraneuronal beta-amyloid aggregates, neurodegeneration, and neuron loss in transgenic mice with five familial Alzheimer's disease mutations: potential factors in amyloid plaque formation. *The Journal of neuroscience : the official journal of the Society for Neuroscience* 26:10129-10140.
- Ojo O, Brooke J (2015) Evaluating the Association between Diabetes, Cognitive Decline and Dementia. *Int J Environ Res Public Health* 12:8281-8294.
- Pavlov VA, Tracey KJ (2015) Neural circuitry and immunity. *Immunol Res* 63:38-57.
- Perlmutter LS, Scott SA, Barron E, Chui HC (1992) MHC class II-positive microglia in human brain: association with Alzheimer lesions. *J Neurosci Res* 33:549-558.
- Perry V, Cunningham C, Holmes C (2007) Systemic infections and inflammation affect chronic neurodegeneration. *Nature reviews Immunology* 7:161-167.
- Phillips RJ, Lutz M, Premack B (2005) Differential signaling mechanisms regulate expression of CC chemokine receptor-2 during monocyte maturation. *J Inflamm (Lond)* 2:14.
- Prinz M, Priller J, Sisodia S, Ransohoff R (2011a) Heterogeneity of CNS myeloid cells and their roles in neurodegeneration. *Nature neuroscience* 14:1227-1235.
- Prinz M, Priller J, Sisodia SS, Ransohoff RM (2011b) Heterogeneity of CNS myeloid cells and their roles in neurodegeneration. *Nat Neurosci* 14:1227-1235.

- Proctor C, Thiennimitr P, Chattipakorn N, Chattipakorn SC (2016) Diet, gut microbiota and cognition. *Metab Brain Dis*.
- Prokop S, Miller KR, Drost N, Handrick S, Mathur V, Luo J, Wegner A, Wyss-Coray T, Heppner FL (2015) Impact of peripheral myeloid cells on amyloid-beta pathology in Alzheimer's disease-like mice. *J Exp Med* 212:1811-1818.
- Qin L, Wu X, Block M, Liu Y, Breese G, Hong J-S, Knapp D, Crews F (2007) Systemic LPS causes chronic neuroinflammation and progressive neurodegeneration. *Glia* 55:453-462.
- Radler ME, Wright BJ, Walker FR, Hale MW, Kent S (2015) Calorie restriction increases lipopolysaccharide-induced neuropeptide Y immunolabeling and reduces microglial cell area in the arcuate hypothalamic nucleus. *Neuroscience* 285:236-247.
- Ransohoff RM, Brown MA (2012) Innate immunity in the central nervous system. *The Journal of clinical investigation* 122:1164-1171.
- Ransohoff RM, Engelhardt B (2012) The anatomical and cellular basis of immune surveillance in the central nervous system. *Nature reviews Immunology* 12:623-635.
- Ransohoff RM, Schafer D, Vincent A, Blachere NE, Bar-Or A (2015) Neuroinflammation: Ways in Which the Immune System Affects the Brain. *Neurotherapeutics : the journal of the American Society for Experimental NeuroTherapeutics* 12:896-909.
- Rezai-Zadeh K, Gate D, Town T (2009) CNS infiltration of peripheral immune cells: D-Day for neurodegenerative disease? *Journal of neuroimmune pharmacology : the official journal of the Society on NeuroImmune Pharmacology* 4:462-475.
- Rijkers ES, de Ruiter T, Baridi A, Veninga H, Hoek RM, Meyaard L (2008) The inhibitory CD200R is differentially expressed on human and mouse T and B lymphocytes. *Mol Immunol* 45:1126-1135.
- Rochfort KD, Collins LE, Murphy RP, Cummins PM (2014) Downregulation of blood-brain barrier phenotype by proinflammatory cytokines involves NADPH oxidase-dependent ROS generation: consequences for interendothelial adherens and tight junctions. *PLoS One* 9:e101815.
- Rosas-Ballina M, Olofsson PS, Ochani M, Valdes-Ferrer SI, Levine YA, Reardon C, Tusche MW, Pavlov VA, Andersson U, Chavan S, Mak TW, Tracey KJ (2011) Acetylcholine-synthesizing T cells relay neural signals in a vagus nerve circuit. *Science* 334:98-101.
- Rose S, Misharin A, Perlman H (2012) A novel Ly6C/Ly6G-based strategy to analyze the mouse splenic myeloid compartment. *Cytometry A* 81:343-350.
- Rosenkranz D, Weyer S, Tolosa E, Gaenslen A, Berg D, Leyhe T, Gasser T, Stoltze L (2007) Higher frequency of regulatory T cells in the elderly and increased suppressive activity in neurodegeneration. *J Neuroimmunol* 188:117-127.
- Saederup N, Cardona A, Croft K, Mizutani M, Coteleur A, Tsou C-L, Ransohoff R, Charo I (2010) Selective chemokine receptor usage by central nervous system myeloid cells in CCR2-red fluorescent protein knock-in mice. *PLoS one* 5.
- Sallusto F, Geginat J, Lanzavecchia A (2004) Central memory and effector memory T cell subsets: function, generation, and maintenance. *Annu Rev Immunol* 22:745-763.
- Sama DM, Mohammad Abdul H, Furman JL, Artiushin IA, Szymkowski DE, Scheff SW, Norris CM (2012) Inhibition of soluble tumor necrosis factor ameliorates synaptic alterations and Ca²⁺ dysregulation in aged rats. *PLoS One* 7:e38170.
- Sanjabi S, Zenewicz LA, Kamanaka M, Flavell RA (2009) Anti-inflammatory and pro-inflammatory roles of TGF-beta, IL-10, and IL-22 in immunity and autoimmunity. *Curr Opin Pharmacol* 9:447-453.

- Sauer BM, Schmalstieg WF, Howe CL (2013) Axons are injured by antigen-specific CD8(+) T cells through a MHC class I- and granzyme B-dependent mechanism. *Neurobiol Dis* 59:194-205.
- Schafer DP, Lehrman EK, Kautzman AG, Koyama R, Mardinly AR, Yamasaki R, Ransohoff RM, Greenberg ME, Barres BA, Stevens B (2012) Microglia sculpt postnatal neural circuits in an activity and complement-dependent manner. *Neuron* 74:691-705.
- Schlager C, Korner H, Krueger M, Vidoli S, Haberl M, Mielke D, Brylla E, Issekutz T, Cabanas C, Nelson PJ, Ziemssen T, Rohde V, Bechmann I, Lodygin D, Odoardi F, Flugel A (2016) Effector T-cell trafficking between the leptomeninges and the cerebrospinal fluid. *Nature* 530:349-353.
- Schneider-Hohendorf T, Rossaint J, Mohan H, Boning D, Breuer J, Kuhlmann T, Gross CC, Flanagan K, Sorokin L, Vestweber D, Zarbock A, Schwab N, Wiendl H (2014) VLA-4 blockade promotes differential routes into human CNS involving PSGL-1 rolling of T cells and MCAM-adhesion of TH17 cells. *J Exp Med* 211:1833-1846.
- Scholz D, Poltl D, Genewsky A, Weng M, Waldmann T, Schildknecht S, Leist M (2011) Rapid, complete and large-scale generation of post-mitotic neurons from the human LUHMES cell line. *J Neurochem* 119:957-971.
- Sedgwick JD, Schwender S, Imrich H, Dorries R, Butcher GW, ter Meulen V (1991) Isolation and direct characterization of resident microglial cells from the normal and inflamed central nervous system. *Proc Natl Acad Sci U S A* 88:7438-7442.
- Sharma H, Castellani R, Smith M, Sharma A (2012) The blood-brain barrier in Alzheimer's disease: novel therapeutic targets and nanodrug delivery. *International review of neurobiology* 102:47-90.
- Smith JA, Das A, Ray SK, Banik NL (2012) Role of pro-inflammatory cytokines released from microglia in neurodegenerative diseases. *Brain Res Bull* 87:10-20.
- Sofroniew MV (2014) Multiple roles for astrocytes as effectors of cytokines and inflammatory mediators. *Neuroscientist* 20:160-172.
- Steed PM et al. (2003) Inactivation of TNF signaling by rationally designed dominant-negative TNF variants. *Science* 301:1895-1898.
- Steinman L (2013a) Inflammatory cytokines at the summits of pathological signal cascades in brain diseases. *Science signaling* 6.
- Steinman L (2013b) Inflammatory cytokines at the summits of pathological signal cascades in brain diseases. *Sci Signal* 6:pe3.
- Swardfager W, Lanctot K, Rothenburg L, Wong A, Cappell J, Herrmann N (2010) A meta-analysis of cytokines in Alzheimer's disease. *Biol Psychiatry* 68:930-941.
- Tanzi RE (2012) The genetics of Alzheimer disease. *Cold Spring Harbor perspectives in medicine* 2.
- Tay TL, Hagemeyer N, Prinz M (2016) The force awakens: insights into the origin and formation of microglia. *Curr Opin Neurobiol* 39:30-37.
- Togo T, Akiyama H, Iseki E, Kondo H, Ikeda K, Kato M, Oda T, Tsuchiya K, Kosaka K (2002) Occurrence of T cells in the brain of Alzheimer's disease and other neurological diseases. *J Neuroimmunol* 124:83-92.
- Togo TA, Haruhiko; Iseki, Eizo; Kondo, Hiromi; Ikeda, Kenji; Kato, Masanori; Oda, Tatsuro; Tsuchiya, Kuniaki; Kosaka, Kenji (2002) Occurrence of T cells in the brain of Alzheimer's disease and other neurological diseases. *J Immunol* 124:83-92.
- Tontsch U, Rott O (1993) Cortical neurons selectively inhibit MHC class II induction in astrocytes but not in microglial cells. *Int Immunol* 5:249-254.

- Underwood EL, Thompson LT (2016) High-fat diet impairs spatial memory and hippocampal intrinsic excitability and sex-dependently alters circulating insulin and hippocampal insulin sensitivity. *Biol Sex Differ* 7:9.
- Varvel NH, Grathwohl SA, Degenhardt K, Resch C, Bosch A, Jucker M, Neher JJ (2015) Replacement of brain-resident myeloid cells does not alter cerebral amyloid-beta deposition in mouse models of Alzheimer's disease. *J Exp Med* 212:1803-1809.
- Walker JM, Harrison FE (2015) Shared Neuropathological Characteristics of Obesity, Type 2 Diabetes and Alzheimer's Disease: Impacts on Cognitive Decline. *Nutrients* 7:7332-7357.
- Walter BA, Valera VA, Takahashi S, Matsuno K, Ushiki T (2006) Evidence of antibody production in the rat cervical lymph nodes after antigen administration into the cerebrospinal fluid. *Arch Histol Cytol* 69:37-47.
- Wan YY, Flavell RA (2009) How diverse--CD4 effector T cells and their functions. *J Mol Cell Biol* 1:20-36.
- Wlodarczyk A, Lobner M, Cedile O, Owens T (2014) Comparison of microglia and infiltrating CD11c(+) cells as antigen presenting cells for T cell proliferation and cytokine response. *J Neuroinflammation* 11:57.
- Yang J, Zhang L, Yu C, Yang XF, Wang H (2014) Monocyte and macrophage differentiation: circulation inflammatory monocyte as biomarker for inflammatory diseases. *Biomark Res* 2:1.
- Yates KF, Sweat V, Yau PL, Turchiano MM, Convit A (2012) Impact of metabolic syndrome on cognition and brain: a selected review of the literature. *Arterioscler Thromb Vasc Biol* 32:2060-2067.
- Zenaro E, Pietronigro E, Della Bianca V, Piacentino G, Marongiu L, Budui S, Turano E, Rossi B, Angiari S, Dusi S, Montresor A, Carlucci T, Nani S, Tosadori G, Calciano L, Catalucci D, Berton G, Bonetti B, Constantin G (2015) Neutrophils promote Alzheimer's disease-like pathology and cognitive decline via LFA-1 integrin. *Nat Med* 21:880-886.
- Zlokovic BV (2008) The blood-brain barrier in health and chronic neurodegenerative disorders. *Neuron* 57:178-201.